EEFECTIVENESS OF TUNED MASS DAMPERS IN MITIGATING EARTHQUAKE GROUND MOTIONS IN LOW AND MEDIUM RISE BUILDINGS

By

ZIXIANG ZHOU

A thesis submitted to the

Graduate School-New Brunswick

Rutgers, The State University of New Jersey

in partial fulfillment of the requirements

for the degree of

Master of Science

Graduate Program in Civil and Environmental Engineering

written under the direction of

Dr. Husam Najm

and approved by

____

____

____

____

New Brunswick, New Jersey

[May 2014]

ABSTRACT OF THE THESIS

EEFECTIVENESS OF TUNED MASS DAMPERS IN MITIGATING EARTHQUAKE GROUND MOTIONS IN LOW AND MEDIUM RISE BUILDINGS

by ZIXIANG ZHOU

Thesis Director:

Dr. HUSAM NAJM

Tuned mass dampers (TMD's) are passive energy devices used to reduce undesired vibrations in a number of structures or structural components such as industrial buildings, floor systems, machine foundations and others. There has been few studies on the effectiveness of TMD's in reducing earthquake effects in low rise and medium rise buildings**.** This paper investigates the effectiveness of tuned mass dampers on the response of low rise and medium rise buildings under earthquake ground motions. Numerical integration methods were used to solve the systems of coupled equations of motion and a MATLAB code was developed to solve the system of equations of motions. Response parameters include roof displacements, base shears, and inter-story drifts. Results from this analysis showed that the TMD can be effective in reducing drift values and base shears in low and medium rise buildings. The reduction was dependent on the TMD properties and location. The numerical solution can be used to obtain the optimum properties of the dampers. A reduction of about 30% was observed in roof displacements for a mass ratio of 10% of the modal mass. A 25% reduction in base shear was also observed for certain cases despite the overall increase of mass of the system. However, this reduction should be interpreted taking into consideration the magnitude of drifts and base shears to justify the use of TMD's. Also it should take into account the size of the TMD and the structural design requirements associated with the added TMD.

Contents

Contents of Tables

Contents of Figures

Introduction

Different from the conventional vibration mitigation techniques, which rely on the strength, stiffness and ductility of the structures, vibration control is a set of technical, in earthquake engineering, in order to mitigate the seismic impacts and response in structural buildings and non-structural components[1] through the installation of various control devices in the structures. Previous researches have given the ideas that vibration control devices can be classified as

- Active, semi-active;
- Passive control[2]; and
- Base isolation:

1. Active, semi-active:

1.1. Active control:

1.1.1. Introduction to Active control:

Active vibration control is the active application of force in an equal and opposite fashion to the forces imposed by external vibration [3]. An active control system generally consists following three components [4]:

1.1.1.1. Sensors: Measure the external excitation and/ or structural and non-structural response and transmit the information to the control system.

1.1.1.2. Computer hardware and software: Compute control forces on the basis of excitation and/ or response, control the drive system through the circuit control signal.

1.1.1.3. Actuator: provide the control force.

1.1.2. Algorithms of active control:

The equation of motion of a SDOF system could be expressed as ([7][8]):

$$\boldsymbol{M}\ddot{\boldsymbol{u}}(\boldsymbol{t}) + \boldsymbol{C}\dot{\boldsymbol{u}}(\boldsymbol{t}) + \boldsymbol{K}\boldsymbol{u}(\boldsymbol{t}) = -\boldsymbol{M}\ddot{\boldsymbol{u}}_{\boldsymbol{g}} \quad \textbf{(1)}$$

Where:

$\boldsymbol{M}, \boldsymbol{C}, \boldsymbol{K}$—mass, damping and stiffness stiffness

$\ddot{\boldsymbol{u}}_{\boldsymbol{g}}$—ground motion acceleration

$\ddot{\boldsymbol{u}}, \dot{\boldsymbol{u}}, u$—acceleration, velocity and displacement due to ground acceleration

The equations of control force can be expressed as:

$$\boldsymbol{M\ddot{Z} + C\dot{Z} + KZ = P} \tag{2}$$

Where:

$\ddot{\boldsymbol{Z}}, \dot{\boldsymbol{Z}}, \boldsymbol{Z}$—acceleration, velocity and displacement due to control force P

The equation of motion based on Eqn. (1) and Eqn. (2) could be expressed as

$$\begin{gathered}\boldsymbol{M}(\ddot{\boldsymbol{u}} + \ddot{\boldsymbol{Z}}) + \boldsymbol{C}(\dot{\boldsymbol{u}} + \dot{\boldsymbol{Z}}) + \boldsymbol{K}(\boldsymbol{u} + \boldsymbol{Z}) = \boldsymbol{P} - \boldsymbol{M}\ddot{\boldsymbol{u}}_{\boldsymbol{g}} \\ \boldsymbol{M}(\ddot{\boldsymbol{u}} + \ddot{\boldsymbol{u}}_{\boldsymbol{g}} + \ddot{\boldsymbol{Z}}) + \boldsymbol{C}(\dot{\boldsymbol{u}} + \dot{\boldsymbol{u}}_{\boldsymbol{g}} + \dot{\boldsymbol{Z}}) + \boldsymbol{K}(\boldsymbol{u} + \boldsymbol{u}_{\boldsymbol{g}}\boldsymbol{Z}) = \boldsymbol{P} + \boldsymbol{C}\dot{\boldsymbol{u}}_{\boldsymbol{g}} + \boldsymbol{K}\boldsymbol{u}_{\boldsymbol{g}}\end{gathered} \tag{3}$$

In the modern control theory, the following algorithms are frequently used to achieve the optimal control procedure [5][9][15][16][17][18][19]

- Classical linear optimal control;
- Instantaneous optimal control;
- Pole assignment;
- Independent modal space control;
- Stochastic optimal control;
- Limit state control;
- Fuzzy control;
- H_∞ optimal control; and
- Variable structure control

1.1.3. Active control devices:

Since the active control requires a lot of labor resources, it is still at the exploration stage. Recent available control devices consist;

1.1.3.1. Active tuned mass control system(AMD): an active mass damper is a feedback control system which is designed to sense structural motions and to generate a corrective control force acting on the structure[5]. AMD control system adjusts energy distribution between the inertial mass and structure through providing a pair of control force between them.

AMD control system consists inertial mass, stiffness elements, damping elements and actuator, which is generated by the actuator[6].

1.1.3.2. Active anchor cable control system: the system can adjust the anchor cable tension by changing the wind deflector windward area to facilitate the vibration control.

1.1.3.3. Active aerodynamic barge board control system: the system adjusts the wind pressure on wind deflector by changing the windward area to suppress wind vibration response of the structure. This system can only be used in wind resistance, and is sensitive to time lag.

1.2. Semi-active control:

1.2.1. Introduction to semi-active control:

Similar with the basis of active control system, semi-active control system combine the best features of both passive and active control systems. Since the semi-active control system aims to realize active optimal control force, Decentralized bang-bang control[10], the methods based on the Lyapunov theory aims to minimize the rate of change of a Lyapunov function[11] or to decrease the total energy of the structure[12], clipped-optimal control[13] and modulated homogeneous friction control[14] are some control algorithms used in semi-active control.

1.2.2. Algorithms of semi-active control:

For a MDOF system subjected to seismic excitation with *n* MR dampers, the equation of motion could be expressed as:

$$\boldsymbol{M\ddot{u}} + \boldsymbol{C\dot{u}} + \boldsymbol{Ku} = \boldsymbol{F\ddot{u}_g} + \boldsymbol{P} \qquad \textbf{(4)}$$

Where:

$\boldsymbol{\ddot{u}}, \boldsymbol{\dot{u}}, \boldsymbol{u} - -$vector of acceleration, velocity and displacement of the structure.

$\boldsymbol{\ddot{u}_g}$—ground acceleration vector.

$\boldsymbol{F}$—transfer matrix of the ground acceleration.

$\boldsymbol{P}$—matrix of control force.

When the state feedback is used, control force could be expressed at[20]

$$\boldsymbol{P} = -\Delta\boldsymbol{Ku} - \Delta\boldsymbol{C\dot{u}} \qquad \textbf{(5)}$$

Substituting Eqn. (5) into Eqn. (4) gives

$$\boldsymbol{M\ddot{u}} + (\boldsymbol{C} + \Delta\boldsymbol{C})\boldsymbol{\dot{u}} + (\boldsymbol{K} + \Delta\boldsymbol{K})\boldsymbol{u} = \boldsymbol{F\ddot{u}_g} \qquad \textbf{(6)}$$

The algorithms of semi-active control also includes the following algorithms

- Classical linear optimal control;
- Instantaneous optimal control;
- Pole assignment;
- Independent modal space control;
- Stochastic optimal control;
- Limit state control;
- Fuzzy control;
- H_∞ optimal control; and
- Variable structure control

1.2.3. Semi-active control devices:

The semi-active control actuators are often a combination of passive stiffness or damping devices with mechanical active control system. Typically, semi-active control system consists:

- Active variable stiffness system, (AVS);
- Active variable damper, (AVD);
- Variable liquid damping control system, (ER/MR)

1.2.3.1. Active variable stiffness system: change the additional stiffness of the structure actively through changing the stiffness of the device, avoid resonance by making the natural frequency of the structure far away from the predominant frequency of the disturbance.

AVS system can achieve following control method:

- Passive-on: controller is in locked state;
- Passive-off: controller is in open state;
- On-off: controller determines the on/ off state of active variable stiffness control device according to some certain control algorithms.

1.2.3.2. Active variable damper system: make the damping force close to the active control force through changing the force of the variable damping control device to achieve the effect of vibration mitigation.

AVD system can only provide damping force at the opposite direction of the structural movement, instead of the control force at any direction. Therefore, AVD system is unconditionally stable with good robustness.

1.2.3.3. Variable liquid damping control system: Electro-rheological fluid and Magneto-rheological fluid is controllable fluid, which is non-colloid suspension liquid consists of non-conductive (magnetic) mother liquor and solid electrolyte particles or magnetic particles spread evenly among them. The fibrous chain will be formed under the action of electric filed or magnetic field. Liquid Newtonian fluid with certain viscosity will be transferred to visco-plastic body with certain yield shear force, producing curing phenomenon.

ER/MR system consists of sensor, Electromagnetic rheological drives, controller and controlled structure. It follows the flow chart

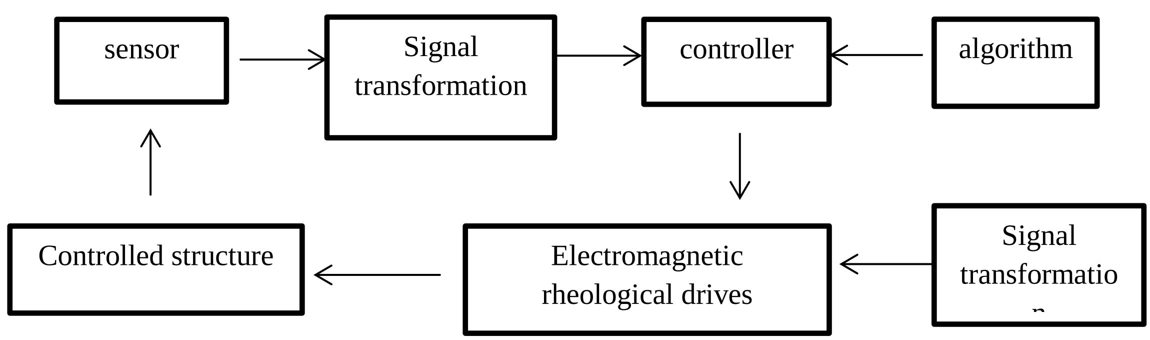

2. Passive control:

Passive control system consists of tuned mass damper systems[23], viscous fluid and viscoelastic dampers, friction dampers, and yielding metallic devices[25].

2.1. **Tuned mass damper:**

A tuned mass damper is a passive energy absorbing device consisting of a mass, a spring, and a viscous damper attached to a vibrating system aims to mitigate the vibration response[24]. The maximum amplitude of the structure can be lowered if the frequency of the damper is tuned properly.

A tuned mass damper (TMD) can be described by three parameters:

Mass ratio: the ratio of the mass of the damper to the total mass of single degree of freedom (SDOF) system or the generalized mass for a given mode of vibration of a multiple degree of freedom (MDOF) system[24].

$$\mu = m/M$$

Frequency ratio: the ratio of the fundamental frequency of the damper to the natural frequency of a SDOF system or the frequency corresponding to the first mode of vibration for a MDOF system.

$$f = \omega_d/\omega_0$$

Damping ratio: the damping ratio of the TMD is

$$\xi = c/2m\omega_d$$

2.2. Viscoelastic devices:

2.2.1. Fluid viscoelastic devices:

The fluid viscoelastic devices, generally known as shock and vibration isolation system, use the resistance of a viscous fluid to mitigate the vibration response. The viscous heating caused by friction dissipates the energy.

Both linear and nonlinear behavior are considered and the fluid is insensitive to the temperature. The generalized Maxwell model is used for viscoelastic devices[26].

2.2.2. Solid viscoelastic devices:

A solid viscoelastic device consists of polymeric material layers bonded between steel plates[25]. The energy is dissipated through transforming the energy to heat under cyclic shear deformations.

2.3. Friction devices:

Friction devices uses the friction between two solids interfaces sliding relative to one another to dissipate the energy.

Several researches have been performed to investigate the properties of the friction devices. Pall used a Friction Damped Braced Frame to dissipate the dynamic energy[34]. Grigorian suggested two types of friction devices, Slotted Bolted Connections (SBCs). In 1990, Aiken and Kelly suggested two types of energy-absorbing devices[36]. The energy-absorbing are a viscoelastic shear damper using an energy approach and a friction device.

It is found that friction devices do not dissipate the energy under minor earthquake, but only act as braces. Therefore, the effect of vibration mitigation is not remarkable. To solve this problem, Tsiatas and Daly suggested to use a friction absorber and a viscous damper as a series system[37]. Under minor earthquake and wind load, only the viscous damper acts as an energy absorber; when subjected to violent earthquake, the friction device take participate in dissipating the energy.

2.4. Base isolation:

The basic principle of base isolation is to extent the natural period of the structures, providing proper damping to reduce the acceleration response. At the same time, to ensure that the large displacement of the structure be taken by the base isolation system instead of by the structure itself [38].

Literature Review

1. Early application of TMD

The concept of tuned mass damper could be traced back to 1909, when Frahm invented a dynamic vibration absorber[39] to control the vibration. Since then, researchers have done a lot of work in the passive control theory and application. In early 1950s, the engineers in former Soviet Union applied percussive pendulum on the steel tower and chimney to reduce the structural vibration under wind load excitation. In 1970s, engineers installed hundreds of tons of TMD on the 343.5m high John Hancock Tower in Boston[40] and the 292.6m high Citicorp Center in New York City[41], and effectively reduced the wind-induced response. In 1980, a TMD was also successfully installed on the Sydney Tower to control the wind-induced vibration in Australia. And in Japan, the first TMD device was installed on the Chiba Port Tower in 1980, and followed by the Funade bridge in Osaka. In 2004, a 660 tons of sphere liked TMD was installed on the Taipei 101 Tower in Taiwan, which is the largest damper in the world.

2. The theoretical research and practical applications of TMD

The development of the theoretical study of TMD can be divided into three stages. The first stage mainly focuses on the research of a single TMD system. Since Den Hartog proposed a principle of optimizing the parameters of the system without TMD, many researchers have studied the parametric problem of the TMD under different forms of excitation. It is observed that the impact of the parameters of the TMD on the structural vibration is nonlinear. And it is practically vilified that the TMD is suitable for high-rise buildings, tall towers and large-span bridges with small damping ratio. The parameters of TMD have a great impact on vibration control.

The second stage focuses on the research of the multiple tuned mass damper(MTMD). In 1988, Clark proposed a new idea to optimize the parameters of MTMD. Since then, many researchers have committed to research in this area. Studies have shown that the MTMD have better vibration control effect than single-TMD system. Given a certain mass ratio, the frequency ratio, damping ratio and the number of TMD are the main parameters of the system. And they play a major role in the structural response

The third stage focuses on the extension of the concept of the TMD. Current research in this area is still in the beginning stage with fewer findings.

Basics of TMD Systems

Consider a single degree of freedom (SDOF) system attached with a tuned mass damper (TMD) shown in Figure 1

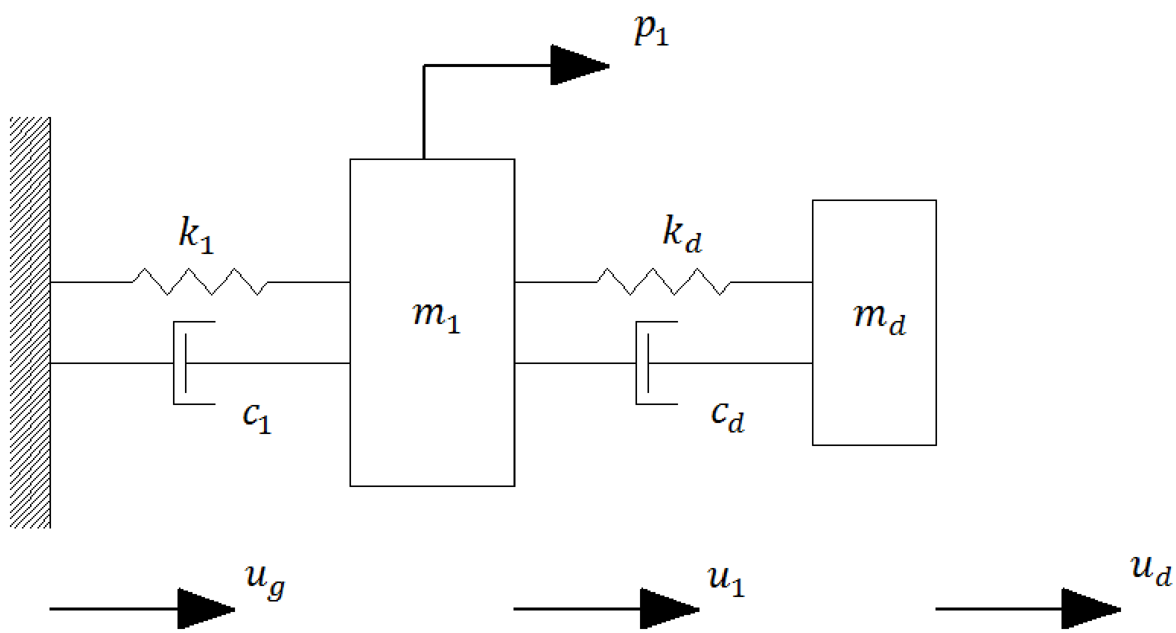

Figure 1: Schematic diagram of damped SDOF system

The equations of motion could be expressed as:

$$m\ddot{u} + c\dot{u} + ku = P - m\ddot{u}_g + c_d\dot{u}_d + k_d u_d \qquad (7)$$

$$m_d\ddot{u}_d + c_d\dot{u}_d + k_d u_d + m_d\ddot{u} = -m_d\ddot{u}_g \qquad \mathbf{(8)}$$

Where:

m, c, k—the mass, damping and the stiffness of the primary structure.

m_d, c_d, k_d—the mass, damping and the stiffness of tuned mass damper.

$\ddot{u}, \dot{u}, u$—the acceleration, velocity and the displacement response of the primary structure.

$\ddot{u}_d, \dot{u}_d, u_d$—the acceleration, velocity and the displacement response of tuned mass damper.

u_d −displacement response of tuned mass damper relative to primary mass, m.

P −the excitation force.

$\ddot{u}_g$ −the ground acceleration.

1. Harmonic excitation:

Assume the system is undamped and excited solely by a harmonic force

$$P(t) = P_0 e^{i\Omega t}$$

In which P_0 is the amplitude of the force and Ω is the angular frequency. Eqn. (7) and Eqn. (8) can be rewritten as:

$$m\ddot{u} + ku = P + c_d\dot{u}_d + k_d u_d$$

$$m_d\ddot{u}_d + c_d\dot{u}_d + k_d u_d + m_d\ddot{u} = 0$$

Rearrange the equations:

$$m\ddot{u} - c_d\dot{u}_d + (ku - k_d u_d) = P \qquad \textbf{(9)}$$

$$(m_d\ddot{u}_d + m_d\ddot{u}) + c_d\dot{u}_d + k_d u_d = 0 \qquad \textbf{(10)}$$

The response of the primary mass and the tuned mass damper could be given as[27]:

$$\begin{aligned} u &= u_0 e^{i\Omega t};\ u_d = u_{d0} e^{i\Omega t} \\ \dot{u} &= i\Omega u_0 e^{i\Omega t};\ \dot{u}_d = i\Omega u_{d0} e^{i\Omega t} \\ \ddot{u} &= -\Omega^2 u_0 e^{i\Omega t};\ \ddot{u}_d = -\Omega^2 u_{d0} e^{i\Omega t} \end{aligned} \qquad \textbf{(11)}$$

Substitute Eqn. (11) into Eqn. (9) and (10) gives

$$\begin{aligned} [k - \Omega^2(m + m_d)]u - \Omega^2 m_d u_d &= P \\ -\Omega^2 m_d u + [k_d + i\Omega c_d - \Omega^2 m_d]u_d &= 0 \end{aligned} \qquad \textbf{(12)}$$

Eqn. (12) can be written in matrix form

$$\begin{bmatrix} k - \Omega^2(m + m_d) & -\Omega^2 m_d \\ -\Omega^2 m_d & k_d + i\Omega c_d - \Omega^2 m_d \end{bmatrix} \begin{Bmatrix} u \\ u_d \end{Bmatrix} = \begin{Bmatrix} P \\ 0 \end{Bmatrix} \qquad \textbf{(13)}$$

The response u and u_d could be solved as

$$\begin{Bmatrix} u \\ u_d \end{Bmatrix} = \begin{bmatrix} k - \Omega^2(m + m_d) & -\Omega^2 m_d \\ -\Omega^2 m_d & k_d + i\Omega c_d - \Omega^2 m_d \end{bmatrix}^{-1} \begin{Bmatrix} P \\ 0 \end{Bmatrix}$$

Therefore, if we define

$$\frac{u}{P/k};\ \frac{u_d}{P/k}$$

be the amplification factors of the primary mass and the damper respectively, the amplification factors could be given as[28]

$$\frac{u}{P/k} = \frac{(k_d + i\Omega c_d - \Omega^2 m_d)k}{[k - \Omega^2(m + m_d)][k_d - \Omega^2 m_d + i\Omega c_d] - (\Omega^2 m_d)^2} \quad \textbf{(14)}$$

$$\frac{u_d}{P/k} = \frac{\Omega^2 m_d k}{[k - \Omega^2(m + m_d)][k_d - \Omega^2 m_d + i\Omega c_d] - (\Omega^2 m_d)^2} \quad \textbf{(15)}$$

Practically, a vibration system is described by its mass m and its natural frequency ω, the damper is generally characterized by a damping ratio ξ_d. Therefore, the following parameter: mass ratio, μ, and damping ratio, ξ_d

$$\mu = \frac{m_d}{m}$$

$$\xi_d = \frac{c_d}{2\omega_d}$$

Are introduced to describe the system.

Substituting the two parameters into Eqn. (14) and Eqn. (15) gives the amplification factor in terms of μ and ξ_d as

$$\frac{u}{P/k} = \frac{\omega^2[\omega_d^2 - \Omega^2 + 2i\xi_d\omega_d\Omega]}{\Omega^4 - [\omega^2 + (1+\mu)\omega_d^2]\Omega^2 + \omega^2\omega_d^2 + 2i\xi_d\omega_d\Omega[\omega^2 - (1+\mu)\Omega^2]} \quad \textbf{(16)}$$

$$\frac{u_d}{P/k} = \frac{\omega^2\Omega^2}{\Omega^4 - [\omega^2 + (1+\mu)\omega_d^2]\Omega^2 + \omega^2\omega_d^2 + 2i\xi_d\omega_d\Omega[\omega^2 - (1+\mu)\Omega^2]} \quad \textbf{(17)}$$

The amplification factor of frequency ratio, $f = \Omega/\omega$ is shown is as

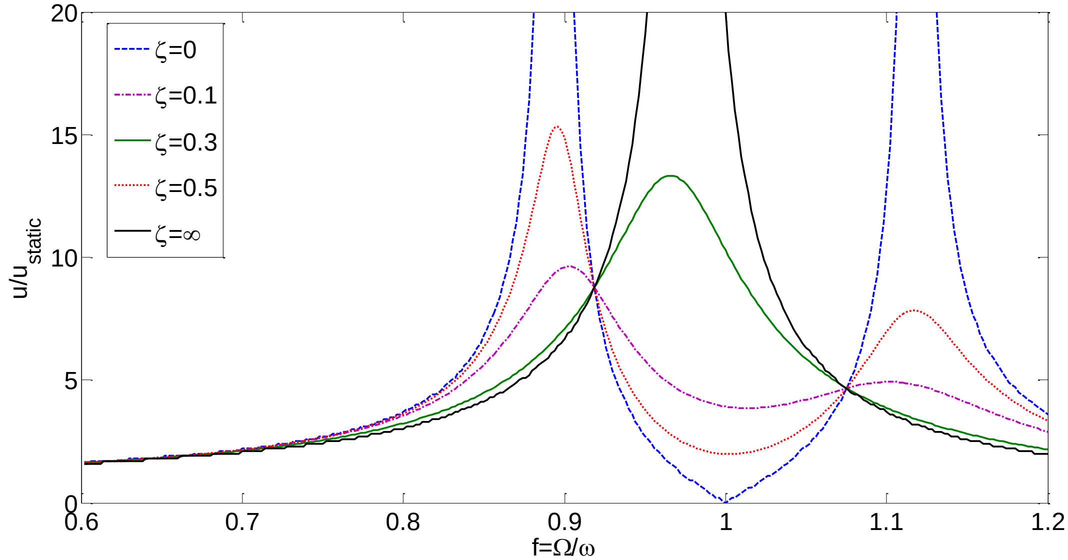

Figure 2: Amplification factor

It has been found that there are two frequencies ω_A and ω_B where the amplification factor is independent from the damping ratio[28]. Den Hartog[29] advised to select a proper damping frequency ω_d so that the amplification factor at point A and B is equal. Based on this, the optimal frequency and optimal damping could be found.

1.1. Optimal frequency:

From Eqn. (16), the amplification factor could be expressed as

$$\frac{u}{P/k} = \frac{A_1 + 2i\xi_d A_2}{A_3 + 2i\xi_d A_4}$$

In which

$$A_1 = \omega^2[\omega_d^2 - \Omega^2]$$

$$A_2 = \omega_d \Omega \omega^2$$

$$A_3 = \Omega^4 - [\omega^2 + (1+\mu)\omega_d^2]\Omega^2 + \omega^2\omega_d^2$$

$$A_4 = \omega_d \Omega[\omega^2 - (1+\mu)\Omega^2]$$

The amplification factor is the absolute value

$$\left\|\frac{u}{P/k}\right\| = \left\|\frac{A_1 + 2i\xi_d A_2}{A_3 + 2i\xi_d A_4}\right\|$$

For the factors corresponding to point A and B which are independent to ξ_d, the limits for $\xi_d = 0$ and $\xi_d \to \infty$ must be equal[28]:

$$\frac{A_1^2}{A_3^2} = \frac{A_2^2}{A_4^2}$$

Substituting A_1, A_2, A_3 and A_4 gives

$$\left[1 - \left(\frac{\Omega}{\omega}\right)^2\right]\left[1 - \left(\frac{\Omega}{\omega_d}\right)^2\right] - \mu\left(\frac{\Omega}{\omega}\right)^2 = \pm\left[1 - \left(\frac{\Omega}{\omega_d}\right)^2\right]\left[1 - (1+\mu)\left(\frac{\Omega}{\omega}\right)^2\right] \quad \textbf{(18)}$$

Plus sign gives the root $\Omega = 0$, which represents the static force $P = P_0$. The minus sign gives

$$\left[1 - \left(\frac{\Omega}{\omega_d}\right)^2\right]\left[2 - (2+\mu)\left(\frac{\Omega}{\omega}\right)^2\right] = \mu\left(\frac{\Omega}{\omega}\right)^2 \quad \textbf{(19)}$$

The roots of this equation are Ω_A^2 and Ω_B^2. Substituting the two roots into Eqn. (19) gives the relation between the two roots

$$\left(\frac{\Omega_A}{\omega}\right)^2 + \left(\frac{\Omega_B}{\omega}\right)^2 = \frac{2}{2+\mu}\left[1 + (1+\mu)\right]\left(\frac{\omega_d}{\omega}\right)^2 \quad \textbf{(20)}$$

Another relation is determined by specifying equal magnitude of amplification at Ω_A^2 and Ω_B^2[28]. The response magnitude is determined when $\xi_d \to \infty$.

$$\frac{u}{P/k} = \frac{1}{1-(1+\mu)\left(\frac{\Omega}{\omega}\right)^2} \quad \textbf{(21)}$$

Substituting two roots, Ω_A^2 and Ω_B^2 into Eqn. (21) gives

$$\frac{1}{1 - (1+\mu)\left(\frac{\Omega_A}{\omega}\right)^2} = -\frac{1}{1 - (1+\mu)\left(\frac{\Omega_B}{\omega}\right)^2}$$

which could be expressed as

$$\left(\frac{\Omega_A}{\omega}\right)^2 + \left(\frac{\Omega_B}{\omega}\right)^2 = \frac{2}{1+\mu} \quad \textbf{(22)}$$

By solving Eqn. (20) and Eqn. (22), the optimal mass ratio could be given as

$$1 + (1+\mu)\left(\frac{\omega_d}{\omega}\right)^2 = \frac{2+\mu}{1+\mu}$$

The optimal damper frequency can be given as

$$\frac{\omega_d}{\omega} = \frac{1}{1+\mu} \quad \textbf{(23)}$$

1.2. Structural amplification factor:

Eqn. (20) gives the dynamic amplification factor at the frequencies Ω_A and Ω_B determined by Eqn. (23)

$$(2+\mu)(1+\mu)^2(\frac{\omega}{\omega_0})^4 - 2(1+\mu)(2+\mu)(\frac{\omega}{\omega_0})^2 + 2 = 0 \qquad \textbf{(24)}$$

The roots of this equation are

$$(1+\mu)\left(\frac{\Omega_{A,B}}{\omega_0}\right)^2 = 1 \pm \sqrt{\frac{\mu}{2+\mu}}$$

Substituting these frequencies into Eqn. (21) gives

$$\frac{u}{P/k} = \frac{1}{1-(1+\mu)\left(\frac{\Omega_{A,B}}{\omega}\right)^2} = \pm\sqrt{\frac{2+\mu}{\mu}} \qquad \textbf{(25)}$$

Therefore, the amplification factors at frequencies Ω_A and Ω_B independent of the damping are[28]

$$\left|\frac{u}{P/k}\right|_{A,B} = \sqrt{\frac{2+\mu}{\mu}} \qquad \textbf{(26)}$$

1.3. Optimal damper tuning:

Brock[30] and Den Hartog[29] suggested that the optimal damping ratio, ξ_d, could be obtained by taking the arithmetic average of the local maximum dynamic amplification at frequency Ω_A and the local minimum dynamic amplification at frequency Ω_B

$$\xi_{classic}^2 = \frac{1}{2}\frac{\mu}{1+\mu} \qquad \textbf{(27)}$$

Steen Krenk and Jan R. Høgsberg[28] suggested that from Figure 2, the suitable damping ratio could be selected to make the dynamic amplification factors equal to the two factors at frequencies Ω_A and Ω_B. If the two mass is joined to one, the optimal frequency tuning Ω could be taken at the geometric mean of ω and ω_d[28]

$$\Omega_\infty = \frac{\omega}{\sqrt{1+\mu}} = \sqrt{\omega_d \omega}$$

The dynamic amplification factor at this frequency is

$$\left|\frac{u}{P/k}\right|^2 = \frac{\mu^2+(2\xi_d)^2(1+\mu)}{\mu^2} \qquad \textbf{(28)}$$

The damping ratio could be given by equating the dynamic amplification at Ω_∞ to that at Ω_A and Ω_B[28]

$$\xi_{opt}^2 = \frac{3}{8}\frac{\mu}{1+\mu} \tag{29}$$

2. Ground motion:

When the SDOF system is loaded by ground acceleration, the equation of motion could be expressed in the form of Eqn. (7) and Eqn. (8) with an equivalent load

$$F = -\begin{Bmatrix} m_1 \\ m_d \end{Bmatrix} \ddot{u}_g$$

and use the absolute displacement response of TMD, u_d, to replace the relative displacement, the equation of motion could be written as

$$\begin{bmatrix} k_1 + k_d + i\omega c_d - \omega^2 m_1 & -k_d - i\omega c_d \\ -k_d - i\omega c_d & k_d + i\omega c_d - \omega^2 m_2 \end{bmatrix} \begin{Bmatrix} u_1 \\ u_d \end{Bmatrix} = -\begin{Bmatrix} m_1 \\ m_d \end{Bmatrix} \ddot{u}_g \tag{30}$$

Substitute

$$\mu = \frac{m_d}{m_1};\ r = \frac{\Omega}{\omega_1}, f = \frac{\omega_d}{\omega_1};\ \xi_1 = \frac{c_1}{2\omega_1};\ \xi_d = \frac{c_d}{2\omega_d}$$

into Eqn. (30) gives[31]

$$\begin{bmatrix} 1 + \mu f^2 - r^2 + 2i\mu f r \xi_d & -\mu f^2 - 2i\mu f r \xi_d \\ -\mu f^2 - 2i\mu f r \xi_d & \mu f^2 - \mu r^2 + 2i\mu f r \xi_d \end{bmatrix} \begin{Bmatrix} u_1 \\ u_d \end{Bmatrix} = -\begin{Bmatrix} m_1 \\ m_d \end{Bmatrix} \ddot{u}_g \tag{31}$$

The response of u_1 could be given by taking the normalized acceleration $\ddot{u}_g/\omega_1^2$ as input

$$u_1 = \frac{(1+\mu)f^2 - r^2 + 2i(1+\mu)fr\xi_d}{[1+\mu f^2 - r^2 + 2i\mu f r\xi_d][f^2 - r^2 + 2ifr\xi_d] - \mu[f^2 + 2ifr\xi_d]^2} \frac{\ddot{u}_g}{\omega_1^2} \tag{32}$$

Numerical Studies

In this section, a SDOF system shown in Figure 3 with TMD is studied to evaluate the effect of TMD on mitigating the vibration response. The derivation of Newmark-β method is presented first. The effect of TMD on vibration response due to free vibration, harmonic force excitation and harmonic ground motions are evaluated.

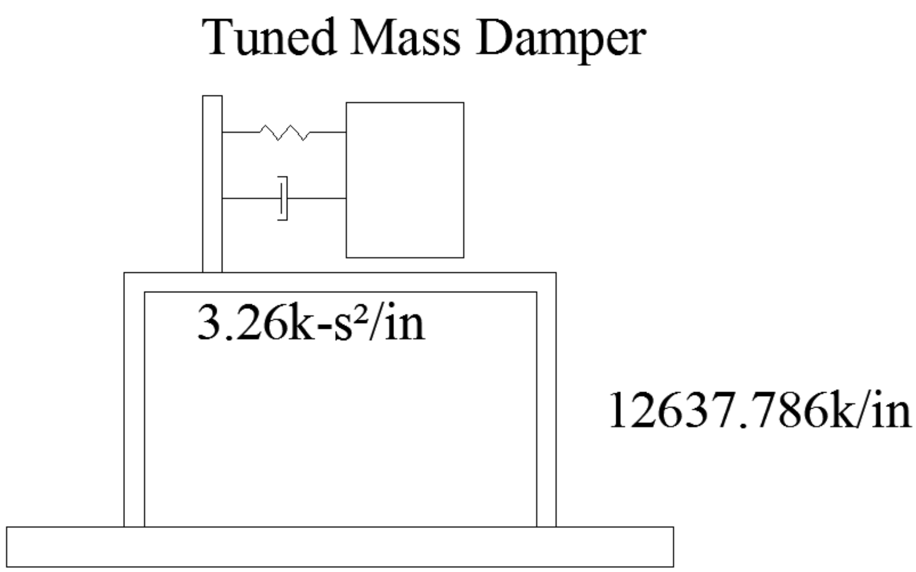

Figure 3: SDOF system with TMD

1. Derivation of numerical calculation

A SDOF system with TMD shown in Figure 1 was studied. The equation of motion of the SDOF system with TMD expressed in Eqn. (7) and Eqn. (8) are rewritten here

$$m\ddot{u}_1 + c\dot{u}_1 + ku_1 - k_d u_d - c_d \dot{u}_d = p_1 - m\ddot{u}_g$$

$$m_d \ddot{u}_d + c_d \dot{u}_d + k_d u_d = -m_d(\ddot{u}_1 - \ddot{u}_g)$$

Newmark-β numerical calculation [32] was performed to express the displacement, velocity of primary mass and damper, respectively, as

$$u_{i+1} = u_i + \Delta\dot{u}_i + \Delta^2\left[\left(\frac{1}{2} - \beta\right)\ddot{u}_i + \beta\ddot{u}_{i+1}\right] \quad \textbf{(33)}$$

$$\dot{u}_{i+1} = \dot{u}_i + \Delta[(1-\gamma)\ddot{u}_i + \gamma\ddot{u}_{i+1}] \quad \textbf{(34)}$$

$$u_{d+1} = u_d + \Delta\dot{u}_d + \Delta^2\left[\left(\frac{1}{2} - \beta\right)\ddot{u}_d + \beta\ddot{u}_{d+1}\right] \quad \textbf{(35)}$$

$$\dot{u}_{d+1} = \dot{u}_d + \Delta[(1-\gamma)\ddot{u}_d + \gamma\ddot{u}_{d+1}] \quad \textbf{(36)}$$

Substitute $u_{i+1};\ \dot{u}_{i+1}$ into Enq. (7) and $u_{d+1};\ \dot{u}_{d+1}$ into Eqn. (8)

$$[m + c\Delta\gamma + k\Delta^2\beta]\ddot{u}_{i+1} + \left[c\Delta(1-\gamma) + k\Delta^2\left(\frac{1}{2} - \beta\right)\right]\ddot{u}_i + [c + k\Delta]\dot{u}_i + ku_i$$

$$= p_{i+1} - f_{i+1} + [k_d\Delta^2\beta + c_d\Delta\gamma]\ddot{u}_{d+1} + \left[k_d\Delta^2\left(\frac{1}{2} - \beta\right) + c_d\Delta(1-\gamma)\right]\ddot{u}_d + [k_d\Delta + c_d]\dot{u}_d + k_d u_d \quad \textbf{(37)}$$

$$[m_d + c_d\Delta\gamma + k_d\Delta^2\beta]\ddot{u}_{d+1} + \left[c_d\Delta(1-\gamma) + k_d\Delta^2\left(\frac{1}{2} - \beta\right)\right]\ddot{u}_d + [c_d + k_d\Delta]\dot{u}_d + k_d u_d$$

$$= -m_d(\ddot{u}_2)_{i+1} - m_d u g_{i+1} \quad \textbf{(38)}$$

Let

$$H_1 = m + c\Delta\gamma + k\Delta^2\beta;\ H_2 = c\Delta(1-\gamma) + k\Delta^2\left(\frac{1}{2} - \beta\right);\ H_3 = c + k\Delta;\ \ H_4 = k$$

$$H_5 = k_d\Delta^2\beta + c_d\Delta\gamma;\ H_6 = k_d\Delta^2\left(\frac{1}{2} - \beta\right) + c_d\Delta(1-\gamma);\ H_7 = k_d\Delta + c_d;\ H_8 = k_d$$

Also let

$$B_1 = m_d + c_d\Delta\gamma + k_d\Delta^2\beta;\ B_2 = c_d\Delta(1-\gamma) + k_d\Delta^2\left(\frac{1}{2} - \beta\right);\ B_3 = c_d + k_d\Delta; B_4 = k_d;\ B_5 = -m_d$$

Eqn. (37) and Eqn. (38) could be expressed as

$$H_1\ddot{u}_{i+1} + H_2\ddot{u}_i + H_3\dot{u}_i + H_4 u_i = p_{i+1} - f_{i+1} + H_5\ddot{u}_{d+1} + H_6\ddot{u}_d + H_7\dot{u}_d + H_8 u_d \quad \textbf{(39)}$$

$$B_1\ddot{u}_{d+1} + B_2\ddot{u}_d + B_3\dot{u}_d + B_4 u_d = B_5(\ddot{u}_2)_{i+1} - m_d u g_{i+1} \quad \textbf{(40)}$$

Let

$$\widetilde{H} = p_{i+1} - f_{i+1} + H_6\ddot{u}_d + H_7\dot{u}_i + H_8u_d - H_2\ddot{u}_i - H_3\dot{u}_i - H_4u_i \tag{41}$$

$$\tilde{B} = B_2\ddot{u}_d + B_3\dot{u}_d + B_4u_d + m_d u g_{i+1} \tag{42}$$

Eqn. (39) and Eqn. (40) could be written as

$$H_1\ddot{u}_{i+1} - H_5\ddot{u}_{d+1} = \widetilde{H} \tag{43}$$

$$B_5(\ddot{u}_2)_{i+1} - B_1\ddot{u}_{d+1} = \tilde{B} \tag{44}$$

Solving the equations (43), (44) gives the acceleration response of primary mass and damper

$$\ddot{u}_{i+1} = \begin{Bmatrix} \ddot{u}_1 \\ \ddot{u}_2 \end{Bmatrix}_{i+1} = \begin{bmatrix} H_1^{11} & H_1^{12} - C_2^1 \\ H_1^{21} & H_1^{22} - C_2^2 \end{bmatrix}^{-1} \begin{Bmatrix} C_1^1 \\ C_1^2 \end{Bmatrix} \tag{45}$$

$$\ddot{u}_{d+1} = \frac{B_5(\ddot{u}_2)_{i+1} - \tilde{B}}{B_1} \tag{46}$$

where

$$C_1 = \widetilde{H} - H_5\frac{\tilde{B}}{B_1};\;\; C_2 = H_5\frac{B_5}{B_1}$$

The algorithm based on the above derivation was given in Table 1 and a Matlab code was developed.

Table 1: algorithm based on the derivation

Initial computations:

Form stiffness $[\boldsymbol{K}], [\boldsymbol{K_d}]$, mass $[\boldsymbol{M}], [M_d]$, damping $[\boldsymbol{C}], [\boldsymbol{C_d}]$

Initialize $\{u_0\}.\{\dot{u}_0\}, \{\ddot{u}_0\}, \{u_{d_0}\}, \{\dot{u}_{d_0}\}, \{\ddot{u}_{d_0}\}$

Select time step Δt, parameters α, β

Form $[\boldsymbol{H_1}], [\boldsymbol{H_2}], [\boldsymbol{H_3}], [\boldsymbol{H_4}], [\boldsymbol{H_5}], [\boldsymbol{H_7}], [\boldsymbol{H_8}]$ and B_1, B_2, B_3, B_4, B_5

For each time step:

Form $[\widetilde{\boldsymbol{H}}], [\boldsymbol{C_1}], [\boldsymbol{C_2}]$ and $\tilde{B}$

Calculate $\{\ddot{u}_{t+1}\}, \{\ddot{u}_{d_{t+1}}\}$

Calculate $\{u_{t+1}\}, \{\dot{u}_{t+1}\}, \{u_{d_{t+1}}\}, \{\dot{u}_{d_{t+1}}\}$

2. Effect of TMD on SDOF system

A SDOF system attached with a TMD was evaluated to study the effect of vibration mitigating due to various dynamic loads. The SDOF system is the same as shown in Figure 3.

Introducing three parameters:

- mass ratio, $\mu = m_d/m$;
- frequency ratio, $f = \omega_d/\omega$; and
- damping ratio, $\xi_d = c_d/2\omega_d$

the mass, stiffness and damping of TMD could be expressed in terms of three parameters and the mass, stiffness and frequency of primary mass as

$$m_d = \mu m;\ k_d = (f\omega)^2(\mu m);\ c_d = 2\xi_d f\omega \qquad \textbf{(47)}$$

The effect of TMD on vibration response due to various loads are evaluated numerically, respectively.

2.1. Effect of TMD due to free vibration

For the SDOF system shown in Figure 3, the vibration displacement response due to free vibration could be performed via inputting an initial displacement, u_0.

For a SDOF system without damping, the initial displacement results steady state vibration, while damping is introduced, the vibration attenuates. Let the initial displacement to be 5% of the height of the system, here, $7.2in$.

Take the following cases to evaluate the effect of TMD on vibration response:

- Case 1: $\mu = 0.05, f = 0.9, \xi_d = 0.01$;
- Case 2: $\mu = 0.05, f = 0.9, \xi_d = 0.05$;
- Case 3: $\mu = 0.05, f = 1.0, \xi_d = 0.01$;

- Case 4: $\mu = 0.05, f = 1.0, \xi_d = 0.05$;
- Case 5: $\mu = 0.05, f = 1.1, \xi_d = 0.01$;
- Case 6: $\mu = 0.05, f = 1.1, \xi_d = 0.05$;

The SDOF system has damping ratio of $\xi = 0.02$. The displacement of SDOF system with and without TMD caused by an initial displacement are shown in Figure 4.

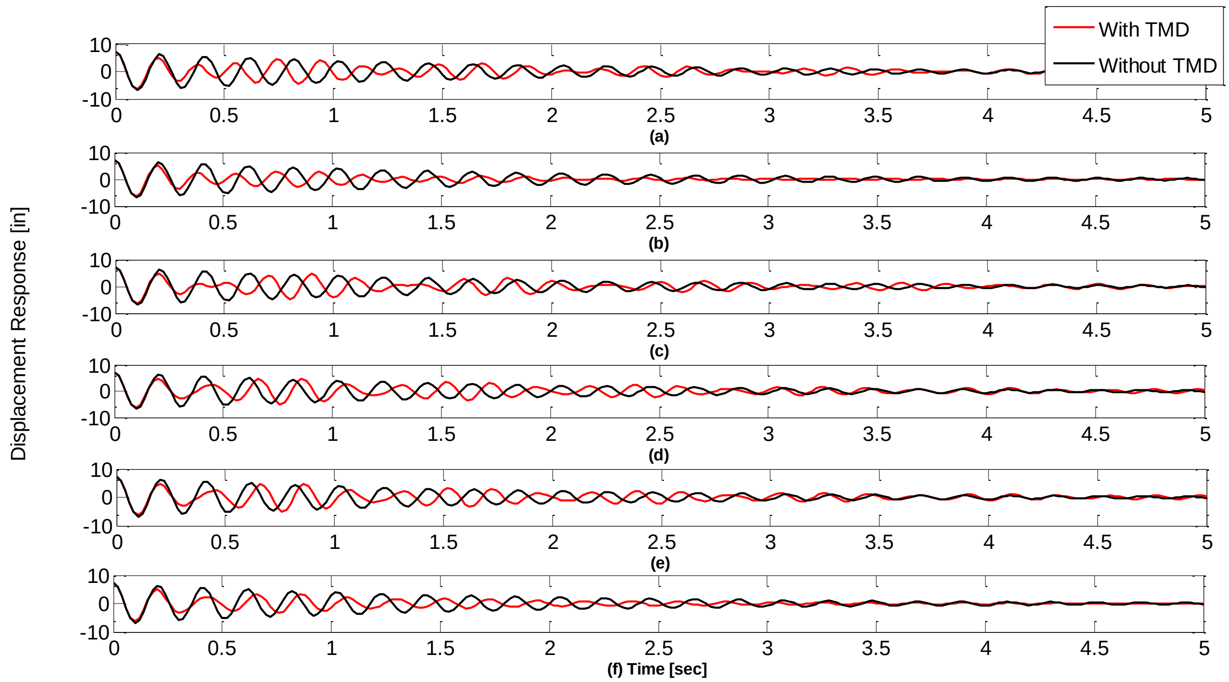

Figure 4: Effect of TMD on SDOF system, (a) case 1; (b) case 2; (c) case 3; (d) case 4; (e) case 5; (f) case 6

It is found that TMD mitigates the displacement vibration due to initial displacement at the beginning of vibration, while with time passes by, the effect of TMD decreases. Generally, for the case of loaded by initial displacement, TMD changed the period of system.

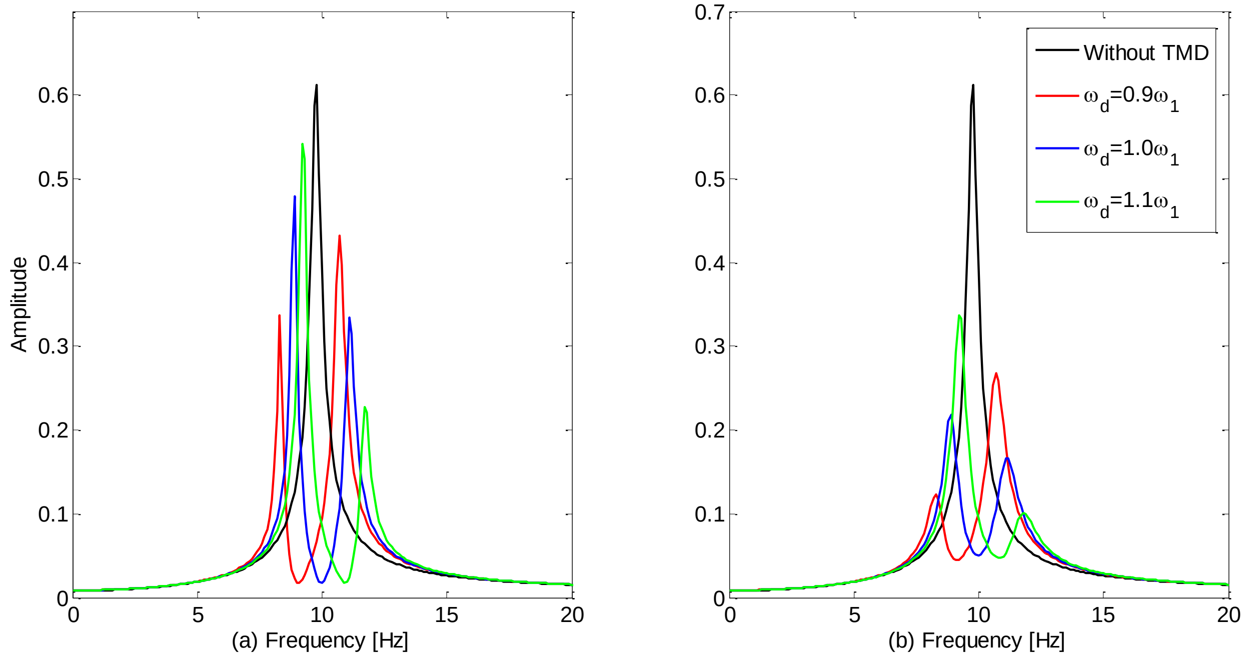

Figure 5: Effect of TMD on displacement in frequency domain, (a) $\xi_d = 0.01$; (b) $\xi_d = 0.05$

The effect of TMD on SDOF system subjected to initial displacement was also studied in frequency domain. Figure 5 shows the response of system in frequency domain. It is observed that for the system without TMD, only one main frequency exists, however, when attached with a TMD, one frequency is added and they deviate from the original frequency. For different frequency ratios, various frequency relationships are presented. For example, when frequency ratio is $f = 0.9$, the amplitude corresponding to the first frequency of the system is lower than that of corresponding to the second frequency; while for $f = 1.0$ and $f = 1.1$, opposite relationship exists. In addition, with the increase of frequency ratio, the amplitude corresponding to the first frequency increases and moves towards the original frequency, while the amplitude corresponding to the second frequency decreases and moves away. It is observed from Figure 5 that a TMD will be optimally tuned when the amplitude corresponding to its first and second frequency are equal. Eqn. (23) gives an equation to find the optimal frequency ratio expressed here as

$$\frac{\omega_d}{\omega} = \frac{1}{1+\mu}$$

For the system discussed here, $\mu = 0.05$, therefore, the frequency ratio is $f = 0.952$. The effect of TMD on displacement response, which is tuned to have $f = 0.952$, in frequency domain were evaluated and plotted in Figure 6. It is found that when tuned to have $f = 0.952$, the two peak amplitudes for the system with $\xi_d = 0.01$ are almost equal; while the second peak amplitude is still larger than the first for the system with $\xi_d = 0.05$, the difference is much less than what is presented in Figure 5(b).

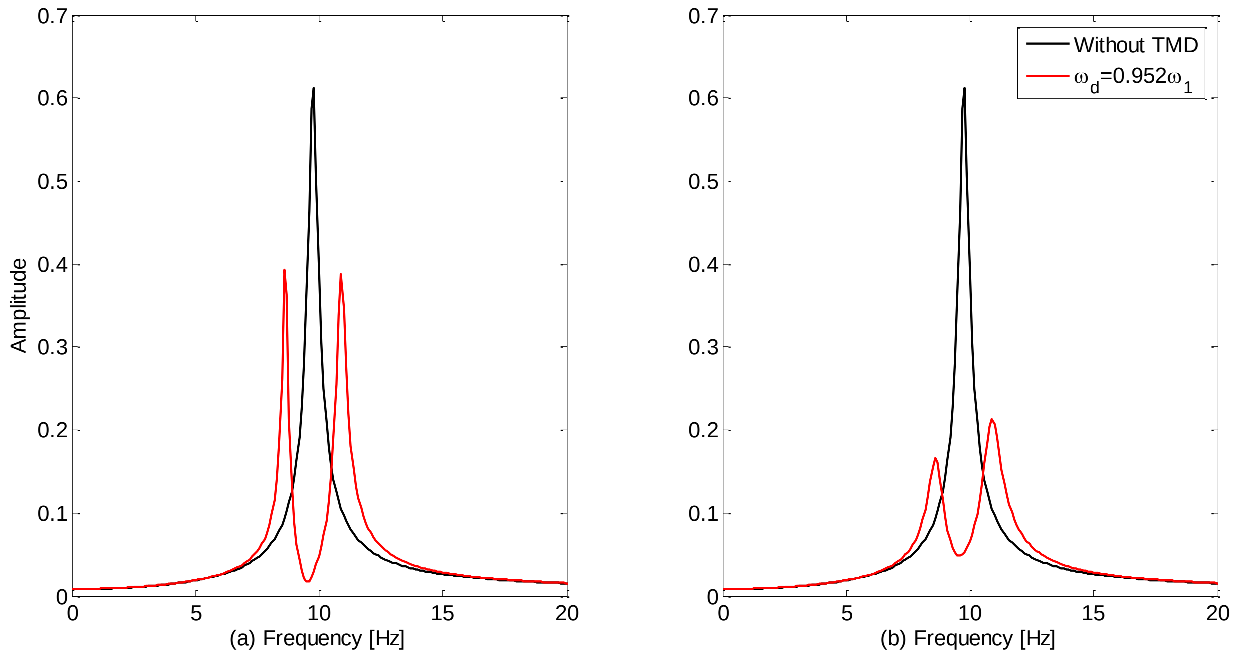

Figure 6: Effect of TMD on displacement in frequency domain with optimal frequency ratio, (a) $\xi_d = 0.01$; (b) $\xi_d = 0.05$

2.2. Effect of TMD due to harmonic excitation

For the same system, a harmonic force excitation was loaded on the primary mass, m_1. The harmonic force is defines as

$$P(t) = P_0 e^{i\Omega t}$$

In which P_0 is the amplitude of the force and Ω is the angular frequency. As discussed in section1.1, for different angular frequency, Ω, following parameters of TMD, mass ratio, frequency ratio, and damping ratio, will affect the effect of vibration mitigation. To evaluate the effect of those parameters, amplification factor defined as Eqn. (16) is introduced. By comparing the difference of amplification factor between the system with and without TMD, the effect of those parameters could be concluded. Take the following cases:

- Case 1: $\mu = 0.05, f = 1.1, \xi_d = 0.00$;
- Case 2: $\mu = 0.05, f = 1.1, \xi_d = 0.50$;
- Case 3: $\mu = 0.05, f = 1.1, \xi_d = \infty$;
- Case 4: $\mu = 0.05, f = 1.0, \xi_d = 0.00$;
- Case 5: $\mu = 0.05, f = 1.0, \xi_d = 0.50$;
- Case 6: $\mu = 0.05, f = 1.0, \xi_d = \infty$;
- Case 7: $\mu = 0.05, f = 0.9, \xi_d = 0.00$;
- Case 8: $\mu = 0.05, f = 0.9, \xi_d = 0.50$; and
- Case 9: $\mu = 0.05, f = 0.9, \xi_d = \infty$

Figure 7shows the effect of those parameters on the amplification factor due to harmonic excitation force. It is found that for the SDOF system without TMD, the amplification factor reaches infinity when the frequency of excitation force resonance with the frequency of SDOF system, $r = \Omega/\omega_1$. For the systems attached with a TMD with variety range of parameter, μ, ξ_d, f. The peak of amplification factor is much less than that of without TMD. In addition, when attached with TMD, the frequency ratio, $r = \Omega/\omega_1$, corresponding to the peaks deviate from $r = 1$. For damping ratio is $\xi_d = 0.00$, two peaks are observed, while for damping ratio is $\xi_d = 0.5$ and $\xi_d = \infty$, only one peak exists.

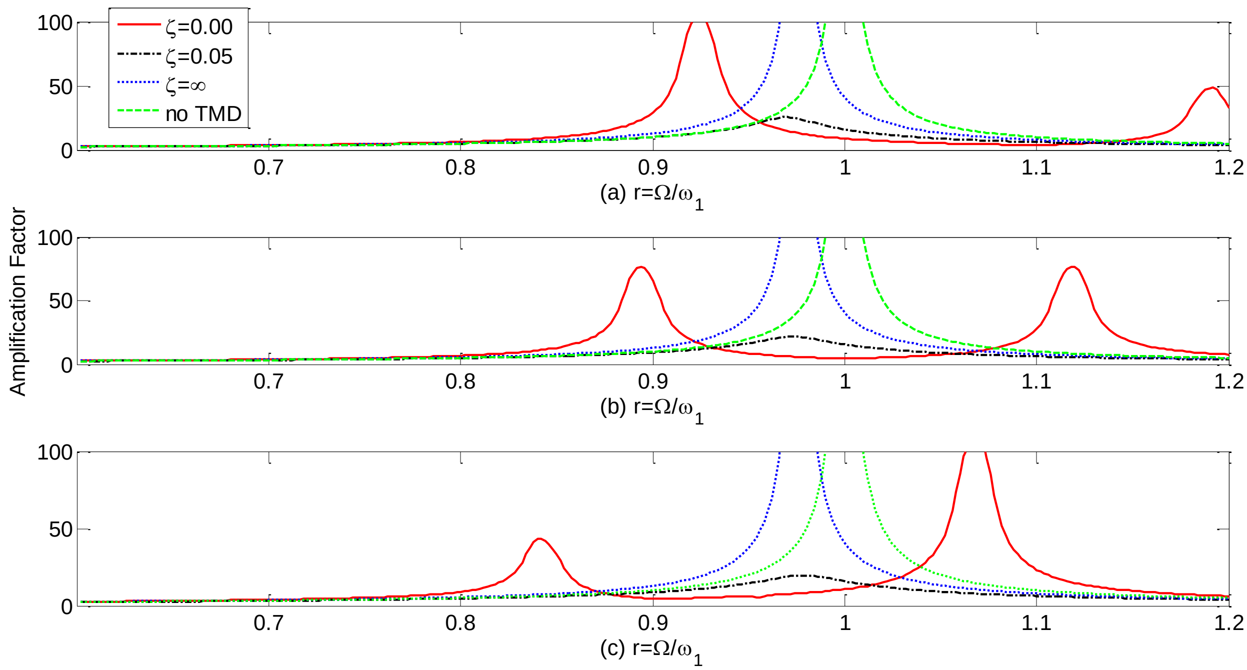

Figure 7: Effect of TMD on amplification factor subjected to harmonic excitation, (a) $f = 1.1$; (b) $f = 1.0$; (c) $f = 0.9$

Eqn. (16) and Eqn. (17) give the analytical equation of the amplification factor. A comparison between the numerical study and theoretical study in Figure 8 shows that the amplification for both numerical and theoretical studies are almost identical at peak. However, slight difference is observed when the frequency ratio, $r = \Omega/\omega_1$, deviate from where the peak amplification factor corresponds to.

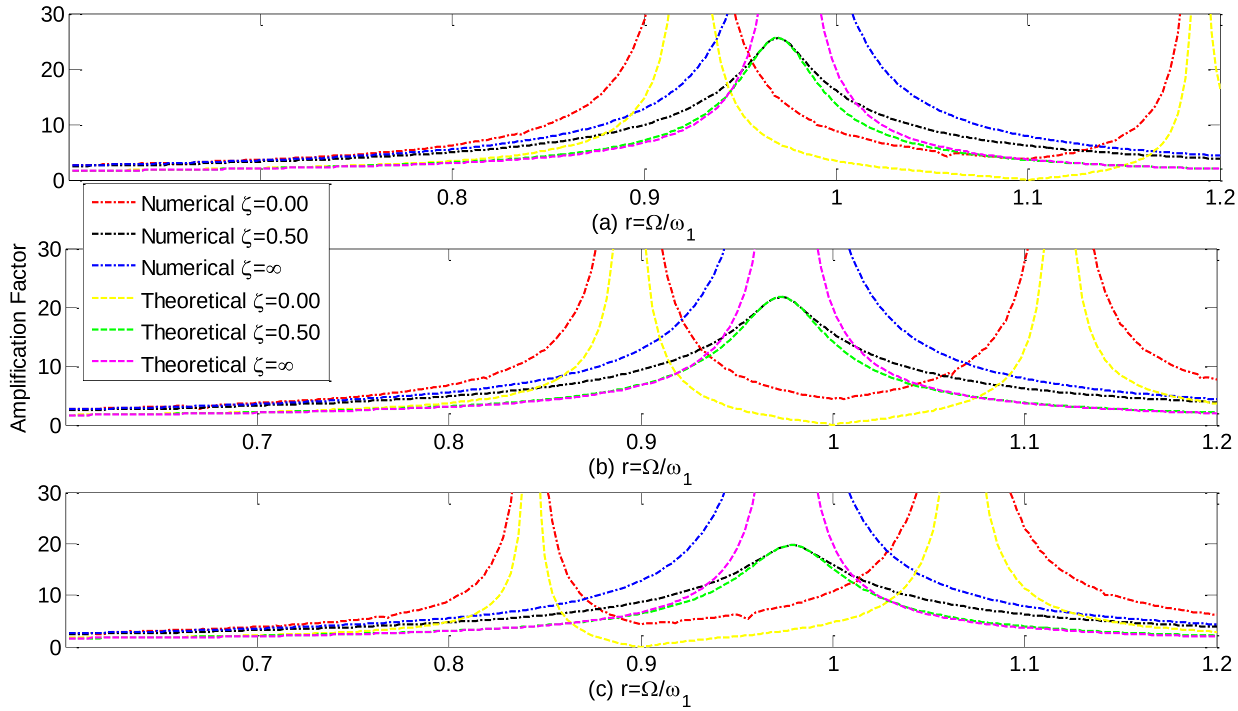

Figure 8: Comparison between numerical and theoretical study of amplification factor, (a) $f = 1.1$; (b) $f = 1.0$; (c) $f = 0.9$

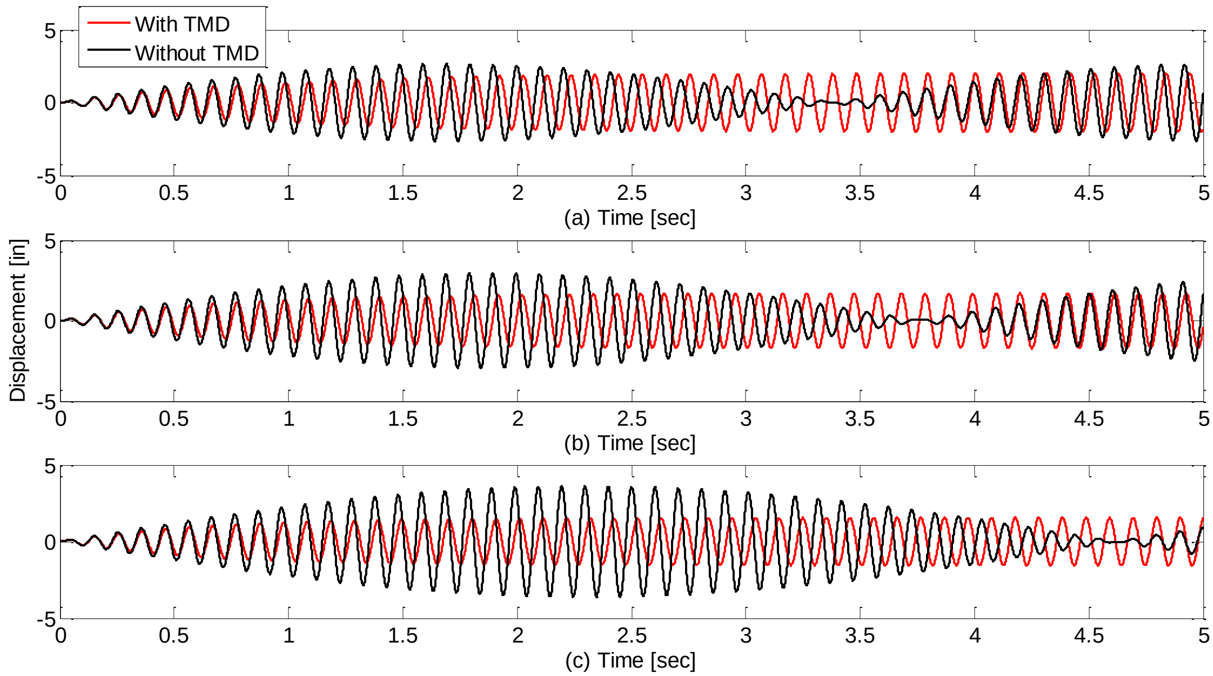

Figure 9: Effect of TMD on displacement of SDOF system in time domain, (a) $f = 1.1$; (b) $f = 1.0$; (c) $f = 0.9$

Figure 9 shows the comparison of displacement between the SDOF system with and without TMD for the following cases:

- Case 1: $f = \omega_d/\omega_1 = 1.1$; $r = 0.97$;
- Case 2: $f = \omega_d/\omega_1 = 1.0$; $r = 0.973$; and
- Case 3: $f = \omega_d/\omega_1 = 0.9$; $r = 0.978$.

Since the damping ratio of the primary system is $\xi_1 = 0.00$, the displacement response due to harmonic ground motion is also harmonic. However, when attached with a TMD, the amplitude of the displacement response decreases and a steady state response occurs. Comparing Figure 9(c) with Figure 9(a) and Figure 9(b) gives that the effect of TMD on displacement reduction increases with the decrease of frequency ratio, $f = \omega_d/\omega_1$.

2.3. Effect of TMD due to harmonic ground motion

The same system was also studied when subjected to harmonic ground motion. Define the harmonic ground motion as

$$\ddot{u}_g(t) = \ddot{u}_{g0}e^{i\Omega t}$$

Therefore, the dynamic load due to harmonic ground motion is obtained by the inertia force on the primary mass and the TMD. The displacement response of the system is affected by the following parameters: the frequency of harmonic ground motion to the frequency of the system, the damping ratio of the TMD, the frequency ratio of the TMD and the mass ratio of the TMD. Similar to what was done in section2.2, amplification factor is used to evaluate the effect of the TMD on the displacement. Here, to obtain the static displacement of the system due to the ground motion, an equivalent force, P_{eq}, obtained via taking the inertia force on the primary mass is introduced, which could be expressed as

$$P_{eq} = m_1\ddot{u}_{g0}$$

Take the same cases in section2.2 as

- Case 1: $\mu = 0.05, f = 1.1, \xi_d = 0.00$;
- Case 2: $\mu = 0.05, f = 1.1, \xi_d = 0.50$;
- Case 3: $\mu = 0.05, f = 1.1, \xi_d = \infty$;
- Case 4: $\mu = 0.05, f = 1.0, \xi_d = 0.00$;
- Case 5: $\mu = 0.05, f = 1.0, \xi_d = 0.50$;
- Case 6: $\mu = 0.05, f = 1.0, \xi_d = \infty$;
- Case 7: $\mu = 0.05, f = 0.9, \xi_d = 0.00$;
- Case 8: $\mu = 0.05, f = 0.9, \xi_d = 0.50$; and
- Case 9: $\mu = 0.05, f = 0.9, \xi_d = \infty$

Figure 10 shows the amplification factor due to harmonic ground motions. It is found that when subjected to harmonic ground motion, the TMD significantly mitigates amplification factor of the SDOF system. For the system without TMD, the amplification factor reached infinity at resonance frequency, $r = \Omega/\omega_1 = 1$.however, when attached with a TMD, the peak of amplification factor drops dramatically. In addition, the peak of amplification factor does not occur at the point of $r = \Omega/\omega_1 = 1$, but deviate from it. For the TMD with damping ratio $\xi_d = 0.5$ and $\xi_d = \infty$, only one peak of amplification factor exists, while for the TMD with $\xi_d = 0.00$, two peaks exist, one corresponds to the frequency ratio less than $r = \Omega/\omega_1 < 1.0$, and the other corresponds to $r = \Omega/\omega_1 > 1.0$.

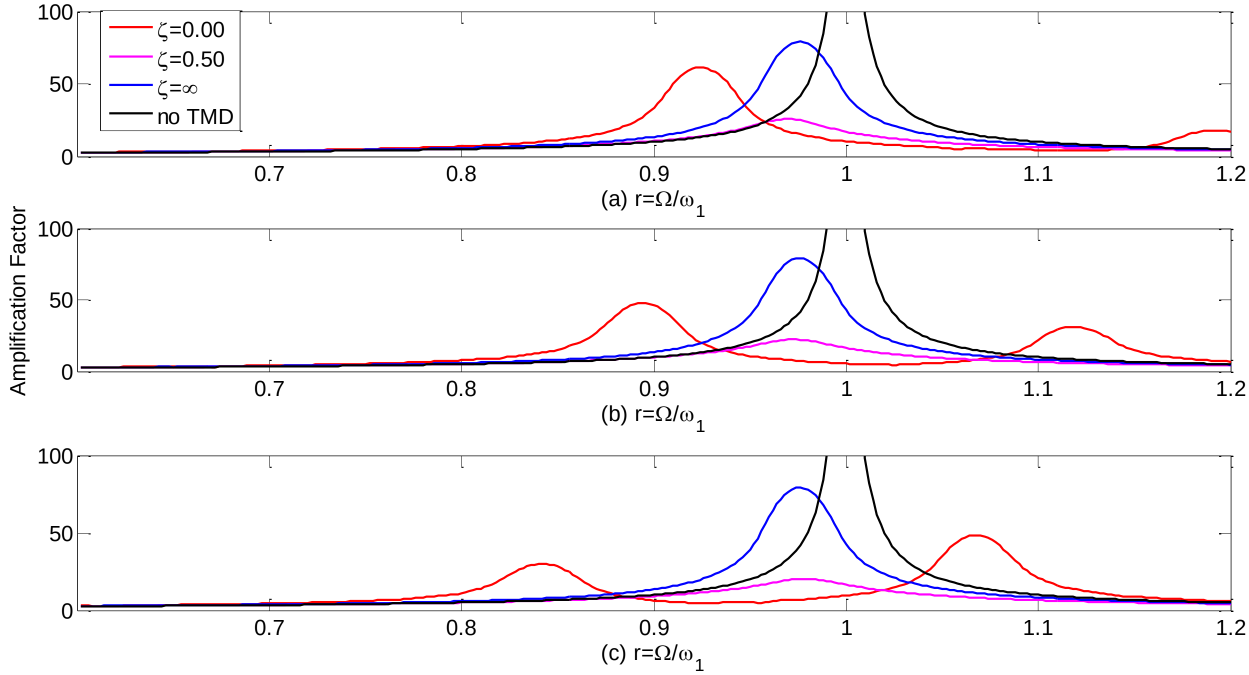

Figure 10: Effect of TMD on amplification factor subjected to harmonic ground motion, (a) $f = 1.1$; (b) $f = 1.0$; (c) $f = 0.9$

Figure 10 also shows that for those cases studied, the system with the TMD has damping ratio of $\xi_d = 0.50$ has the best effect of vibration mitigation at resonance frequency. When frequency ratio $f = \omega_d/\omega_1 = 1.1$, the resonance frequency ratio is $r = 0.97$; when $f = \omega_d/\omega_1 = 1.0$, the resonance frequency ratio is $r = 0.973$; and when $f = \omega_d/\omega_1 = 0.9$, the resonance frequency ratio is $r = 0.978$. The comparison of displacement response between the system with and without TMD is plotted in Figure 11.

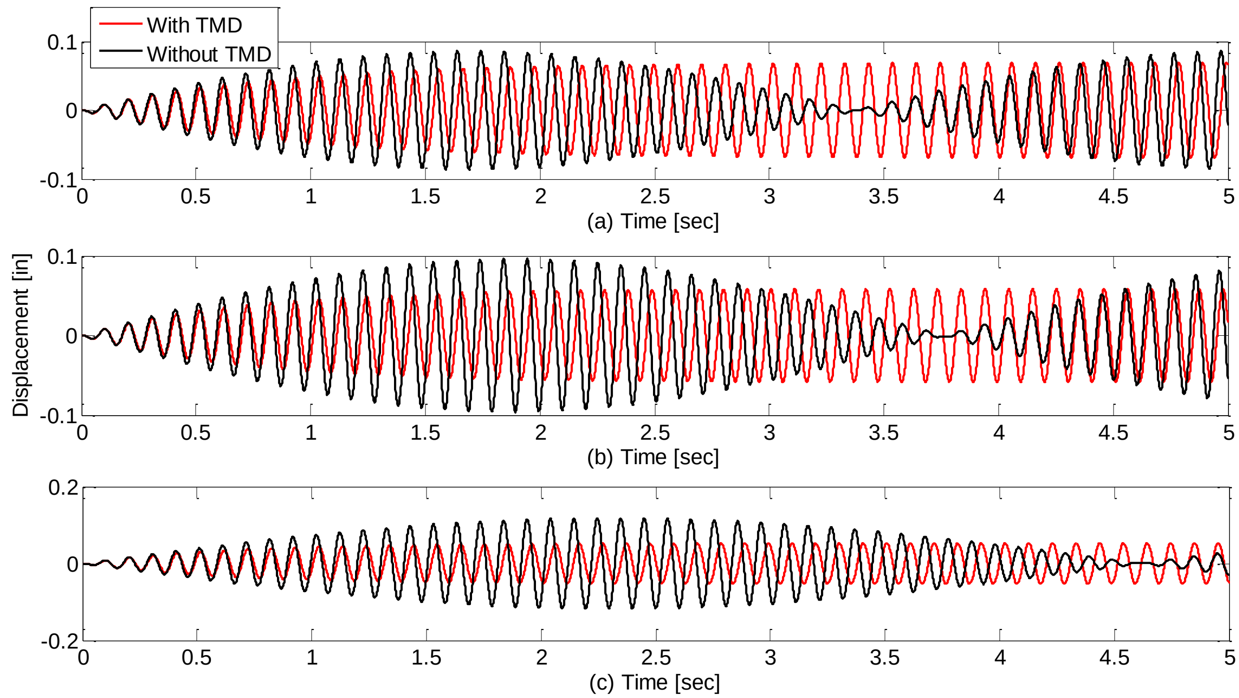

Figure 11: Effect of TMD on displacement of SDOF system in time domain, (a) $f = 1.1$; (b) $f = 1.0$; (c) $f = 0.9$

Similar with the displacement due to harmonic force excitation, the TMD reduced the displacement response due to the harmonic ground motion. The effect of TMD on displacement increase as the frequency ratio decreases.

3. Effect of TMD on MDOF system

A MDOF system attached with a TMD is shown in Figure 12

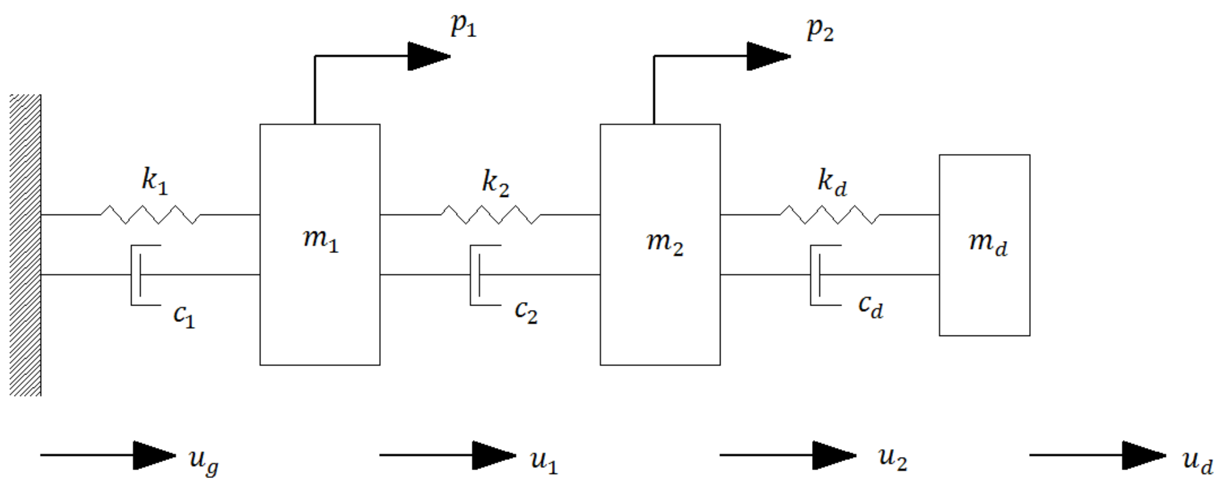

Figure 12: MDOF system with TMD

The equation of motion for the MDOF system could be expressed as

$$\begin{gathered} m_1\ddot{u}_1 + c_1\dot{u}_1 + k_1u_1 - k_2(u_2 - u_1) - c_2(\dot{u}_2 - \dot{u}_1) = p_1 - m_1\ddot{u}_g \\ m_2\ddot{u}_2 + c_2\dot{u}_2 + k_2u_2 - k_3(u_2 - u_3) - c_3(\dot{u}_2 - \dot{u}_3) = p_2 - m_2\ddot{u}_g \\ \vdots \\ m_n\ddot{u}_n - c_n\dot{u}_{n-1} + c_n\dot{u}_n - k_nu_{n-1} + k_nu_n - k_du_d - c_d\dot{u}_d = p_n - m_n\ddot{u}_g \\ m_d\ddot{u}_d + c_d\dot{u}_d + k_du_d = -m_d(\ddot{u}_n - \ddot{u}_g) \end{gathered} \tag{48}$$

which could be written in matrix form as

$$\begin{gathered} \boldsymbol{M}\ddot{u} + \boldsymbol{C}\dot{u} + \boldsymbol{K}u = \boldsymbol{P} - \boldsymbol{F} + \boldsymbol{K_d}u_d + \boldsymbol{C_d}\dot{u}_d \\ m_d\ddot{u}_d + c_d\dot{u}_d + k_du_d = -m_d\left(\ddot{u}_n - \ddot{u}_g\right) \end{gathered} \tag{49}$$

where

$$\boldsymbol{M} = \begin{bmatrix} m_1 & 0 & \cdots & 0 \\ 0 & m_2 & 0 & \vdots \\ \vdots & 0 & \ddots & \vdots \\ 0 & \cdots & \cdots & m_n \end{bmatrix};\ \boldsymbol{C} = \begin{bmatrix} c_1 + c_2 & -c_2 & \cdots & 0 \\ -c_2 & c_2 + c_3 & \cdots & \vdots \\ \vdots & \vdots & \ddots & \vdots \\ 0 & \cdots & \cdots & m_n \end{bmatrix};\ \boldsymbol{K} = \begin{bmatrix} k_1 + k_2 & -k_2 & \cdots & 0 \\ -k_2 & k_2 + k_3 & \cdots & \vdots \\ \vdots & \vdots & \ddots & \vdots \\ 0 & \cdots & \cdots & k_n \end{bmatrix}$$

$$\boldsymbol{P} = \begin{bmatrix} P_1 \\ P_2 \\ \vdots \\ P_n \end{bmatrix};\ \boldsymbol{F} = \begin{bmatrix} F_1 \\ F_2 \\ \vdots \\ F_n \end{bmatrix} = \boldsymbol{MI}\ddot{u}_g;\ \boldsymbol{K_d} = \begin{bmatrix} 0 \\ 0 \\ \vdots \\ k_d \end{bmatrix};\ \boldsymbol{C_d} = \begin{bmatrix} 0 \\ 0 \\ \vdots \\ c_d \end{bmatrix}$$

Similar with what was derivated for SDOF system with TMD, the Newmark-β method is also used to carry out the numerical calculation[32]. Substituting Eqn. (33) through Eqn. (36) into Eqn. (49)gives the following equations

$$[\boldsymbol{M} + \boldsymbol{C}\Delta\gamma + \boldsymbol{K}\Delta^2\beta]\ddot{u}_{i+1} + \left[\boldsymbol{C}\Delta(1-\gamma) + \boldsymbol{K}\Delta^2\left(\tfrac{1}{2} - \beta\right)\right]\ddot{u}_i + [\boldsymbol{C} + \boldsymbol{K}\Delta]\dot{u}_i + \boldsymbol{K}u_i$$
$$= \boldsymbol{P_{i+1}} - \boldsymbol{F_{i+1}} + [\boldsymbol{K_d}\Delta^{\boldsymbol{2}}\boldsymbol{\beta} + \boldsymbol{C_d}\Delta\boldsymbol{\gamma}]\boldsymbol{\ddot{u}_{d+1}} + \left[\boldsymbol{K_d}\Delta^{\boldsymbol{2}}\left(\tfrac{\boldsymbol{1}}{\boldsymbol{2}} - \boldsymbol{\beta}\right) + \boldsymbol{C_d}\Delta(\boldsymbol{1} - \boldsymbol{\gamma})\right]\boldsymbol{\ddot{u}_d} + [\boldsymbol{K_d}\Delta + \boldsymbol{C_d}]\boldsymbol{\dot{u}_d} + \boldsymbol{K_d}\boldsymbol{u_d}$$
$$[m_d + c_d\Delta\gamma + k_d\Delta^2\beta]\ddot{u}_{d+1} + \left[c_d\Delta(1-\gamma) + k_d\Delta^2\left(\tfrac{1}{2} - \beta\right)\right]\ddot{u}_d + [c_d + k_d\Delta]\dot{u}_d + k_d u_d$$
$$= -m_d(\ddot{u}_2)_{i+1} - m_d ug_{i+1}$$

(50)

let

$$\boldsymbol{H_1} = \boldsymbol{M} + \boldsymbol{C}\Delta\gamma + \boldsymbol{K}\Delta^2\beta;\ \boldsymbol{H_2} = \boldsymbol{C}\Delta(1-\gamma) + \boldsymbol{K}\Delta^2\left(\frac{1}{2} - \beta\right);\ \boldsymbol{H_3} = \boldsymbol{C} + \boldsymbol{K}\Delta;\ \ \boldsymbol{H_4} = \boldsymbol{K}$$
$$\boldsymbol{H_5} = \boldsymbol{K_d}\Delta^2\beta + \boldsymbol{C_d}\Delta\gamma;\ \boldsymbol{H_6} = \boldsymbol{K_d}\Delta^2\left(\frac{1}{2} - \beta\right) + \boldsymbol{C_d}\Delta(1-\gamma);\ \boldsymbol{H_7} = \boldsymbol{K_d}\Delta + \boldsymbol{C_d};\ \boldsymbol{H_8} = \boldsymbol{K_d}$$

and

$$B_1 = m_d + c_d\Delta\gamma + k_d\Delta^2\beta;\ B_2 = c_d\Delta(1-\gamma) + k_d\Delta^2\left(\frac{1}{2} - \beta\right);\ B_3 = c_d + k_d\Delta; B_4 = k_d;\ B_5 = -m_d$$

to simplify the expression, where

$$\boldsymbol{H_1}, \boldsymbol{H_2}, \boldsymbol{H_3}, \boldsymbol{H_4}, \boldsymbol{H_5}, \boldsymbol{H_6}, \boldsymbol{H_7}$$

are $n \times n$ matrixes. Similar with Eqn. (43) and Eqn. (44), Eqn. (50) could be written as

$$\boldsymbol{H_1}\ddot{u}_{i+1} - \boldsymbol{H_5}\ddot{u}_{d+1} = \boldsymbol{\widetilde{H}}$$
$$B_5(\ddot{u}_n)_{i+1} - B_1\ddot{u}_{d+1} = \tilde{B} \qquad \textbf{(51)}$$

in which

$$\boldsymbol{\widetilde{H}} = \boldsymbol{P_{i+1}} - \boldsymbol{F_{i+1}} + \boldsymbol{H_6}\ddot{u}_d + \boldsymbol{H_7}\dot{u}_i + \boldsymbol{H_8}u_d - \boldsymbol{H_2}\ddot{u}_i - \boldsymbol{H_3}\dot{u}_i - \boldsymbol{H_4}u_i$$

$$\tilde{B} = B_2\ddot{u}_d + B_3\dot{u}_d + B_4u_d + m_d ug_{i+1}$$

from the second equation of Eqn. (51), $\ddot{u}_{d+1}$ could be determined from Eqn. (51) as

$$\ddot{u}_{d+1} = \frac{B_5(\ddot{u}_n)_{i+1} - \tilde{B}}{B_1}$$

Substituting $\ddot{u}_{d+1}$ into Eqn. (51) gives

$$\boldsymbol{H_1}\ddot{u}_{i+1} - \boldsymbol{H_5}\left[\frac{B_5(\ddot{u}_n)_{i+1} - \tilde{B}}{B_1}\right] = \widetilde{\boldsymbol{H}} \qquad \textbf{(52)}$$

let

$$\boldsymbol{C_1} = \widetilde{\boldsymbol{H}} - \boldsymbol{H_5}\frac{\tilde{B}}{B_1};\ \ \boldsymbol{C_2} = \boldsymbol{H_5}\frac{B_5}{B_1}$$

Eqn. (52), therefore, could be expressed as

$$\boldsymbol{H_1}\ddot{u}_{i+1} - \boldsymbol{C_2}(\ddot{u}_n)_{i+1} = \boldsymbol{C_1} \qquad \textbf{(53)}$$

Writing Eqn. (53) in matrix form as

$$\begin{bmatrix} H_1^{11} & H_1^{12} & \cdots & H_1^{1n} \\ H_1^{21} & H_1^{22} & \cdots & H_1^{2n} \\ \vdots & \vdots & \ddots & \vdots \\ H_1^{n1} & H_1^{n2} & \cdots & H_1^{nn} \end{bmatrix} \begin{Bmatrix} \ddot{u}_1 \\ \ddot{u}_2 \\ \vdots \\ \ddot{u}_n \end{Bmatrix}_{i+1} + \begin{Bmatrix} C_2^1 \\ C_2^2 \\ \vdots \\ C_2^n \end{Bmatrix} (\ddot{u}_n)_{i+1} = \begin{Bmatrix} C_1^1 \\ C_1^2 \\ \vdots \\ C_1^n \end{Bmatrix}$$

Rearranging this equation

$$\begin{bmatrix} H_1^{11} & H_1^{12} & \cdots & H_1^{1n} - C_2^1 \\ H_1^{21} & H_1^{22} & \cdots & H_1^{2n} - C_2^2 \\ \vdots & \vdots & \ddots & \vdots \\ H_1^{n1} & H_1^{n2} & \cdots & H_1^{nn} - C_2^n \end{bmatrix} \begin{Bmatrix} \ddot{u}_1 \\ \ddot{u}_2 \\ \vdots \\ \ddot{u}_n \end{Bmatrix}_{i+1} = \begin{Bmatrix} C_1^1 \\ C_1^2 \\ \vdots \\ C_1^n \end{Bmatrix}$$

Therefore, the acceleration of the primary system and the TMD for the next time step are

$$\ddot{u}_{i+1} = \begin{Bmatrix} \ddot{u}_1 \\ \ddot{u}_2 \\ \vdots \\ \ddot{u}_n \end{Bmatrix}_{i+1} = \begin{bmatrix} H_1^{11} & H_1^{12} & \cdots & H_1^{1n} - C_2^1 \\ H_1^{21} & H_1^{22} & \cdots & H_1^{2n} - C_2^2 \\ \vdots & \vdots & \ddots & \vdots \\ H_1^{n1} & H_1^{n2} & \cdots & H_1^{nn} - C_2^n \end{bmatrix}^{-1} \begin{Bmatrix} C_1^1 \\ C_1^2 \\ \vdots \\ C_1^n \end{Bmatrix}$$

$$\ddot{u}_{d+1} = \frac{B_5(\ddot{u}_n)_{i+1} - \tilde{B}}{B_1}$$

The above derivation is performed for the MDOF system with a TMD placed at roof level. For other cases where the TMD is placed at other levels but roof level, Eqn. (48) could be written as the following form. Take the case where the TMD is placed at $(n-1)^{\text{th}}$ level, the equation of motion could be expressed as

$$
\begin{gathered}
m_1\ddot{u}_1 + c_1\dot{u}_1 + k_1u_1 - k_2(u_2 - u_1) - c_2(\dot{u}_2 - \dot{u}_1) = p_1 - m_1\ddot{u}_g \\
\vdots \\
m_{n-1}\ddot{u}_{n-1} - c_{n-1}\dot{u}_{n-2} + (c_{n-1} + c_n)\dot{u}_{n-1} - c_n\dot{u}_n - k_{n-1}u_{n-2} + (k_{n-1} + k_n)u_{n-1} - k_nu_n - k_du_d - c_d\dot{u}_d \\
= p_{n-1} - m_{n-1}\ddot{u}_g \\
m_n\ddot{u}_n - c_n\dot{u}_{n-1} + c_n\dot{u}_n - k_nu_{n-1} + k_nu_n = P_n - m_n\ddot{u}_g \\
m_d\ddot{u}_d + c_d\dot{u}_d + k_du_d = -m_d(\ddot{u}_n - \ddot{u}_g)
\end{gathered}
$$

(54)

In matrix form, the equation of motion could be written as

$$
\begin{gathered}
\boldsymbol{M}\ddot{u} + \boldsymbol{C}\dot{u} + \boldsymbol{K}u = \boldsymbol{P} - \boldsymbol{F} + \boldsymbol{K_d}u_d + \boldsymbol{C_d}\dot{u}_d \\
m_d\ddot{u}_d + c_d\dot{u}_d + k_du_d = -m_d\left(\ddot{u}_n - \ddot{u}_g\right)
\end{gathered}
$$

in which $\boldsymbol{K_d}$ and $\boldsymbol{C_d}$ are expressed as

$$
\boldsymbol{K_d} = \begin{bmatrix} 0 \\ \vdots \\ k_d \\ 0 \end{bmatrix}, \boldsymbol{C_d} = \begin{bmatrix} 0 \\ \vdots \\ c_d \\ 0 \end{bmatrix}
$$

The above derivation could be followed for other cases where the TMD is placed at any level and a Matlab code was developed to carry out the numerical integration. The Matlab code is shown in Appendix I.

The effect of the TMD on roof level displacement subjected to various dynamic loads are evaluated in the following section. Unlike what was performed for SDOF system, displacement response in time domain is performed for MDOF system t=with and without TMD. It is hard to find the theoretical solution of the amplification factor, therefore, numerical integration was carried out to obtain the displacement response.

3.1. Effect of TMD due to free vibration

Similar with what was defined for SDOF system, free vibration can be introduced via inputting an initial displacement. For a MDOF system, each degree of freedom can have an initial displacement. Therefore, different combination of initial displacement has different influence on the roof level displacement. In this study, following cases were carried out to evaluated the effect of TMD placed at roof level on the roof level displacement of a 4-DOF structure shown in Figure 13.

- Case 1: Inverted-triangular initial placement with roof displacement is 2ft, $f = 0.9$, $\xi_d = 0.05$;
- Case 2: Inverted-triangular initial placement with roof displacement is 2ft, $f = 1.0$, $\xi_d = 0.05$;
- Case 3: Inverted-triangular initial placement with roof displacement is 2ft, $f = 1.1$, $\xi_d = 0.05$;
- Case 4: Uniform initial displacement of 2ft, , $f = 0.9$, $\xi_d = 0.05$;
- Case 5: Uniform initial displacement of 2ft, , $f = 1.0$, $\xi_d = 0.05$; and
- Case 6: Uniform initial displacement of 2ft, , $f = 1.1$, $\xi_d = 0.05$;

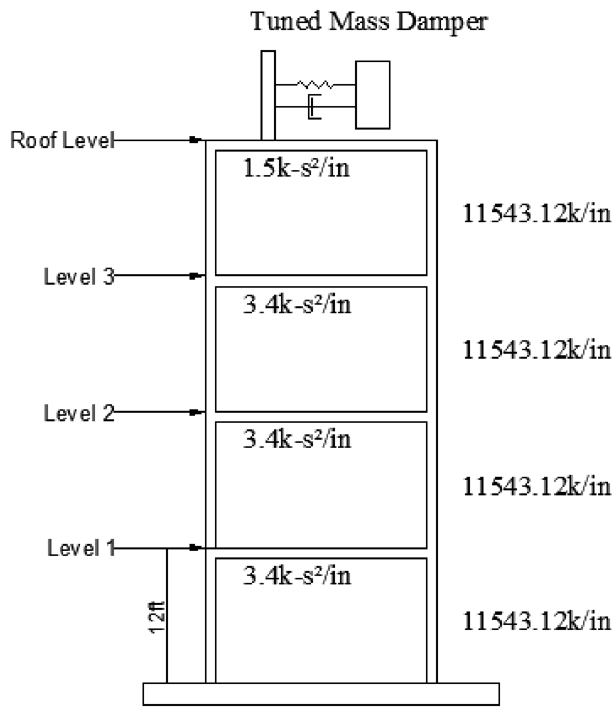

Figure 13: 4-DOF system with TMD

Figure 14 and Figure 15 show the effect of TMD on roof displacement with different initial displacement in time domain. Figure 14 shows the 4-DOF system with inverted-triangular initial displacement, and Figure 15 shows that the 4-DOF system with uniform initial displacement. Both figures show the TMD has a mass ratio is $\mu = 10\%$ and the primary system has damping ratio of $\xi_1 = \xi_2 = 0.02$. the figures show that different initial displacement has different effect impact on the roof displacement. When attached with a TMD, the displacement was reduced. Comparing each figures gives the result that the TMD with frequency ratio is $f = 0.9$ has better effect on mitigating the vibration displacement than the TMD has frequency ratio is $f = 1.0$ and $f = 1.1$.

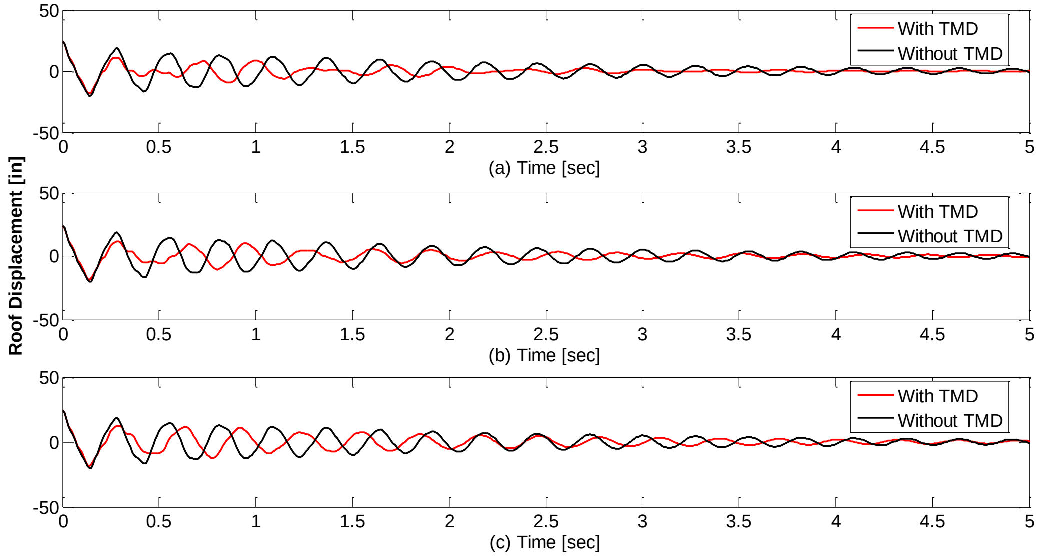

Figure 14: Effect of TMD on roof level displacement with inverted-triangular initial displacement, (a) case 1; (b) case 2; (c) case 3

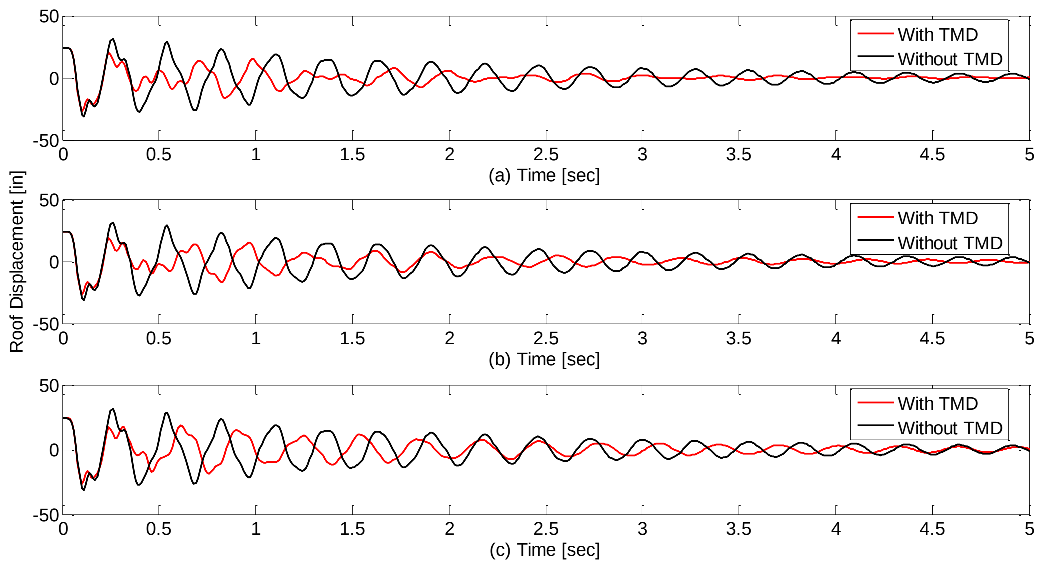

Figure 15: Effect of TMD on roof level displacement with uniform initial displacement, (a) case 4; (b) case 5; (c) case 6

3.2. Effect of TMD due to real ground motion

The same 4-DOF system in Figure 13 was also evaluated subjected to real ground motion. Particularly, El Centro ground motion was picked. Following cases were studied to evaluate the effect of the frequency ratio of the TMD on roof displacement subjected to El Centro ground motion.

- Case 1: $\mu = 0.10, f = 0.9, \xi_d = 0.05$;
- Case 2: $\mu = 0.10, f = 1.0, \xi_d = 0.05$; and
- Case 3: $\mu = 0.10, f = 1.1, \xi_d = 0.05$

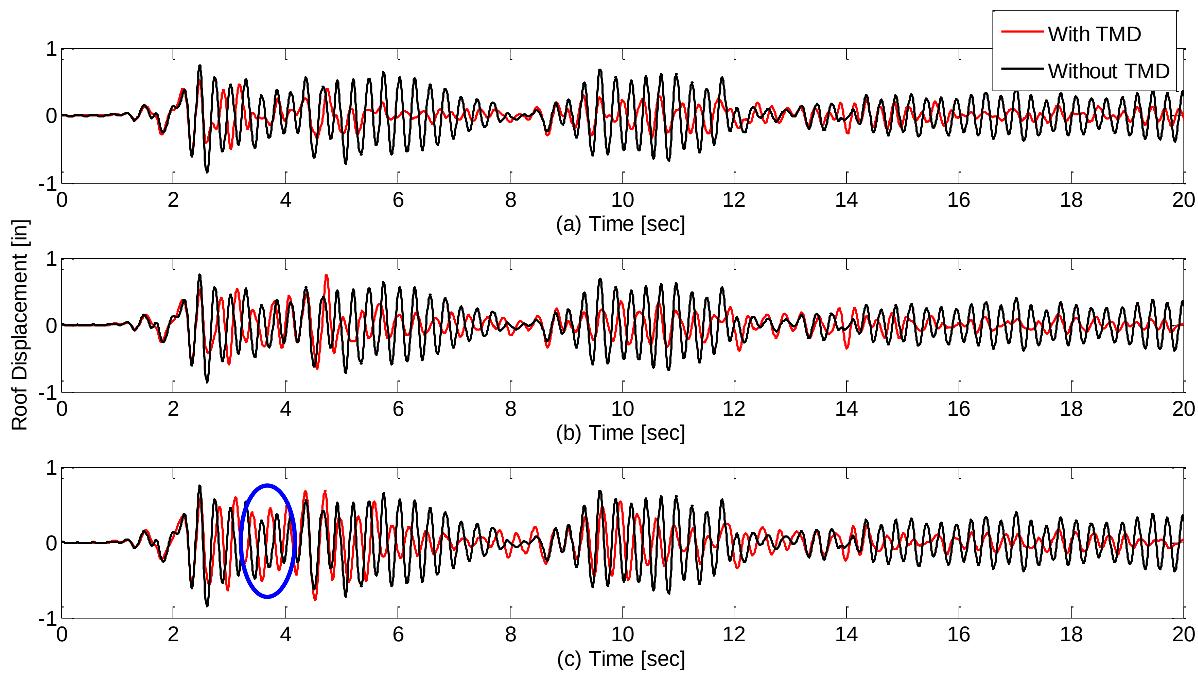

Figure 16: Effect of TMD on roof level displacement subjected to El Centro ground motion, (a) case 1; (b) case 2; (c) case 3

Figure 16 shows the roof displacement response of the 4-DOF system with and without TMD subjected to El Centro ground motion in time domain. It is obviously found that the frequency ratio affects the effect of the TMD on displacement reducing. Comparing Figure 16(a) to Figure 16(b) and Figure 16(c) gives the result that when frequency ratio is 0.9, the TMD has better effect on reducing the displacement response, while when frequency ratio is 1.1, the TMD even amplifies the displacement response between time from 3sec to 4sec.

The damping ratio of the TMD also affects the effect of reducing the displacement. To study it, frequency ratio is $f = 0.9$ was selected and a variety range of damping ratio was picked as shown in the following cases

- Case 1: $\mu = 0.10, f = 0.9, \xi_d = 0.005$;
- Case 2: $\mu = 0.10, f = 0.9, \xi_d = 0.05$;
- Case 3: $\mu = 0.10, f = 0.9, \xi_d = 0.20$; and
- Case 4: $\mu = 0.10, f = 0.9, \xi_d = 0.40$

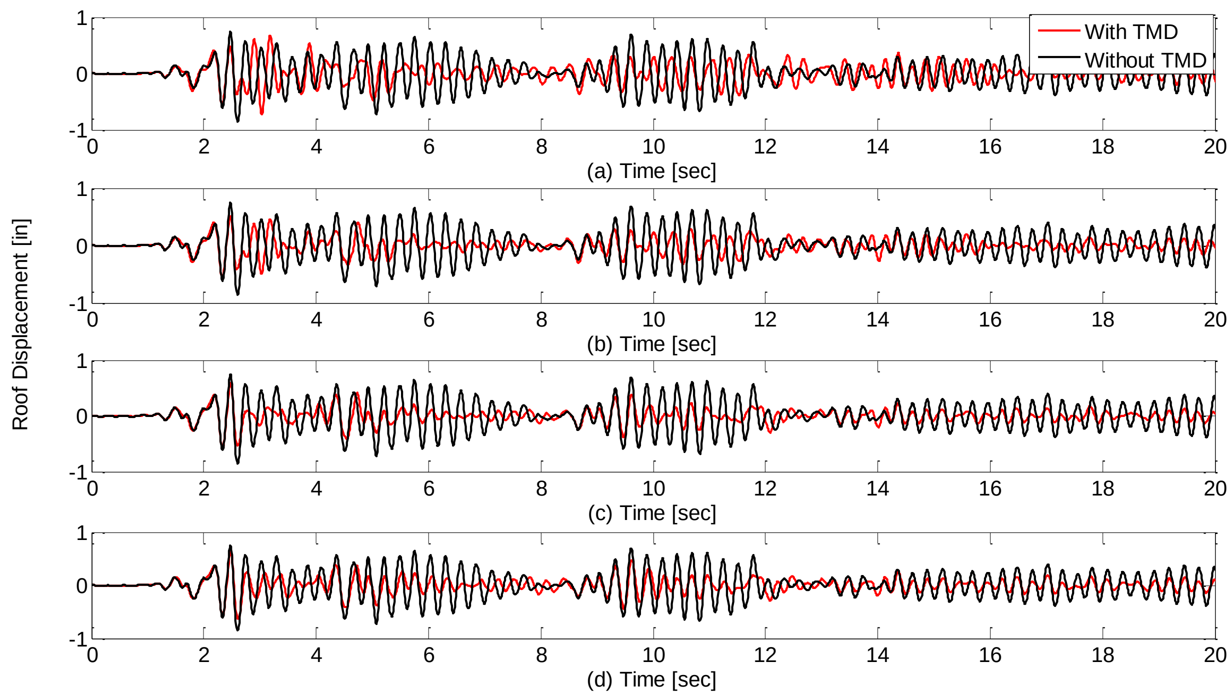

Figure 17: Effect of TMD on roof level displacement subjected to El Centro ground motion, (a) case 1; (b) case 2; (c) case 3; (d) case 4

Figure 17 shows the displacement response of the 4-DOF system subjected to El Centro ground motion with and without TMD at roof level. Although tuned to a preferable frequency ratio, different damping ratio impacts the effect of reducing the displacement response lot. Comparing Figure 17(c) to Figure 17(a), (b) and (d), it is observed that when the TMD has a damping ratio of 0.20, the effect of reducing the displacement response is better than other damping ratios. However, when the TMD has a damping ratio of 0.005, the TMD amplifies the displacement response between time from 2sec to 4sec.

The above studies show that the mass ratio, μ, frequency ratio, f, and damping ratio, ξ_d affects the effect of TMD on reducing the vibration response. Here, the mass ratio is defined as the ratio of the mass of the TMD, m_d, to the first mode mass of the primary structure[33], $\widetilde{M}_1$. Therefore, an optimally tuned TMD could be defined as a TMD has an optimal frequency ratio and optimal damping ratio. The effect of optimally tuned TMD on reducing the displacement and base shear are discussed in the following section.

Analysis Results and Discussion

1. Properties of the two MDOF systems

To evaluate the effect of the TMD on reducing the displacement response, the base shear and the story drift of a MDOF system, two MDOF buildings shown in Figure 18 were selected. The first building is a 4-story building, the typical story height is $12ft$. The other building is a 10-story building, also has a typical story height of $12ft$. The two buildings were particularly designed for this study via ETABS program. The buildings can resist the vertical load caused by the combination of dead load and live load. And they have the following parameters tabulated in Table 2 and Table 3.

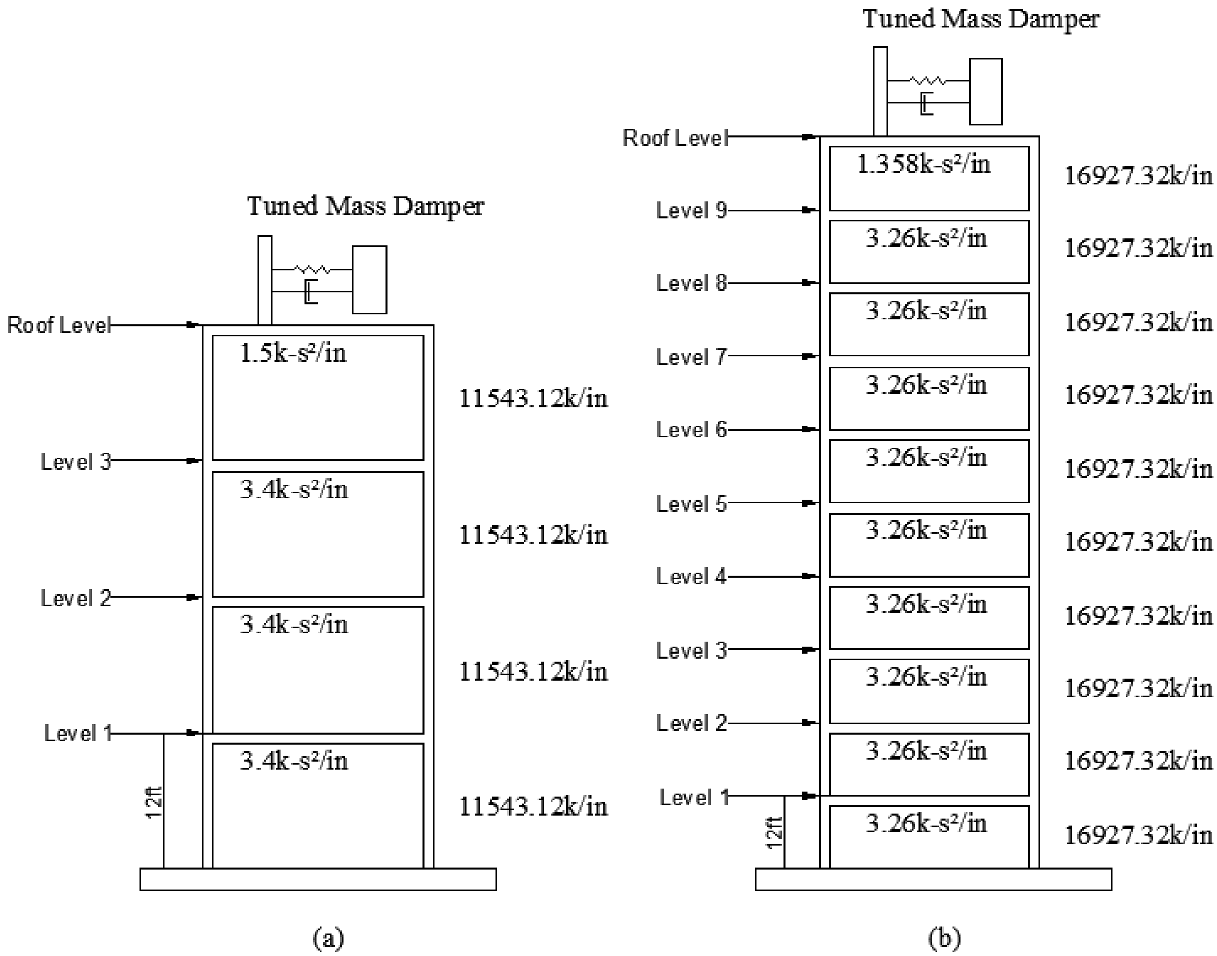

Figure 18: Two MODF buildings, (a) 4-story building; (b) 10-story building

Table 2: Properties of the 4-story building

Properties of Structure			
Natural Frequency (ω)	Natural Period(sec)	Orthogonal Modal Mass($k \cdot s^2/in$)	Effective Modal Mass($k \cdot s^2/in$)
23.0740	0.2723	6.6998	10.5773
65.7103	0.0956	6.6973	0.9316

98.3501	0.0639	6.6854	0.1806
116.3728	0.0540	4.5764	0.0105

Table 3: Properties of the 10-story building

Properties of Structure			
Natural Frequency (ω)	Natural Period (sec)	Orthogonal Modal Mass($k \cdot s^2/in$)	Effective Modal Mass($k \cdot s^2/in$)
11.4024	0.5510	16.1660	26.095
33.9264	0.1852	16.1827	2.8030
55.6148	0.1130	16.1441	0.9407
75.9333	0.0827	16.2305	0.4291
94.3810	0.0666	16.3985	0.2201
110.5028	0.0569	16.3819	0.1165
123.8993	0.0507	17.0646	0.0593
134.2325	0.0468	15.5327	0.0263
141.2054	0.0445	14.2848	0.0078
146.1564	0.0430	4.6929	0.0001

Table 2 shows a fundamental period of vibration of 0.272sec for mode 1 for the 4-story building. It also shows a modal mass for mode 1 equal to $6.6998k \cdot s^2/in$, and the effective mass for mode 1 is $10.57738k \cdot s^2/in$. Table 3 shows a fundamental period of 0.551sec for a 10-story building and a modal mass equal to $16.166k \cdot s^2/in$. Also, the effective mass for mode 1 is $26.095k \cdot s^2/in$. In addition, considering the effect of the structural damping, two structural damping, 0.02 and 0.05, were selected.

2. Effect of TMD on the response of the 4-story building

The 4-story building structure shown in Figure 18(a) was subjected to the El Centro ground motions. Two other ground motions, Lexington and Altadena were also evaluated for comparisons. As discussed previously, the mass ratio, μ, the frequency ratio, f, the damping ratio, ξ_d, and the location where the TMD is placed at affect the effect of the TMD on the response of the MDOF system. However, in practical way, engineers design the TMD via selecting its mass ratio. Therefore, in this study, the mass ratio of the TMD is defined as a predetermined parameter. The effect of the TMD on the displacement response, the base shear, and the story drift were evaluated with a variety range of mass ratio.

2.1. Optimal damping ratio and optimal frequency ratio

The effect of the frequency ratio, f, and the damping ratio, ξ_d, on the displacement response for a certain mass ratio, μ, was evaluated using the numerical integration method.

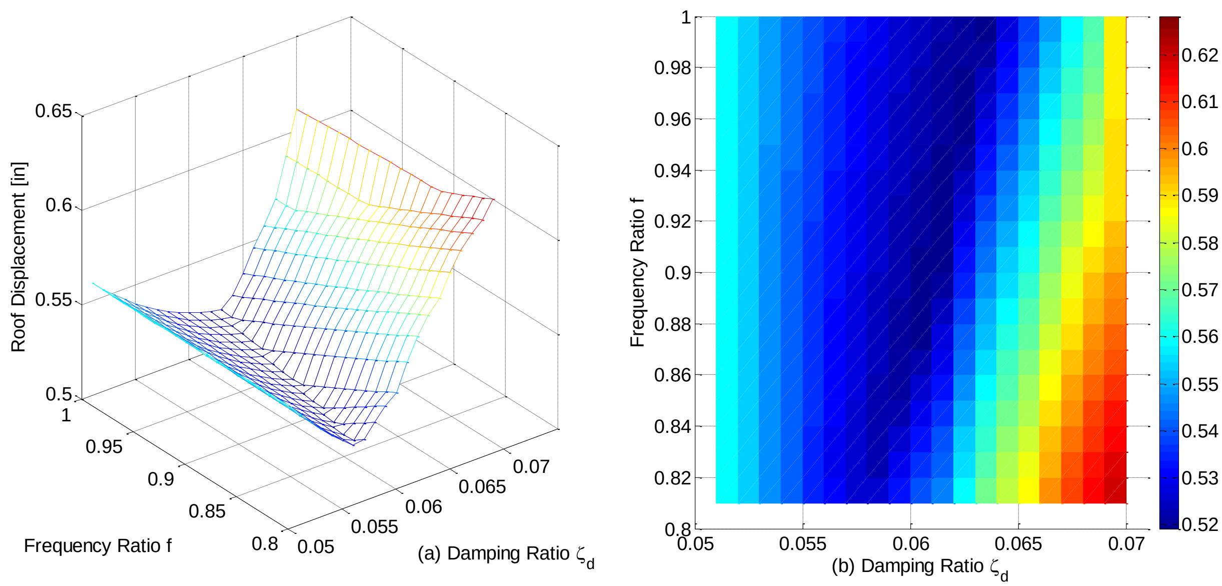

Figure 19: Effect of the frequency ratio and damping ratio on the displacement when mass ratio is 15% and TMD at 4th level, (a) 3-D view; (b) X-Y view

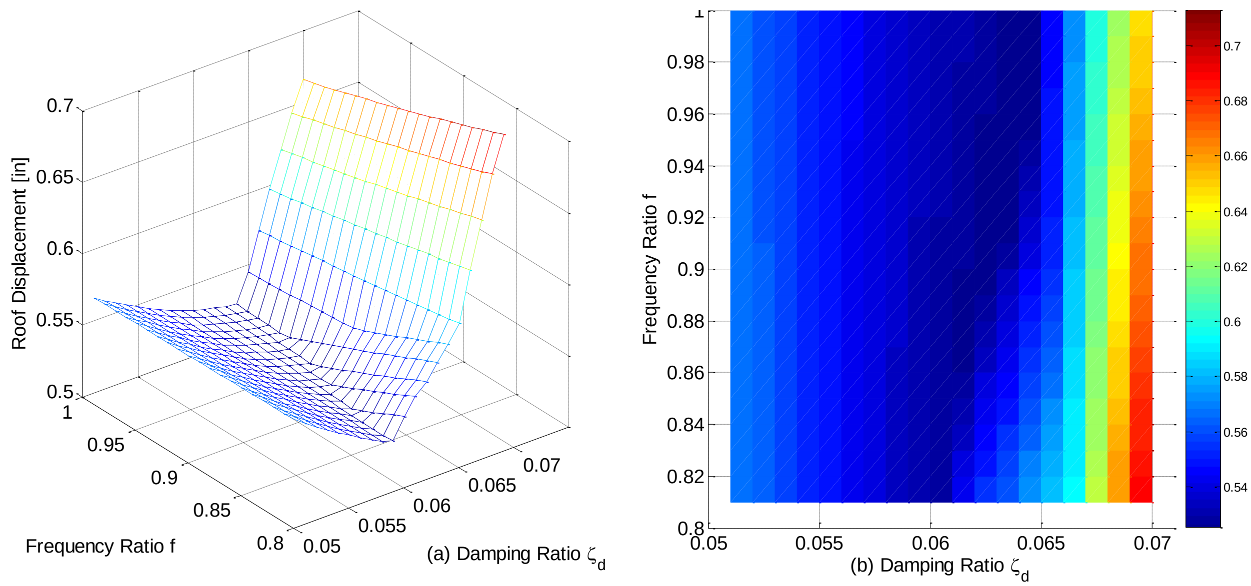

Figure 20: Effect of the frequency ratio and damping ratio on the displacement when mass ratio is 15% and TMD at 3rd level, (a) 3-D view; (b) X-Y view

Figure 19 shows the effect of the frequency ratio and the damping ratio on the roof displacement response when the mass ratio is 15% for the 4-story building subjected to the El Centro ground motion, and the TMD is placed at the roof level. Figure 20 shows the effect of the frequency ratio and the damping ratio on the roof displacement response when the mass ratio is 15% for the 4-story building subjected to the El Centro ground motion, and the TMD is placed at the 3rd level. It is observed from both figures that the effect of damping ratio, ξ_d, has a remarkable impact on the roof displacement, while the effect of the frequency ratio, f, is much less remarkable. Since for both cases, the similar trend are found for the effect of damping ratio and frequency ratio on the roof displacement, a similar procedure was followed to find the optimal damping ratio and optimal frequency ratio for variety range of mass ratio. Table 4 and Table 5 show the optimal damping ratio and optimal frequency ratio for the 4-story building structure subjected to El Centro ground motion with the TMD placed at various levels. With the increase of the mass ratio, the damping ratio increases from 0.00 to 0.45 for the building with structural damping is 0.02, in average, and to 0.6 for the building with structural damping is 0.05 in average. However, when the mass ratio increases, the frequency ratio decreases.

Table 4: Optimal damping ratio, ξ_d

Mass ratio, μ	Structural Damping Ratio is 0.02: TMD placed at 4th level	Structural Damping Ratio is 0.02: TMD placed at 3rd level	Structural Damping Ratio is 0.05: TMD placed at 4th level	Structural Damping Ratio is 0.05: TMD placed at 3rd level
0.01	0.0006	0.0001	0.0001	0.0001
0.02	0.0016	0.0001	0.0001	0.0001
0.03	0.014	0.014	0.0001	0.0001
0.04	0.02	0.0169	0.0026	0.0001
0.05	0.0326	0.0234	0.0206	0.0066
0.06	0.0422	0.0329	0.0237	0.0171
0.07	0.0452	0.0421	0.0292	0.025
0.08	0.0447	0.0502	0.0607	0.0301
0.09	0.0386	0.0602	0.0359	0.0501
0.1	0.0473	0.0802	0.0331	0.0711
0.11	0.0566	0.051	0.0384	0.0891
0.12	0.0609	0.0569	0.0388	0.0376
0.13	0.0657	0.055	0.0369	0.0396
0.14	0.0626	0.0589	0.0423	0.0421
0.15	0.0603	0.062	0.0655	0.0388
0.16	0.0712	0.0649	0.0956	0.0438
0.17	0.1069	0.0639	0.1025	0.0485
0.18	0.1164	0.0612	0.0878	0.0691
0.19	0.1311	0.0701	0.1159	0.086
0.2	0.1435	0.0986	0.15	0.0954
0.25	0.2001	0.1502	0.3517	0.1431
0.3	0.3741	0.2081	0.411	0.3425
0.35	0.408	0.3776	0.5893	0.381

0.4	0.567	0.355	0.7037	0.516

Table 5: Optimal frequency ratio, *f*

Mass ratio, μ	Structural Damping Ratio is 0.02		Structural Damping Ratio is 0.05	
	TMD placed at 4th level	TMD placed at 3rd level	TMD placed at 4th level	TMD placed at 3rd level
0.01	1.084	1.087	1.075	1.089
0.02	1.071	1.084	1.068	1.081
0.03	1.078	1.08	1.07	1.069
0.04	1.07	1.059	1.063	1.068
0.05	1.071	1.059	1.05	1.047
0.06	0.983	1.069	1.049	1.048
0.07	0.957	1.071	1.047	1.044
0.08	0.945	0.991	1.043	1.053
0.09	0.94	0.965	0.934	1.053
0.1	0.941	0.974	0.932	1.055
0.11	0.943	0.94	0.932	1.03
0.12	0.94	0.94	0.92	0.93
0.13	0.94	0.936	0.91	0.93
0.14	0.919	0.933	0.912	0.928
0.15	0.91	0.931	0.91	0.912
0.16	0.938	0.931	0.925	0.924
0.17	0.925	0.92	0.892	0.919
0.18	0.89	0.91	0.85	0.908
0.19	0.892	0.938	0.873	0.904
0.2	0.89	0.93	0.9	0.89
0.25	0.895	0.889	0.5	0.889

0.3	0.5	0.889	0.458	0.5
0.35	0.47	0.5	0.371	0.474
0.4	0.398	0.497	0.3	0.404

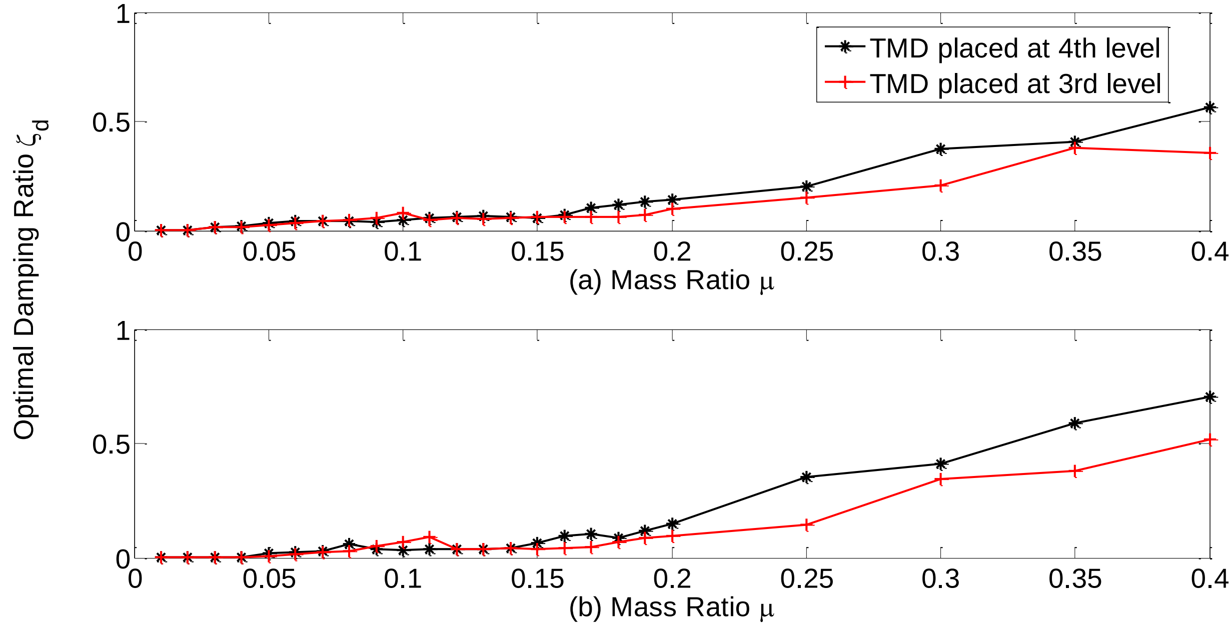

Figure 21: Optimal damping ratio, (a) structural damping ratio is 0.02; (b) structural damping ratio is 0.05

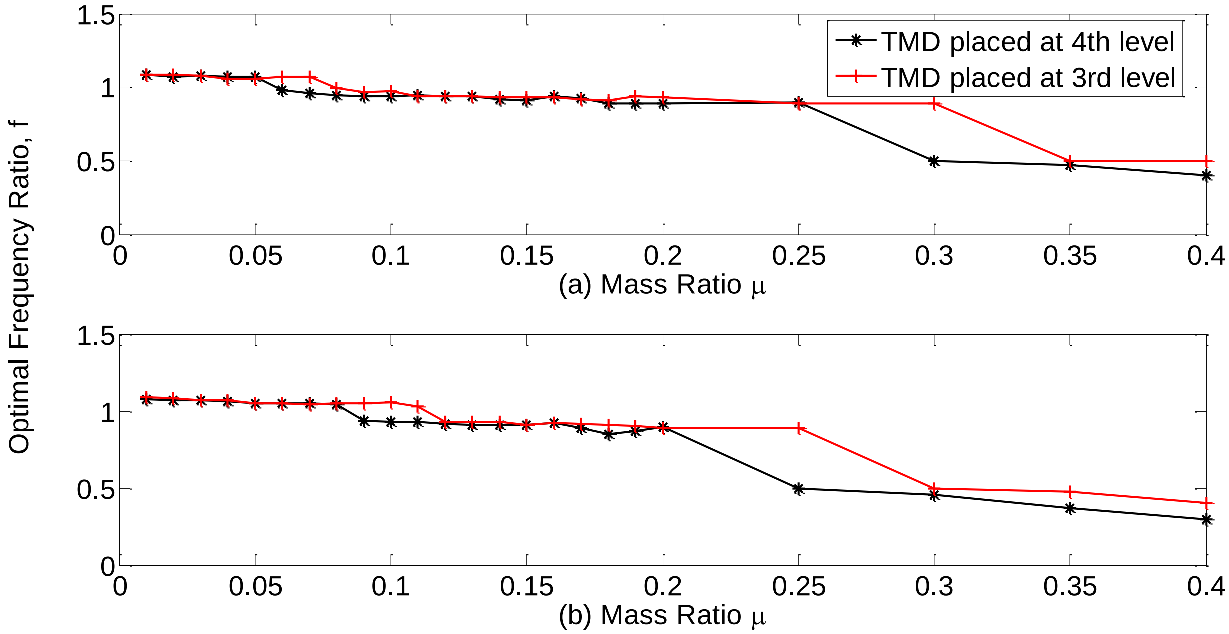

Figure 22: Optimal frequency ratio, (a) structural damping ratio is 0.02; (b) structural damping ratio is 0.05

Figure 21 and Figure 22 show the effect of damping ratio and frequency ratio on the roof displacement. Similar trend is observed for both the damping ratio, ξ_d, and the frequency ratio, f. For a certain mass ratio, the optimal damping ratio for the TMD placed at 4th level is higher than that when the TMD is placed at 3rd level. While for frequency ratio, the frequency ratio for the 4-story building with the TMD placed at 4th level is lower than that when the TMD is placed at 3rd level.

2.2. Effect of the TMD on displacement response

To evaluate the effect of TMD, a single TMD was placed at the roof level and the 3rd level respectively. In order to evaluate the effect of the TMD with the mass ratio, a variety range of mass ratio from $\mu = 0.01$ to $\mu = 0.40$ were studied. As defined previously, the mass ratio of the TMD is $\mu = m_d/\widetilde{M}_1$, therefore, when the mass ratio is 0.01, the mass of the TMD is $m_d = 0.07k \cdot s^2/in$, and when the mass ratio is 0.40, the mass of the TMD is $m_d = 2.68k \cdot s^2/in$, which in practical is a large additional mass. The effect of the optimally tuned TMD with the optimal damping ratio and the optimal frequency ratio discussed in section422.1 were evaluated. To evaluate the effect of the TMD on reducing the roof displacement response, displacement reduction is introduced defined as the ratio of the displacement response with TMD to the displacement response without TMD.

Table 6 shows the displacement reduction of the 4-story building structure with the optimally tuned TMD. When the mass ratio of the TMD is 1%, the displacement when the TMD is placed at 4^{th} level of the building with structural damping 0.02 is 88.7% of the original displacement, when the TMD is placed at 3^{rd} level, the displacement is 89.84% of the original. For the structural damping is 0.05, the roof displacement when the TMD is placed at 4^{th} level is 89.67% of the original, and when the TMD is placed at the 3^{rd} level, the displacement is 90.78% of the original displacement. With the increase of the mass ratio, the roof displacement decreases. For example, when the mass ratio is increased to 10%, the displacement for the 4-story building with structural damping is 0.02 are 64.26% and 64.82% of the original displacement for the TMD placed at 4^{th} level and 3^{rd} level, respectively. And when the mass ratio is increased to 20%, the displacement for the 4-story building with structural damping is 0.02 are 62.16% and 59.81% of the original displacement for the TMD placed at 4^{th} level and 3^{rd} level, respectively.

The roof displacement reduction is shown in Figure 23. It is observed that when the TMD was placed at the roof level, the roof displacement was lower than that when the TMD was placed at 3^{rd} level. An opposite trend is observed when mass ratio is between $\mu = 0.15$ and $\mu = 0.25$.

Table 6: Roof displacement reduction

	Structural Damping Ratio is 0.02		Structural Damping Ratio is 0.05	
Mass ratio,	TMD placed at 4^{th}	TMD placed at 3^{rd}	TMD placed at 4^{th}	TMD placed at 3^{rd}

μ	level	level	level	level
0.01	0.887	0.8984	0.8967	0.9078
0.02	0.7973	0.8098	0.8067	0.823
0.03	0.7516	0.753	0.7495	0.7557
0.04	0.7105	0.723	0.7263	0.7263
0.05	0.6918	0.6897	0.7281	0.7151
0.06	0.6965	0.6797	0.713	0.7087
0.07	0.6757	0.6754	0.7085	0.7006
0.08	0.6648	0.6675	0.7221	0.6973
0.09	0.6532	0.6555	0.7261	0.7063
0.1	0.6426	0.6482	0.7141	0.7135
0.11	0.6341	0.6424	0.705	0.7175
0.12	0.6263	0.6334	0.6968	0.7024
0.13	0.6193	0.6242	0.6876	0.6934
0.14	0.6121	0.6172	0.6812	0.6857
0.15	0.604	0.6104	0.6879	0.6782
0.16	0.6041	0.6039	0.6977	0.6706
0.17	0.6137	0.5975	0.6995	0.6668
0.18	0.6177	0.5904	0.6999	0.6747
0.19	0.6196	0.5906	0.7026	0.6795
0.2	0.6216	0.5981	0.7111	0.6819
0.25	0.6366	0.6074	0.6823	0.6897
0.3	0.6024	0.618	0.67	0.6741
0.35	0.588	0.5955	0.6528	0.6544
0.4	0.5722	0.5762	0.6451	0.6406

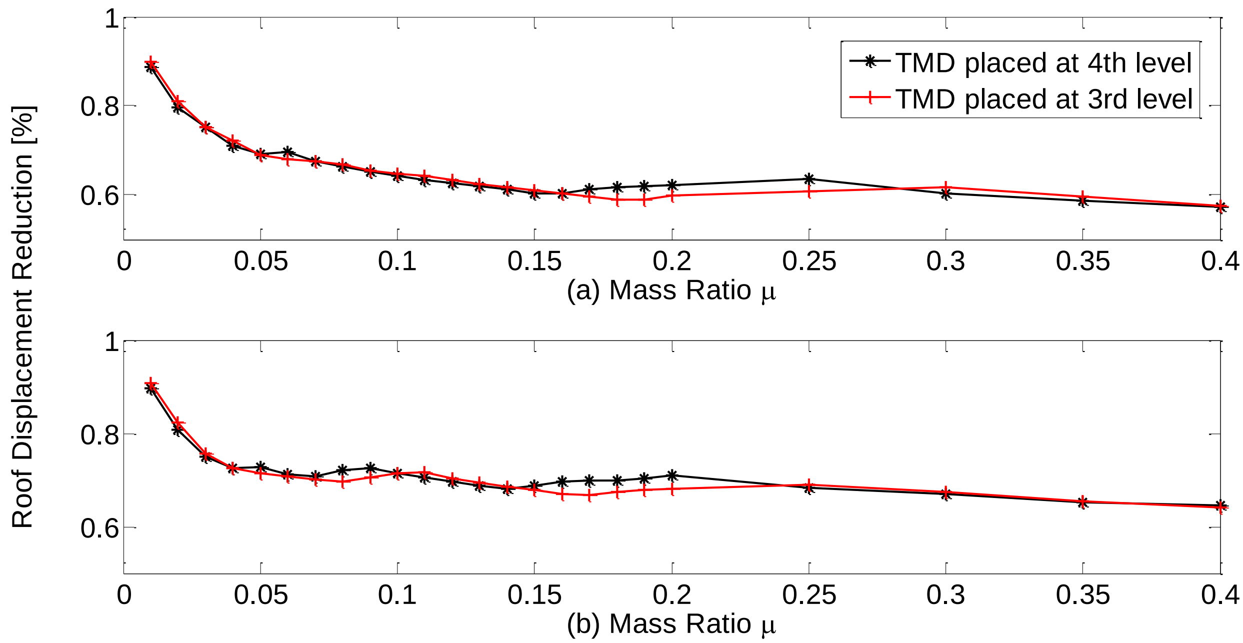

Figure 23: Roof displacement reduction

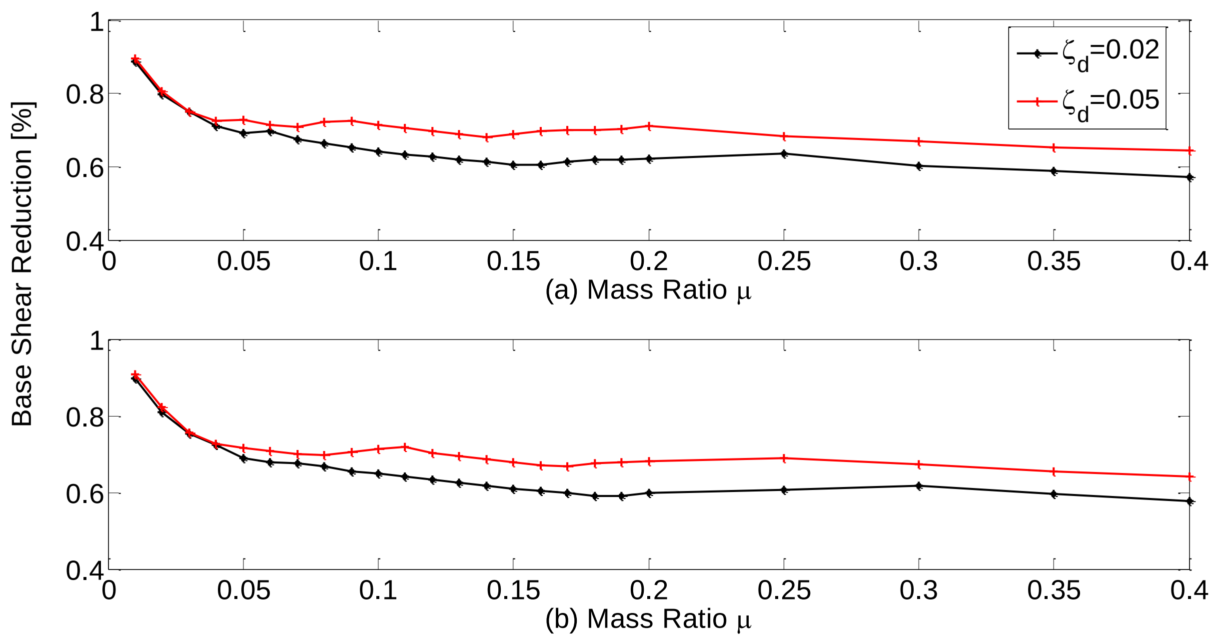

Figure 24: Roof displacement reduction

The effect of the damping ratio of the primary structure on the roof displacement reduction is also shown from Figure 24. It is observed that for a value of $\mu = 15\%$, the reduction in roof displacement for $\xi = 0.05$ and $\xi = 0.02$ is 68.79% and 60.4%, respectively. For $\mu = 25\%$, the reduction in roof displacement are 68.23% and 63.66%, respectively. It also shows that the effect of the TMD with higher structural damping ratio is less remarkable. However, the absolute displacement was still lower for the higher damping ratio. For example, for $\xi = 0.02$, the roof displacement was 0.8575in, whole it decreases to 0.7014in for $\xi = 0.05$ as expected. With a TMD and mass ratio is $\mu = 15\%$, the roof displacement for $\xi = 0.02$ was 0.5179in, while the roof displacement for $\xi = 0.05$ was 0.4825in.

2.3. Effect of the TMD on story drift

The story drift is defined as

$$\Delta_i = \frac{u_i - u_{i-1}}{H_i}$$

in which

u_i, u_{i-1} −displacement of level i and level $i - 1$

H_i −story height of level i

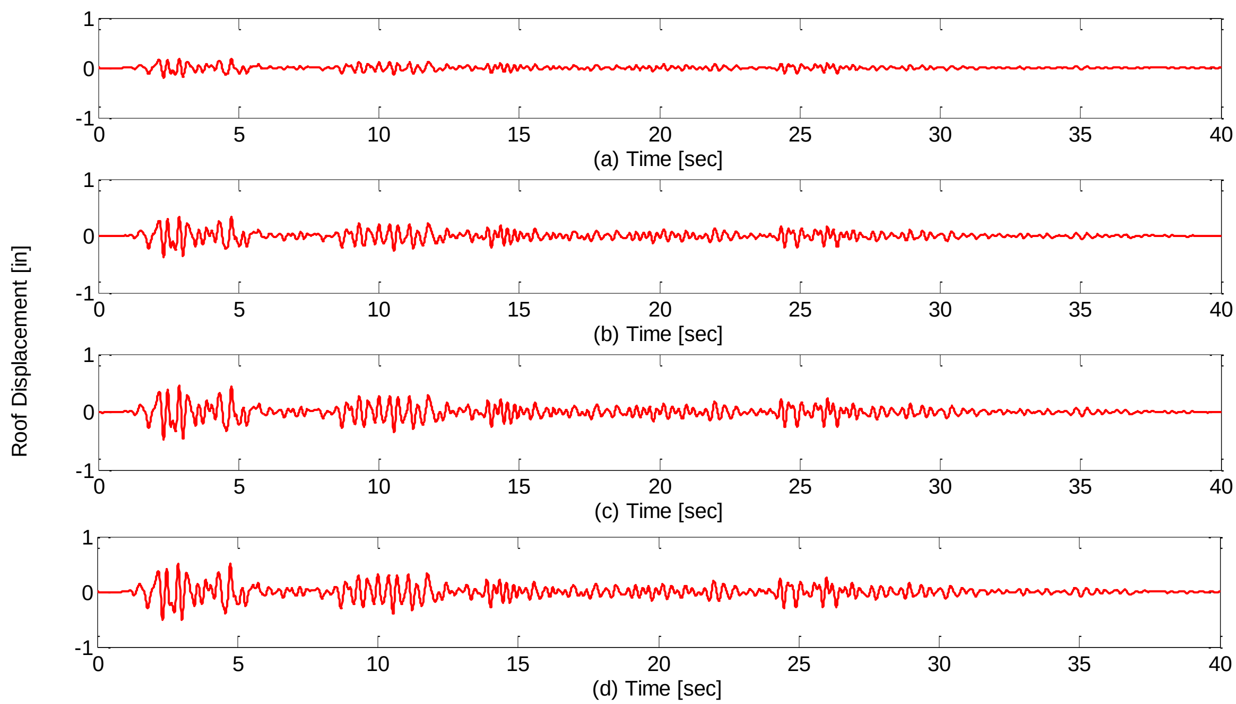

Figure 25: Displacement response with TMD placed at 4th level, (a) 1st level; (b) 2nd level; (c) 3rd level; (d) 4th level

Figure 25 shows the displacement of the 4-story building with the TMD placed at 4th level subjected to the El Centro ground motion. The displacement of 1st level to 4th level are shown from Figure 25(a) to (d), respectively. The mass ratio is 15%, specifically. The maximum displacement for each level are: 0.1816in for level 1; 0.3392in for level 2; 0.4564in for level 3; and 0.5109in for level 4. It is found that although the maximum displacement increases as the level moves up, the story drift, 0.14% for level 1; 0.117% for level 2; 0.074% for level 3; and 0.029% for level 4 drops down significantly.

Table 7: Story drift when TMD placed at 4th level with structural damping 0.02

Mass ratio, μ	Story drift, Δ_1	Story drift, Δ_2	Story drift, Δ_3	Story drift, Δ_4
0.01	0.002118	0.001735	0.001081	0.000349
0.05	0.001664	0.001306	0.000814	0.000336
0.10	0.001499	0.00125	0.000794	0.000292
0.15	0.0014	0.001165	0.000743	0.000289
0.20	0.001415	0.001182	0.000772	0.000333
0.25	0.001423	0.00119	0.000781	0.000397
0.30	0.00146	0.00119	0.000734	0.000203
0.35	0.001415	0.001147	0.000719	0.000221
0.40	0.001356	0.00111	0.000688	0.000253

Table 8: Story drift when TMD placed at 3rd level with structural damping 0.02

Mass ratio, μ	Story drift, Δ_1	Story drift, Δ_2	Story drift, Δ_3	Story drift, Δ_4
0.01	0.002158	0.001769	0.001104	0.000319
0.05	0.001679	0.001344	0.000868	0.000215
0.10	0.001537	0.001269	0.000836	0.000218
0.15	0.001435	0.001208	0.000789	0.000203

0.20	0.001417	0.001181	0.000791	0.000173
0.25	0.001442	0.001207	0.000801	0.000166
0.30	0.001473	0.001243	0.000824	0.00014
0.35	0.001453	0.001195	0.000726	0.000172
0.40	0.001408	0.001155	0.000714	0.000155

Table 9: Story drift when TMD placed at 4th level with structural damping 0.05

Mass ratio, μ	Story drift, Δ_1	Story drift, Δ_2	Story drift, Δ_3	Story drift, Δ_4
0.01	0.001756	0.001431	0.000902	0.000279
0.05	0.001381	0.001132	0.000738	0.000296
0.10	0.001372	0.001129	0.000715	0.000262
0.15	0.001305	0.001077	0.000691	0.000278
0.20	0.001318	0.001097	0.000724	0.000325
0.25	0.001335	0.001118	0.000675	0.000195
0.30	0.001297	0.001081	0.000666	0.00022
0.35	0.001265	0.00104	0.000642	0.000233
0.40	0.001251	0.001028	0.000635	0.000228

Table 10: Story drift when TMD placed at 3rd level with structural damping 0.05

Mass ratio, μ	Story drift, Δ_1	Story drift, Δ_2	Story drift, Δ_3	Story drift, Δ_4
0.01	0.00179	0.00146	0.000905	0.000267
0.05	0.001415	0.001122	0.000743	0.000203
0.10	0.001471	0.001109	0.000721	0.000175
0.15	0.001319	0.001093	0.000706	0.000185
0.20	0.001319	0.0011	0.000735	0.000167
0.25	0.001337	0.001119	0.00074	0.000163

0.30	0.001337	0.001092	0.000666	0.000188
0.35	0.001297	0.001059	0.000683	0.000148
0.40	0.001278	0.001044	0.000653	0.000144

Table 7, Table 8, Table 9 and Table 10 show the story drift of the 4-story building structure with the TMD placed at 4th level and 3rd level, respectively.

Figure 26 shows the effect of mass ratio on the story drift subjected to the El Centro ground motion. The same trend is observed that the story drift decreases with the increase of mass ratio. The effect of TMD for different mass ratio at various levels on story drift is given in Figure 27. It is observed that the story drift below the level where TMD was placed are similar. However, the TMD reduces the story drift above that level significantly. For example, for the 4-story building with structural damping is 0.02. When the mass ratio is 15%, the story drift Δ_3 is 0.0789% for the TMD placed at 3rd level, which is higher than that when the TMD is placed at 4th level, $\Delta_4 = 0.0743\%$. However, the roof level story drift for the TMD placed at 3rd level is $\Delta_4 = 0.0203\%$, which is lower than that when the TMD is placed at 4th level, $\Delta_4 = 0.0289\%$.

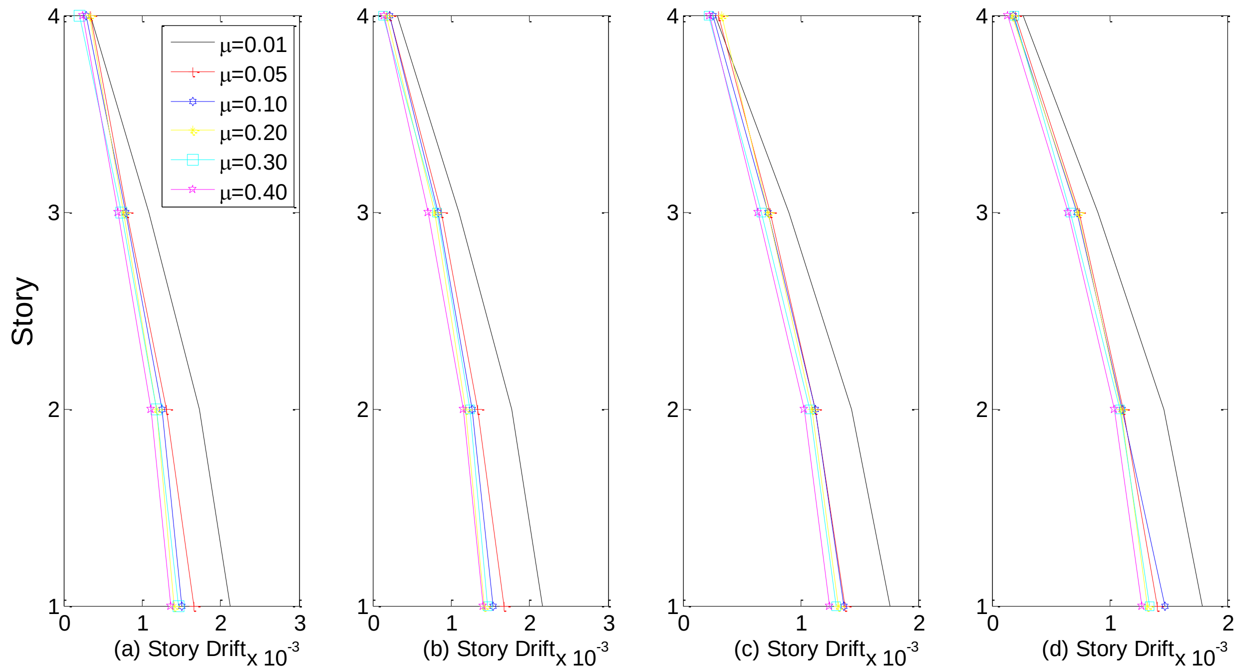

Figure 26: Effect of mass ratio on story drift, (a) TMD placed at 4th level and $\xi = 0.02$; (b) TMD placed at 3rd level and $\xi = 0.02$; (c) TMD placed at 4th level and $\xi = 0.05$; (d) TMD placed at 3rd level and $\xi = 0.05$

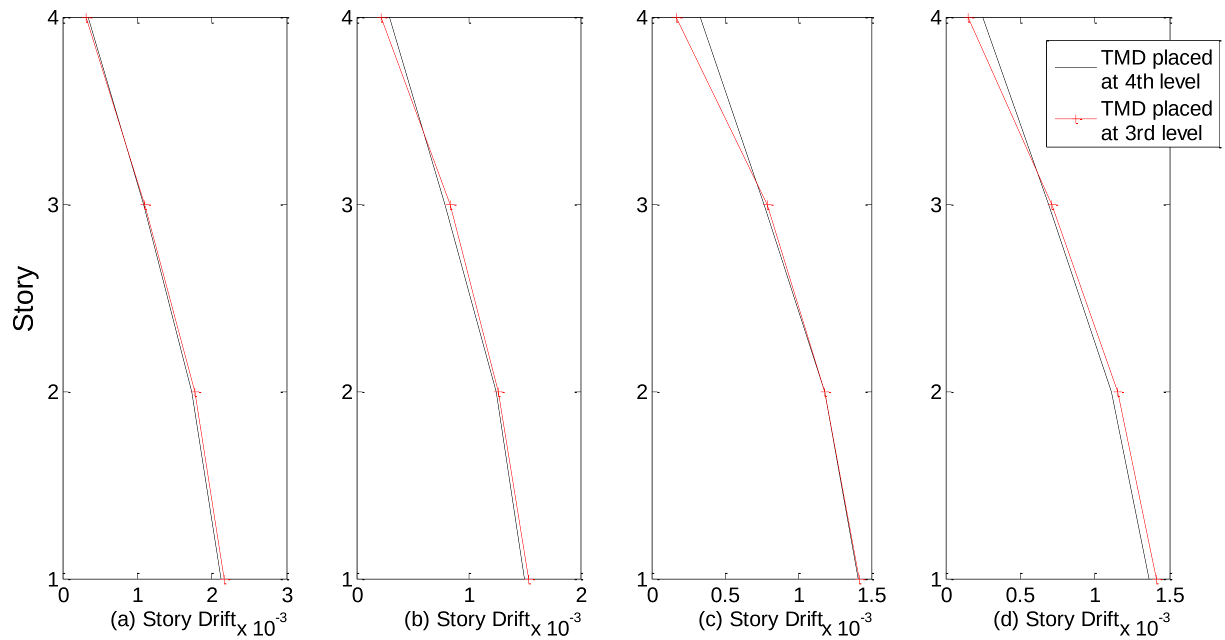

Figure 27: Effect of TMD at various levels on story drift, (a) mass ratio is 0.01; (b) mass ratio is 0.10; (c) mass ratio is 0.20; (d) mass ratio is 0.40

2.4. Effect of TMD on the base shear

The base shear of a building structure subjected to ground motion is very important in design. The base shear is defined as

$$V = \sum_{i=1}^{n} V_i = \sum_{i=1}^{n} (m_i \ddot{u}_i)$$

From the definition, the base shear is determined by the mass and the acceleration of the building. Although the TMD reduces the acceleration of the building, it, however, the TMD increases the mass of the building.

To evaluate the effect of the TMD on the base shear, base shear reduction is introduced. The base shear reduction is defined as the ratio of the base shear for the building with the TMD to the original base shear (without TMD). Table 11 shows the base shear reduction for the 4-story building structure subjected to the El Centro ground motion. It is observed that the increase of the mass ratio affects the base shear reduction in a significant way. For example, when the mass ratio is 1%, the base shear for the building with the TMD is 94% of the original base shear when the TMD placed at 4^{th} level, and the structural damping ratio is 0.02. When the mass ratio is increased to 10%, the base shear decreases to 75.18% of the original base shear. Furthermore, when the mass ratio is 20%, the base shear is 66.24% of the original base shear. However, when the mass ratio is increased to 40%, the base shear is 60.87% of the original one. That means when the mass ratio is less than 20%, increasing the mass of the TMD decreases the base shear remarkably. However, when the mass of the TMD is larger than 20% of the first mode mass of the primary system, increasing the mass of the TMD does not affect the base shear reduction a lot.

Figure 28 shows the effect of the TMD on the base shear. The similar trend is observed that increasing the mass ratio of the TMD decreases the base shear. The effect is obvious when the mass ratio is less than 20% for all cases. However, when the mass ratio is larger than 20%, the base shear due to the increasing mass of the damper offsets the base shear reduction by the damper. This explains why there was no increase in base shear due to added mass of the TMD.

The base shear decreases with the increase of the damping ratio of the primary structure, while the base shear reduction increases with higher damping. For example, when the mass ratio is $\mu = 0.1$, and $\xi_1 = \xi_2 = 0.02$, the base shear is $3453.6 kips$ and the reduction is 75.18% when the TMD placed at the 4^{th} level, as shown in Figure 18(a). For $\xi_1 = \xi_2 = 0.05$, the base shear is $3038.9 kips$ and reduction is 75.46% as shown in Figure 28(b).

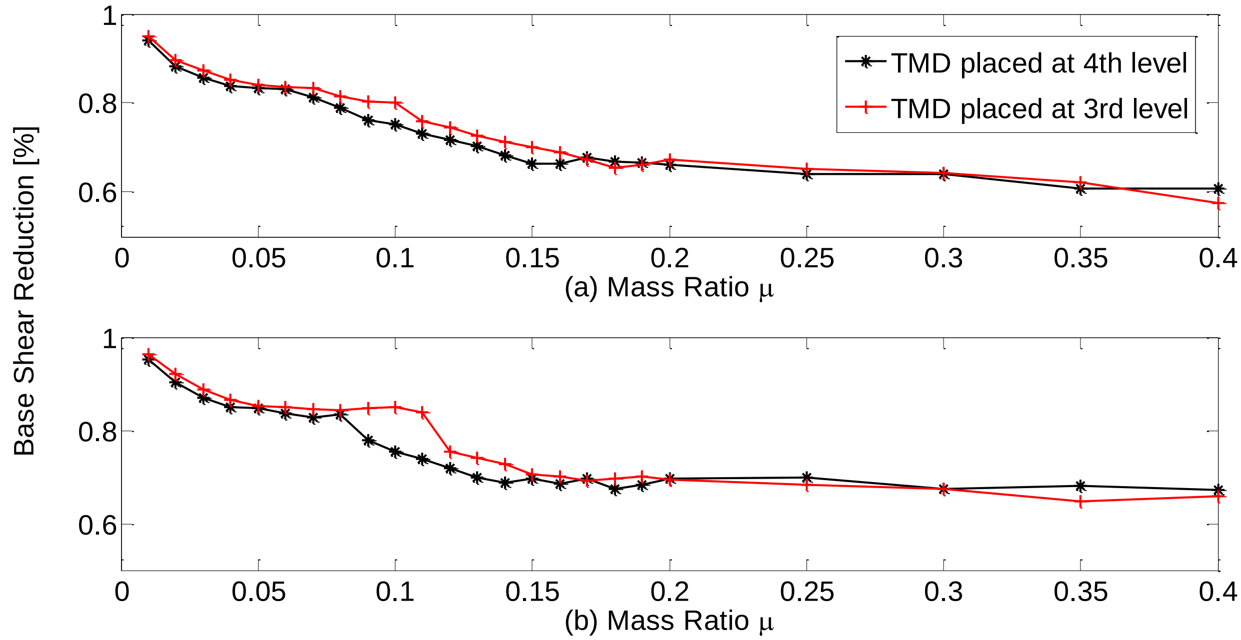

Figure 28: Base shear reduction of 4-story structure, (a) structural damping ratio is 0.02; (b) structural damping ratio is 0.05

Table 11: Base shear reduction

Mass ratio, μ	Structural Damping Ratio is 0.02		Structural Damping Ratio is 0.05	
	TMD placed at 4th level	TMD placed at 3rd level	TMD placed at 4th level	TMD placed at 3rd level
0.01	0.940003	0.950649	0.952226	0.963574
0.02	0.88251	0.896443	0.903856	0.92089
0.03	0.857715	0.873846	0.870534	0.887245
0.04	0.839146	0.851598	0.848906	0.865021
0.05	0.83379	0.839799	0.848559	0.851588
0.06	0.831113	0.836381	0.836615	0.84975
0.07	0.813393	0.833573	0.827875	0.844958
0.08	0.789686	0.815809	0.835324	0.843394
0.09	0.760972	0.803923	0.778338	0.847665

0.1	0.751829	0.800657	0.754575	0.85057
0.11	0.732345	0.758425	0.739528	0.839471
0.12	0.717019	0.74545	0.719862	0.75455
0.13	0.704001	0.72625	0.699253	0.74062
0.14	0.681971	0.713406	0.688575	0.727758
0.15	0.663292	0.701062	0.696248	0.705286
0.16	0.663858	0.690069	0.685894	0.701289
0.17	0.677443	0.672806	0.697663	0.692126
0.18	0.668278	0.654802	0.674174	0.697341
0.19	0.666188	0.661638	0.682244	0.700494
0.2	0.6624	0.673002	0.696198	0.694336
0.25	0.641349	0.652473	0.698408	0.684106
0.3	0.639542	0.643787	0.67395	0.673702
0.35	0.608629	0.622649	0.680257	0.647704
0.4	0.608782	0.574669	0.671889	0.6593

2.5. Effect of TMD in frequency domain

The effect of the TMD on the 4-story building subjected to the El Centro ground motion was also evaluated in frequency domain.

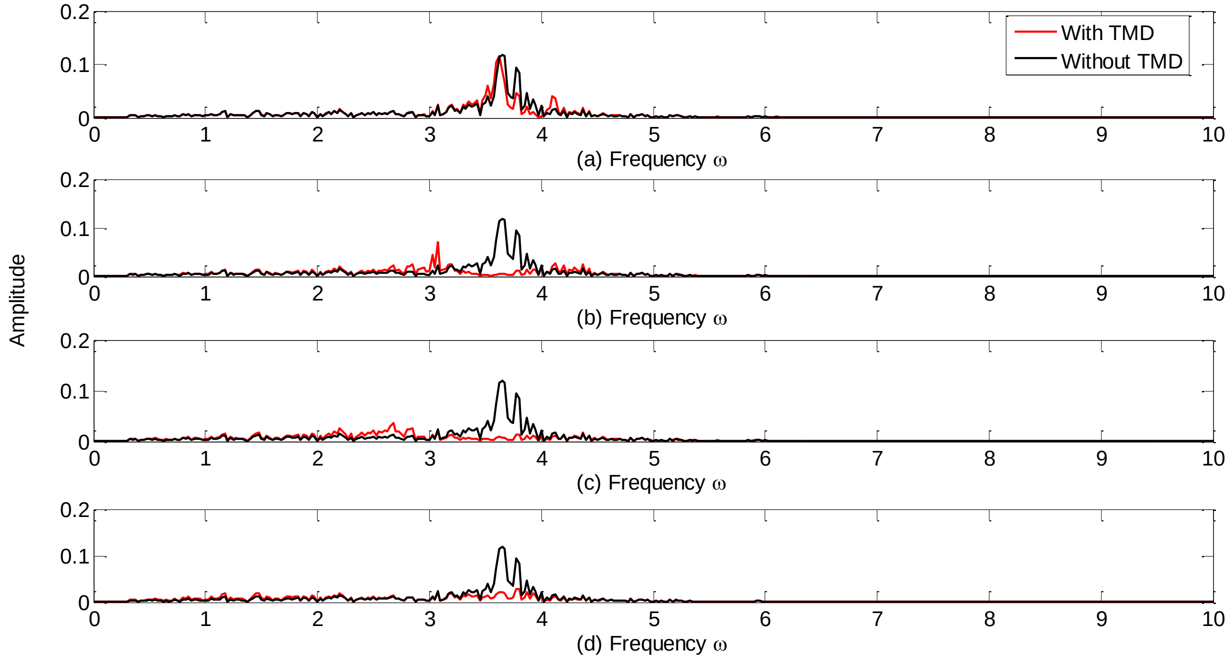

Figure 29: Effect of TMD on 4-story building in frequency domain when the TMD is placed at 4th level and the structural damping is 0.02, (a) $\mu = 0.01$; (b) $\mu = 0.10$; (c) $\mu = 0.20$; (d) $\mu = 0.40$

Figure 29 shows the effect of the TMD on the displacement in frequency domain. Comparing from Figure 29(a) to Figure 29(d) gives that when the mass ratio is 1%, the effect of the TMD is not obvious, with the increase of the mass ratio, the peak amplitude of the building decreases

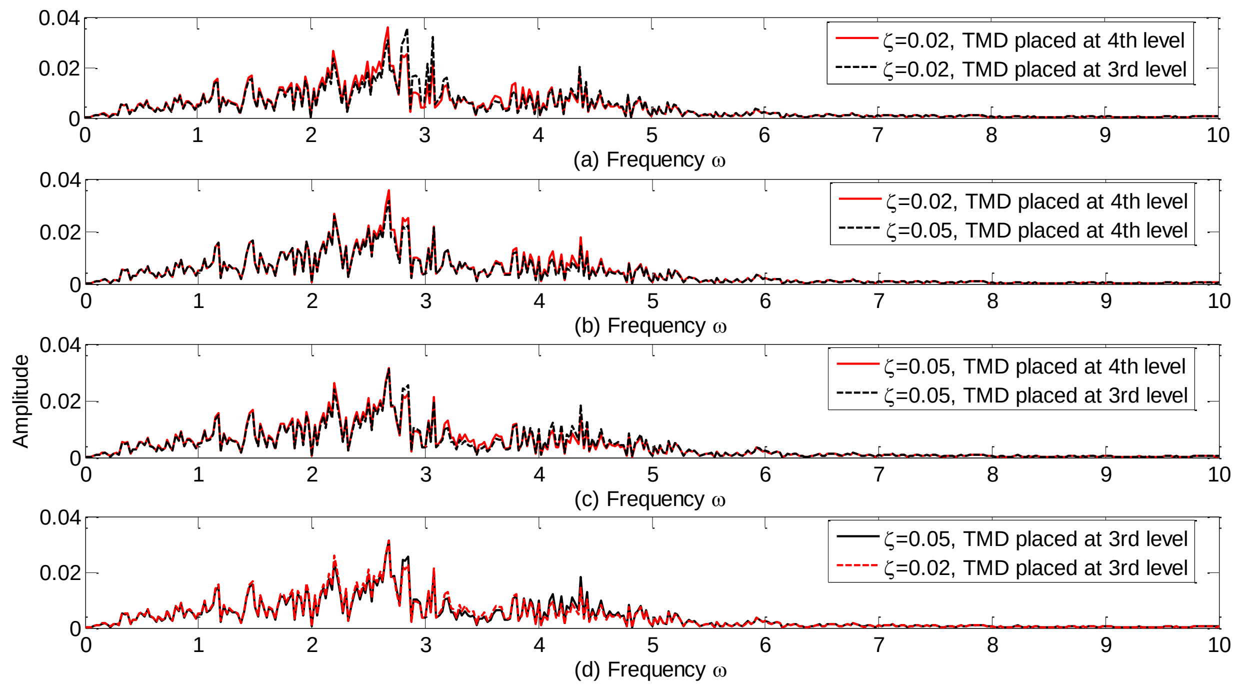

Figure 30: Effect of TMD on 4-story building in frequency domain

Figure 30 shows the effect of TMD at various levels on the 4-story building with various structural damping ratio. It is observed that for the 4-story building with TMD placed at 3rd level has higher amplitude at high frequency than that when TMD placed at 4th level, and for the 4-story building with various structural damping ratio, the peak amplitude for the system with higher damping ratio is less than that with lower damping ratio.

3. Comparison of the effect of the TMD on the 4-story building subjected to various ground motions

The effect of the TMD on the 4-story building subjected to the El Centro ground motion was evaluated in the previous sections. To compare the effect of the TMD under various ground motions, Altadena ground motion and Lexington ground motion were picked.

Table 12 shows the effect of the TMD on the 4-story building with structural damping ratio is 0.02 subjected to the Lexington ground motion. And Table 13 shows the effect of the TMD on the 4-story building with structural damping ratio is 0.02 subjected to the Altadena ground motion. It is found that for Lexington ground motion, the TMD amplifies the roof level displacement and the base shear. The same conclusion could be found for Altadena ground motion. For example, when the mass ratio is 1%, the TMD amplifies the roof level displacement to 112.39% of the original displacement when placed at the 4th level, it also amplifies the base shear to 120.73% of the original base shear when placed at 4th level.

Table 12: Effect of TMD on the displacement and base shear subjected to Lexington ground motion

	Roof Level Displacement		Base Shear	
Mass ratio, μ	TMD placed at 4th level	TMD placed at 3rd level	TMD placed at 4th level	TMD placed at 3rd level
0.01	1.1239	1.126	1.207273	1.207213
0.02	1.1155	1.1198	1.194453	1.192955
0.04	1.0987	1.1074	1.223267	1.220751
0.06	1.0819	1.095	1.25969	1.253699
0.08	1.071	1.0826	1.226502	1.286048
0.10	1.0618	1.0749	1.185407	1.24693
0.12	1.0535	1.0666	1.143114	1.22177
0.14	1.0441	1.0596	1.110106	1.184209
0.16	1.0355	1.0533	1.071886	1.144072
0.18	1.0269	1.0465	1.035763	1.107231
0.20	1.0168	1.0383	1.020727	1.087761
0.22	1.0072	1.0309	1.019589	1.062481
0.24	0.9973	1.0226	1.018091	1.039118
0.26	0.9669	1.0154	1.134308	1.028156
0.28	0.9572	1.0068	1.109387	1.027377
0.30	0.9459	1	1.114779	1.026119
0.32	0.9339	0.9927	1.115138	1.023423
0.34	0.9231	0.9835	1.122087	1.023064

0.36	0.9114	0.9763	1.123525	1.021147
0.38	0.8999	0.9695	1.125502	1.017732
0.40	0.8912	0.9617	1.096268	1.015456

Table 13: Effect of TMD on the displacement and base shear subjected to Altadena ground motion

	Roof Level Displacement		Base Shear	
Mass ratio, μ	TMD placed at 4th level	TMD placed at 3rd level	TMD placed at 4th level	TMD placed at 3rd level
0.01	1.4035	1.4126	0.890793	0.895952
0.02	1.3476	1.3652	0.863444	0.865682
0.04	1.2403	1.2738	1.010442	0.976857
0.06	1.1453	1.196	1.035657	1.039075
0.08	1.0829	1.1159	1.010194	1.085422
0.10	1.0419	1.0798	0.983156	1.031658
0.12	1.0151	1.0463	0.953487	1.015435
0.14	0.9962	1.0239	0.922409	0.987486
0.16	0.9726	1.0061	0.894336	0.962334
0.18	0.9524	0.9884	0.861683	0.936021
0.20	0.9296	0.9699	0.83305	0.90975
0.22	0.9099	0.9508	0.800377	0.883893
0.24	0.8888	0.9318	0.771599	0.857519
0.26	0.8706	0.9121	0.737434	0.83332
0.28	0.8575	0.8925	0.700058	0.810819
0.30	0.8277	0.8737	0.706916	0.788029
0.32	0.821	0.8591	0.678117	0.757013

0.34	0.8148	0.8492	0.669187	0.720777
0.36	0.8067	0.827	0.669498	0.718891
0.38	0.7999	0.8204	0.664816	0.687876
0.40	0.794	0.8139	0.656901	0.667426

The roof displacement reduction and base shear subjected to Altadena and Lexington ground motion are shown in Figure 31Figure 32. For the Lexington and Altadena ground motions, similar trend was observed for the roof displacement reduction and base shear reduction compared to the El Centro ground motion with the increase in mass ratio, both the roof displacement and the base shear decrease. However, it was observed when subjected to the Altadena ground motion, the optimally tuned TMD amplifies the roof displacement when the mass ratio is less than 15%. Similarly, when subjected to Lexington ground motion, a optimally tuned TMD acts as an amplifier when the mass of TMD is less than 25% of the first mode mass, $\widetilde{M}_1$.

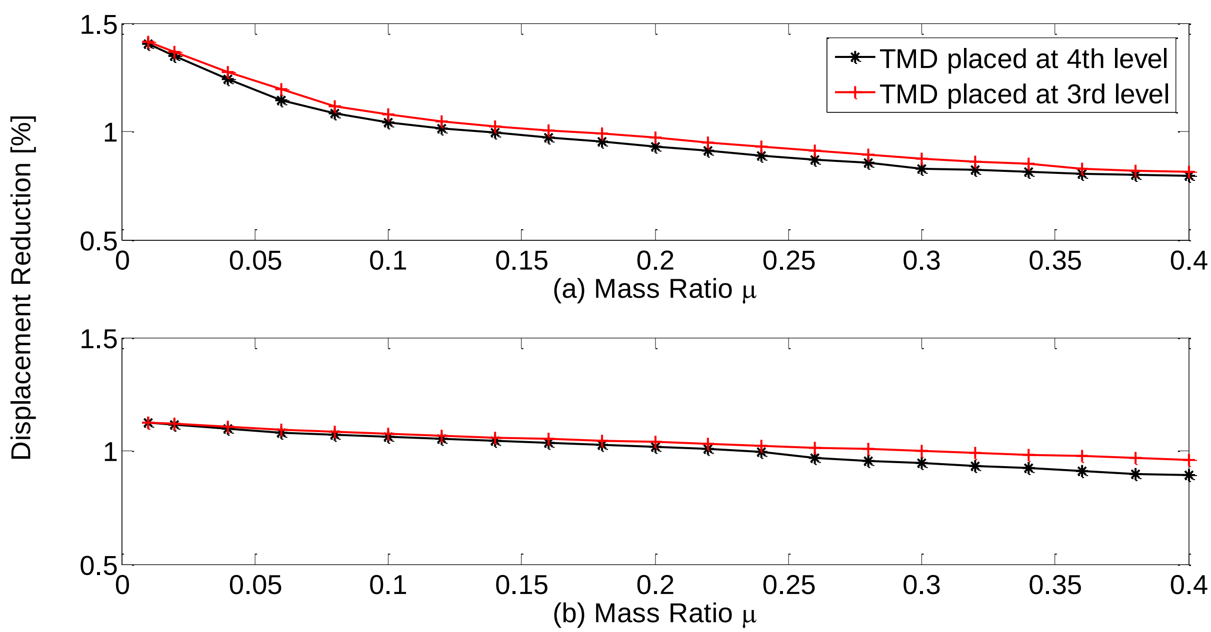

Figure 31: Displacement reduction of roof level of 4-story structure with $\xi_1 = \xi_2 = 0.02$, (a) subjected to Altadena ground motion; (b) subjected to Lexington

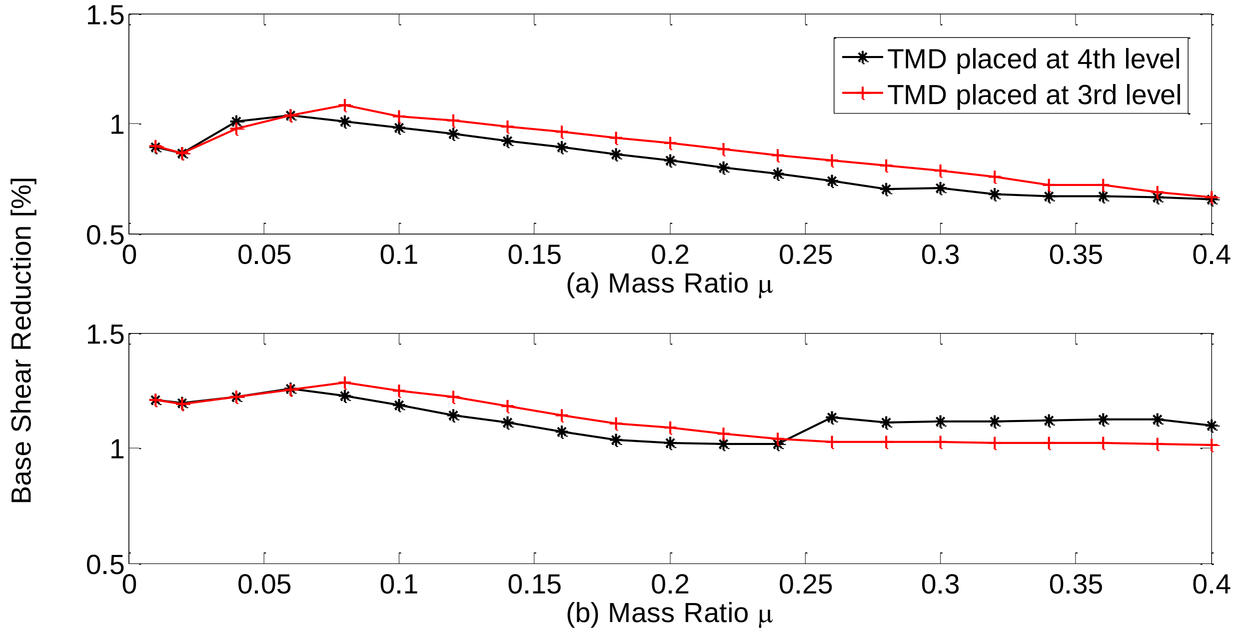

Figure 32: Base shear reduction of roof level of 4-story structure with $\xi_1 = \xi_2 = 0.02$, (a) subjected to Altadena ground motion; (b) subjected to Lexington

The TMD also amplifies the base shear if mass ratio is between 4% and 12% when subjected to the Altadena ground motion. For Lexington ground motion, the optimally tuned TMD inevitably enlarges the base shear from 1.02 to 1.28 times of the original base shear. Again, these trends were not observed when the building structure with the TMD was subjected to the El Centro ground motion.

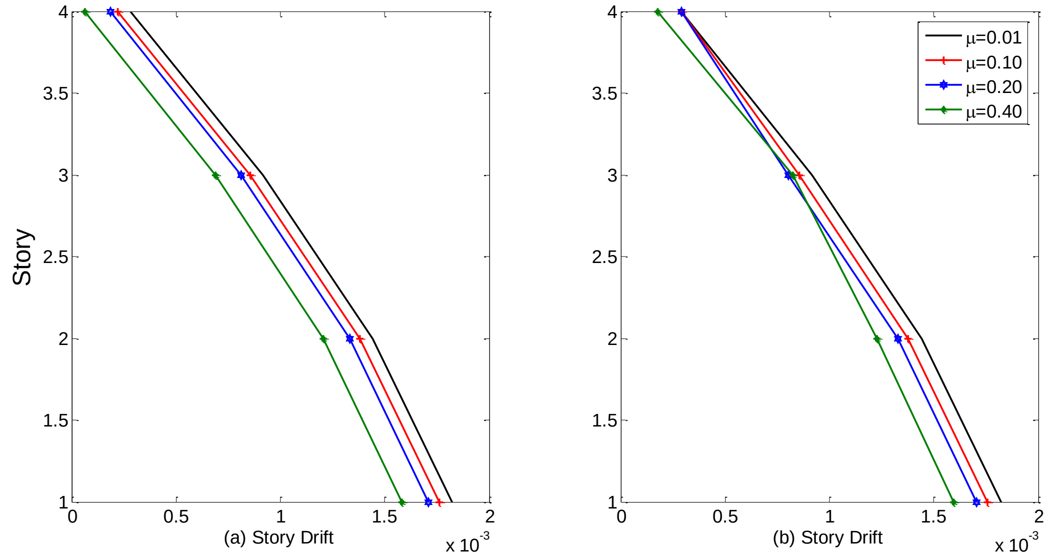

Figure 33: Story drift subjected to Lexington ground motion, (a) TMD placed at 4th level and damping ratio is 0.02; (b) TMD placed at 3rd level and damping ratio is 0.02

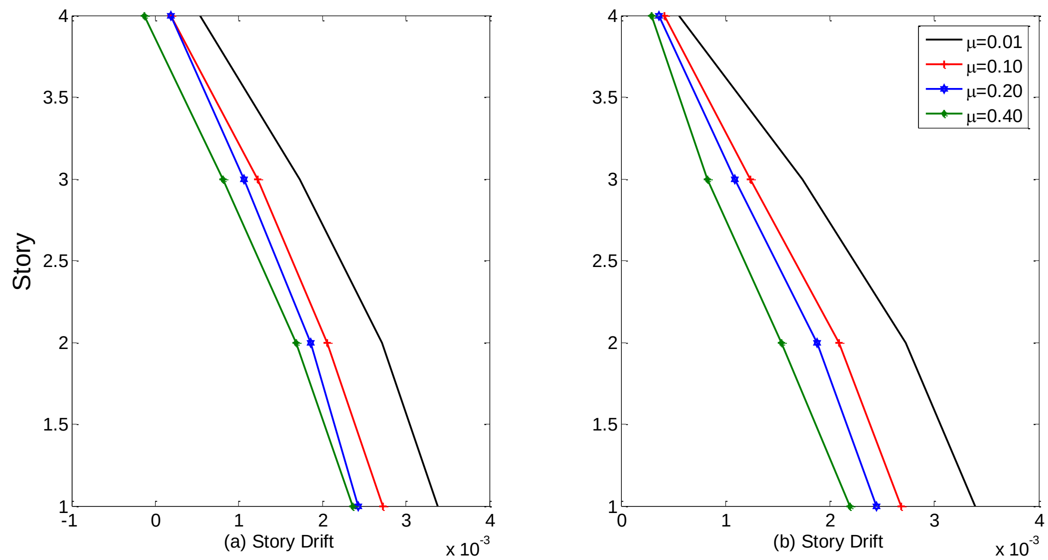

Figure 34: Story drift subjected to Altadena ground motion, (a) TMD placed at 4th level and damping ratio is 0.02; (b) TMD placed at 3rd level and damping ratio is 0.02

Figure 33 and Figure 34 show the story drift of the 4-story building subjected to the Lexington ground motion and the Altadena ground motion, respectively. It is found from the figures that for Lexington ground motion, the story drift decreases with higher level. And the increase of the mass ratio increases the story drift. For instance, when the mass ratio is 1%, the story drift Δ_4 is 0.028%, when the mass ratio is 10%, the story drift, Δ_4, is 0.022%. when the mass ratio is 20%, the story drift, Δ_4, is 0.019%, and when the mass ratio is 40%, the story drift is increased 0.0065%. It is also found that the story drift increases with the TMD placed at lower level. For example, for the mass ratio is 10%, when the TMD placed at 4th level, the story drift is $\Delta_4 = 0.022\%$, when the TMD placed at 3rd level, $\Delta_4 = 0.029$.

For the Altadena ground motion, similar trend is observed from Figure 34(b). for example, for the TMD placed at 4th level, when the mass ratio is 1%, the story drift is $\Delta_4 = 0.029\%$, when the mass ratio is 10%, $\Delta_4 = 0.029\%$, when the mass ratio is increased to 20%, the story drift is $\Delta_4 = 0.08\%$; and when the mass ratio is 40%, $\Delta_4 = 0.018\%$.

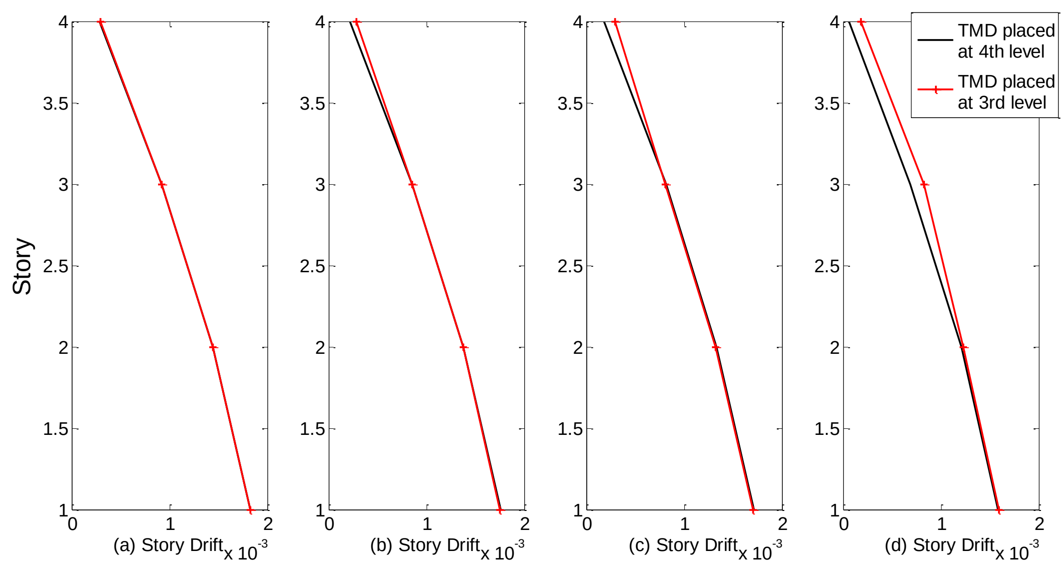

Figure 35: Effect of TMD at various levels on story drift subjected to Lexington ground motion, (a) mass ratio is 0.01; (b) mass ratio is 0.10; (c) mass ratio is 0.20; (d) mass ratio is 0.40

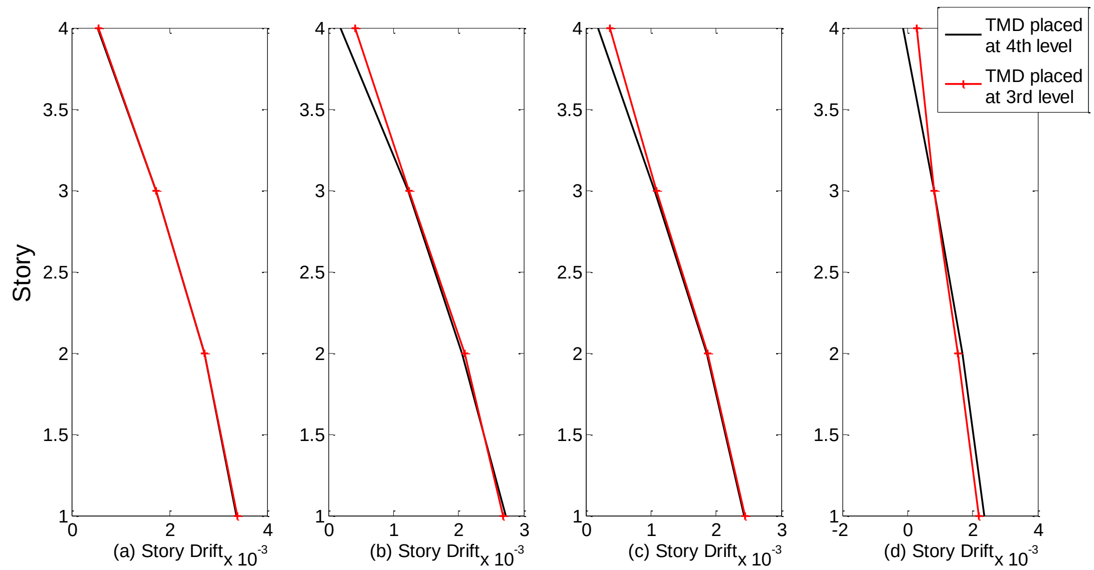

Figure 36: Effect of TMD at various levels on story drift subjected to Altadena ground motion, (a) mass ratio is 0.01; (b) mass ratio is 0.10; (c) mass ratio is 0.20; (d) mass ratio is 0.40

Figure 35 and Figure 36 show the effect of the TMD at various levels on the story drift of the 4-story building subjected to the Lexington ground motion and the Altadena ground motion, respectively. It is found from Figure 35 that for the Lexington ground motion, the TMD amplifies the story drift above the level where the TMD is placed at. For example, from Figure 35, the difference between the story drift with the TMD placed at 4th level and the 3rd level increases at story 3, where is the level where the TMD is placed at. Figure 36 shows the similar trend that the TMD amplifies the story drift above the level where the TMD is placed at subjected to the Altadena ground motion. For instance, for the 4-story building with the mass ratio is 10% and subjected to the Altadena ground motion, the story drift when the TMD is placed at 4 story are $\Delta_3 = 0.123\%$ and $\Delta_4 = 0.019\%$; when the TMD is placed at 3rd level, the story drift are $\Delta_3 = 0.124\%$ and $\Delta_4 = 0.042\%$.

4. Effect of TMD on the response of 10-story building

The 10-story building structure shown in Figure 18**Error! Reference source not found.**(b) was subjected to the El Centro ground motions. Two other ground motions, Lexington and Altadena were also evaluated for comparisons. As discussed previously, the mass ratio, μ, the frequency ratio, f, the damping ratio, ξ_d, and the location where the TMD is placed at affect the effect of the TMD on the response of the MDOF system. However, in practical way, engineers design the TMD via selecting its mass ratio. Therefore, in this study, the mass ratio of the TMD is defined as a predetermined parameter. The effect of the TMD on the displacement response, the base shear, and the story drift were evaluated with a variety range of mass ratio.

4.1. Optimal damping ratio and optimal frequency ratio

The effect of the frequency ratio, f, and the damping ratio, ξ_d, on the displacement response for a certain mass ratio, μ, was evaluated using the numerical integration method.

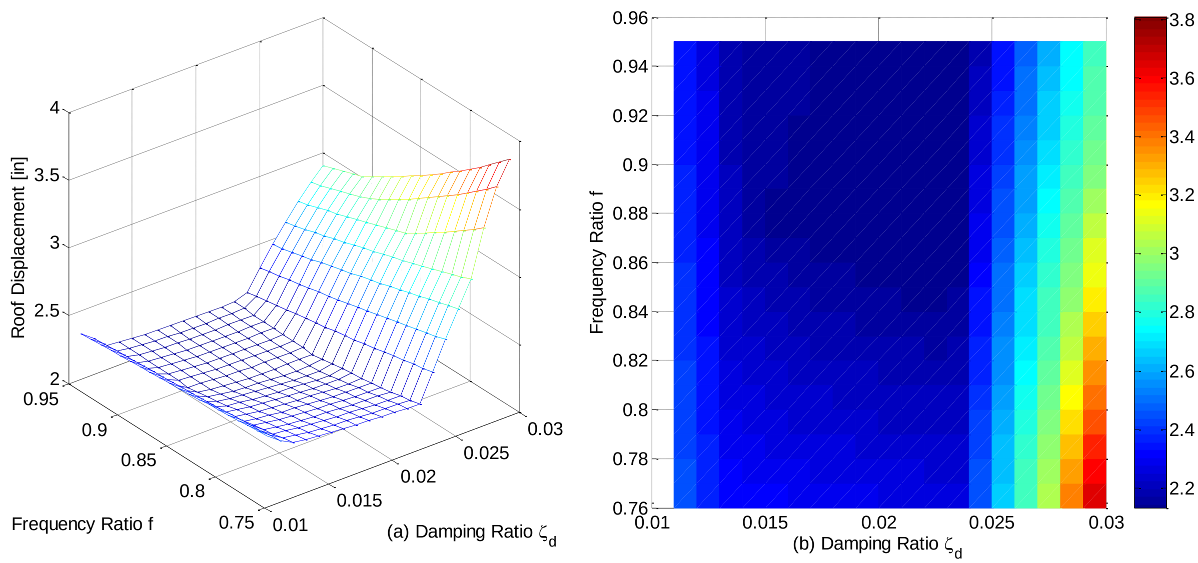

Figure 37: Effect of the frequency ratio and damping ratio on the displacement when mass ratio is 15% and TMD at 10th level, (a) 3-D view; (b) X-Y view

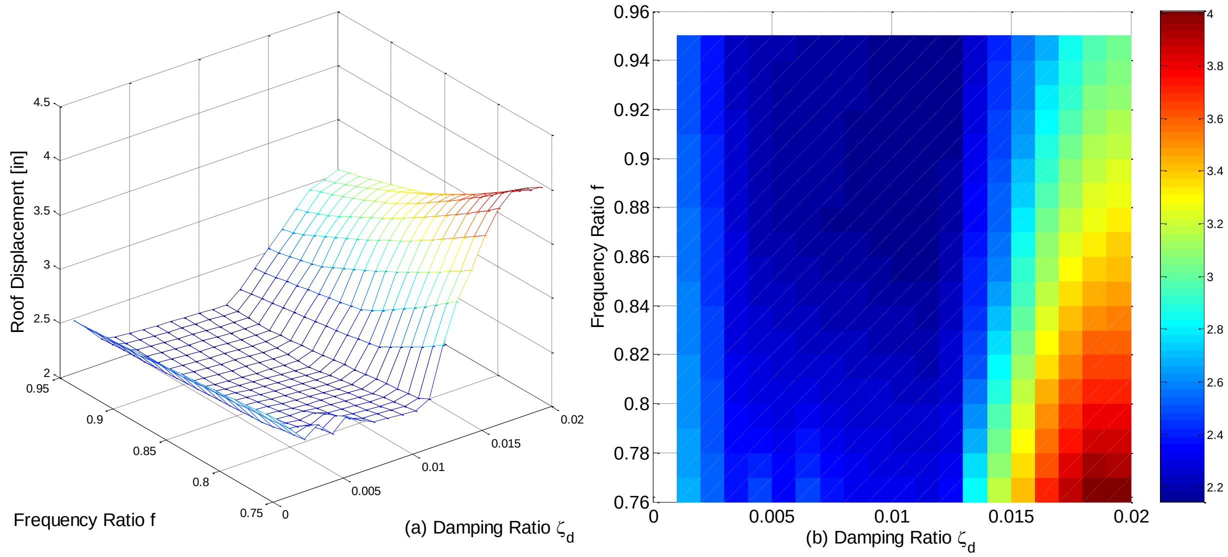

Figure 38: Effect of the frequency ratio and damping ratio on the displacement when mass ratio is 15% and TMD at 8th level, (a) 3-D view; (b) X-Y view

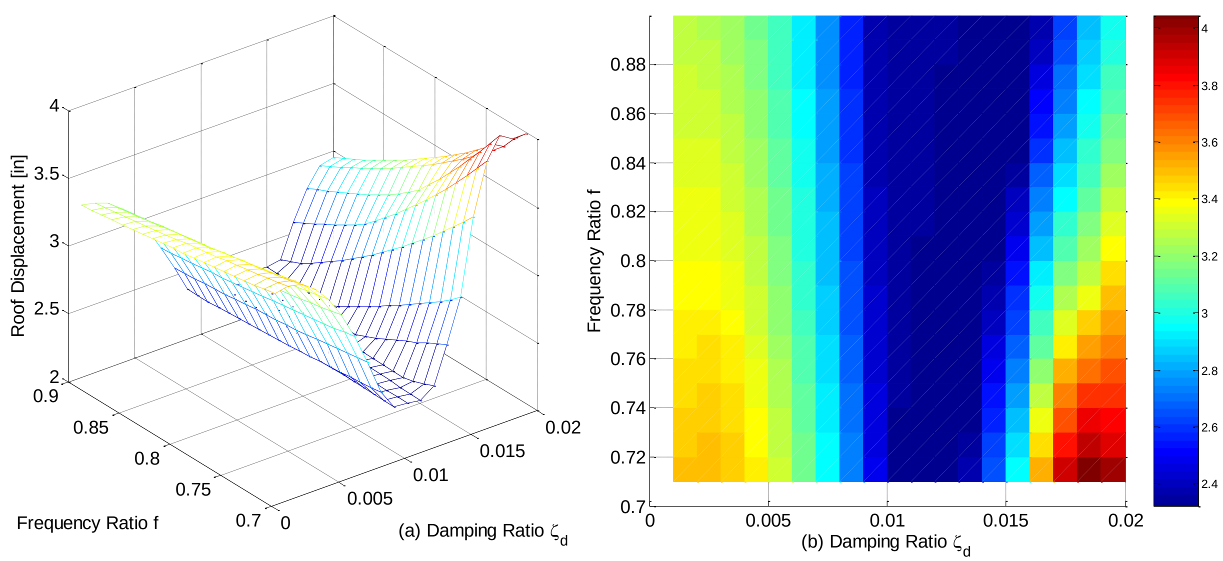

Figure 39: Effect of the frequency ratio and damping ratio on the displacement when mass ratio is 15% and TMD at 6th level, (a) 3-D view; (b) X-Y view

Figure 37 shows the effect of the frequency ratio and the damping ratio on the roof displacement response when the mass ratio is 15% for the 10-story building subjected to the El Centro ground motion, and the TMD is placed at the 10th level. Also, Figure 38 and Figure 39 show the effect of the frequency ratio and the damping ratio on the roof displacement response when the mass ratio is 15% for the 10-story building subjected to the El Centro ground motion, and the TMD is placed at the 8th and 6th level. It is observed from both figures that the effect of damping ratio, ξ_d, has a remarkable impact on the roof displacement, while the effect of the frequency ratio, f, is much less remarkable. Since for both cases, the similar trend are found for the effect of damping ratio and frequency ratio on the roof displacement, a similar procedure was followed to find the optimal damping ratio and optimal frequency ratio for variety range of mass ratio. Table 14 and Table 15 show the optimal damping ratio and optimal frequency ratio for the 10-story building structure subjected to El Centro ground motion with the TMD placed at various levels. With the increase of the mass ratio, the damping ratio increases from 0.00 to 0.08 for the building with structural damping is 0.02, in average, and to 0.1159 for the building with structural damping is 0.05 in average. However, when the mass ratio increases, the frequency ratio decreases.

Table 14: Optimal damping ratio, ξ_d

	Structural Damping Ratio is 0.02			Structural Damping Ratio is 0.05
Mass ratio, μ	TMD placed at 10th level	TMD placed at 8th level	TMD placed at 6th level	TMD placed at 10th level
0.01	0.0001	0.0001	0.0101	0.0001
0.02	0.0001	0.0001	0.0001	0.0001
0.03	0.0001	0.0001	0.0001	0.0001
0.04	0.0021	0.0001	0.0001	0.0001
0.05	0.0046	0.0001	0.0001	0.0005
0.06	0.0078	0.0001	0.0001	0.0001
0.07	0.0076	0.0002	0.0001	0.0001

0.08	0.0125	0.0101	0.0001	0.0003
0.09	0.0001	0.0201	0.0001	0.0007
0.1	0.0001	0.0301	0.0044	0.0001
0.11	0.0005	0.0034	0.0101	0.0001
0.12	0.0013	0.0023	0.0201	0.0001
0.13	0.0076	0.0033	0.0301	0.0001
0.14	0.0138	0.005	0.0301	0.0051
0.15	0.0206	0.0113	0.0031	0.0111
0.16	0.027	0.0172	0.0051	0.0198
0.17	0.0326	0.0229	0.0006	0.0199
0.18	0.0376	0.0282	0.0022	0.0268
0.19	0.0421	0.0329	0.0052	0.0311
0.2	0.0459	0.0373	0.0087	0.0368
0.25	0.0702	0.0535	0.0297	0.0821
0.3	0.1211	0.0932	0.0443	0.0658
0.35	0.0792	0.1301	0.0601	0.0843
0.4	0.095	0.0746	0.0842	0.1159

Table 15: Optimal frequency ratio, *f*

	Structural Damping Ratio is 0.02			Structural Damping Ratio is 0.05
Mass ratio, μ	TMD placed at 10th level	TMD placed at 8th level	TMD placed at 6th level	TMD placed at 10th level
0.01	0.956	0.967	0.973	0.951
0.02	0.956	0.964	0.963	0.943
0.03	0.956	0.961	0.961	0.947

0.04	0.952	0.957	0.959	0.949
0.05	0.954	0.954	0.956	0.952
0.06	0.958	0.969	0.954	0.886
0.07	0.915	0.99	0.954	0.911
0.08	0.843	0.919	0.967	0.846
0.09	0.82	0.922	0.975	0.85
0.1	0.83	0.914	0.912	0.854
0.11	0.84	0.83	0.919	0.861
0.12	0.851	0.84	0.923	0.855
0.13	0.865	0.85	0.909	0.854
0.14	0.867	0.86	0.917	0.85
0.15	0.862	0.866	0.829	0.845
0.16	0.848	0.87	0.84	0.836
0.17	0.843	0.869	0.84	0.812
0.18	0.836	0.865	0.849	0.824
0.19	0.828	0.847	0.86	0.819
0.2	0.821	0.84	0.865	0.813
0.25	0.833	0.821	0.851	0.822
0.3	0.749	0.822	0.825	0.62
0.35	0.63	0.761	0.821	0.622
0.4	0.625	0.627	0.833	0.628

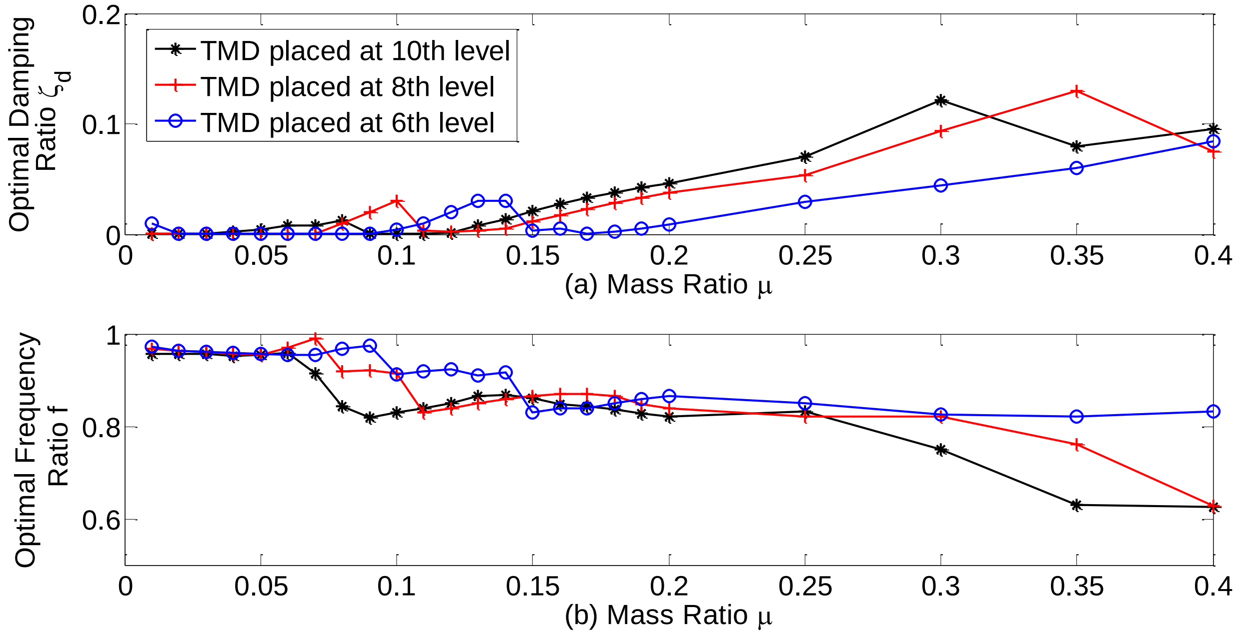

Figure 40: Optimal damping ratio and optimal frequency ratio versus mass ratio of 10-story structure with $\xi_1 = \xi_2 = 0.02$, (a) Optimal damping ratio versus mass ratio; (b) optimal frequency ratio versus mass ratio

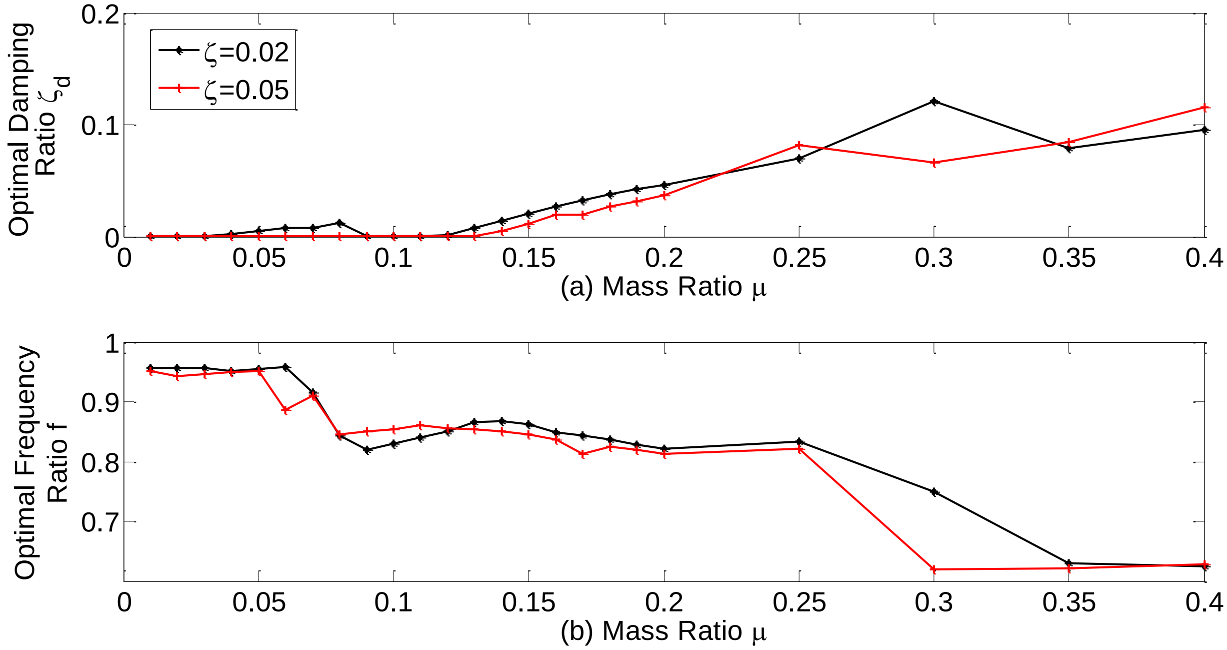

Figure 41: Optimal damping ratio and optimal frequency ratio versus mass ratio of 10-story structure when TMD placed at 10th level, (a) Optimal damping ratio versus mass ratio; (b) optimal frequency ratio versus mass ratio

Figure 40 and Figure 41 show the effect of damping ratio and frequency ratio on the roof displacement. Similar trend is observed for both the damping ratio, ξ_d, and the frequency ratio, f. Figure 40 shows the optimal damping ratio and optimal frequency ratio with the mass ratio for the 10-story building with structural damping ratio is 0.02. The TMD was placed at the 10th level, 8th level, and 6th level, respectively. For example, when the mass ratio is 15%, the optimal damping ratio when the TMD was placed at 10th level is 0.0206, which is larger than that when TMD placed at 8th level, which is 0.0133, and also larger than that when TMD placed at 6th level, 0.0031. While for optimal frequency, an opposite trend is observed. For a mass ratio is 15%, the optimal frequency ratio when the TMD placed at 10th level is 0.862, less than that when TMD placed at 8th level.

4.2. Effect of the TMD on displacement response

To evaluate the effect of TMD, a single TMD was placed at the roof level the 8th level, and the 6th level respectively.

To evaluate the effect of the TMD with the mass ratio, a variety range of mass ratio from $\mu = 0.01$ to $\mu = 0.40$ were studied. As defined previously, the mass ratio of the TMD is $\mu = m_d/\widetilde{M}_1$, therefore, when the mass ratio is 0.01, the mass of the TMD is $m_d = 0.31k \cdot s^2/in$, and when the mass ratio is 0.40, the mass of the TMD is $m_d = 12.28k \cdot s^2/in$, which in practical is a large additional mass.

The effect of the optimally tuned TMD with the optimal damping ratio and the optimal frequency ratio discussed in section4.1 were evaluated. To evaluate the effect of the TMD on reducing the roof displacement response, displacement reduction is introduced defined as the ratio of the displacement response with TMD to the displacement response without TMD.

Table 16 shows the displacement reduction of the 10-story building structure with the optimally tuned TMD. When the mass ratio of the TMD is 1%, the displacement when the TMD is placed at 10th level of the building with structural damping 0.02 is 65.72% of the original displacement, when the TMD is placed at 8th level, the displacement is 65.83% of the original, when the TMD is placed at 6th level, the displacement is 66.38% of the original. For the structural damping is 0.05, the roof displacement when the TMD is placed at 10th level is 89.22% of the original displacement. With the increase of the mass ratio, the roof displacement decreases. For example, when the mass ratio is increased to 10%, the displacement for the 10-story building with structural damping is 0.02 are 53.93%, 55.11% and 57.04% of the original displacement for the TMD placed at 10th level, 8th level and 6th level, respectively. And when the mass ratio is increased to 20%, the displacement for the 10-story building with structural damping is 0.02 are 47.22%, 47.48% and 50.02% of the original displacement for the TMD placed at 10th, 8th, and 6th level, respectively.

The roof displacement reduction is shown in Figure 42(a). It is observed that when the TMD was placed at the roof level, the roof displacement was lower than that when the TMD was placed at 8th and 6th level.

Table 16: Roof displacement reduction

	Structural Damping Ratio is 0.02	Structural Damping Ratio is 0.05

Mass ratio, μ	TMD placed at 10th level	TMD placed at 8th level	TMD placed at 6th level	TMD placed at 10th level
0.01	0.6572	0.6583	0.6638	0.8922
0.02	0.6393	0.6413	0.6506	0.8707
0.03	0.6227	0.6254	0.6385	0.8506
0.04	0.6077	0.6104	0.627	0.8319
0.05	0.5943	0.5963	0.616	0.8145
0.06	0.5829	0.5834	0.6055	0.7978
0.07	0.5691	0.5742	0.5954	0.7799
0.08	0.5652	0.5633	0.5862	0.7703
0.09	0.553	0.5565	0.5778	0.7544
0.1	0.5393	0.5511	0.5704	0.7385
0.11	0.5262	0.5393	0.5637	0.7231
0.12	0.5139	0.5262	0.5598	0.7102
0.13	0.5059	0.5145	0.5567	0.6975
0.14	0.5004	0.5038	0.5503	0.6893
0.15	0.4957	0.497	0.5403	0.6826
0.16	0.4912	0.4921	0.5312	0.6786
0.17	0.4865	0.4876	0.5218	0.6685
0.18	0.4818	0.4834	0.5134	0.6632
0.19	0.4771	0.4791	0.5059	0.6568
0.2	0.4722	0.4748	0.5002	0.6519
0.25	0.4565	0.4529	0.4835	0.6501
0.3	0.4573	0.4514	0.4674	0.6436
0.35	0.4394	0.4483	0.4546	0.6155
0.4	0.4227	0.4333	0.4515	0.5999

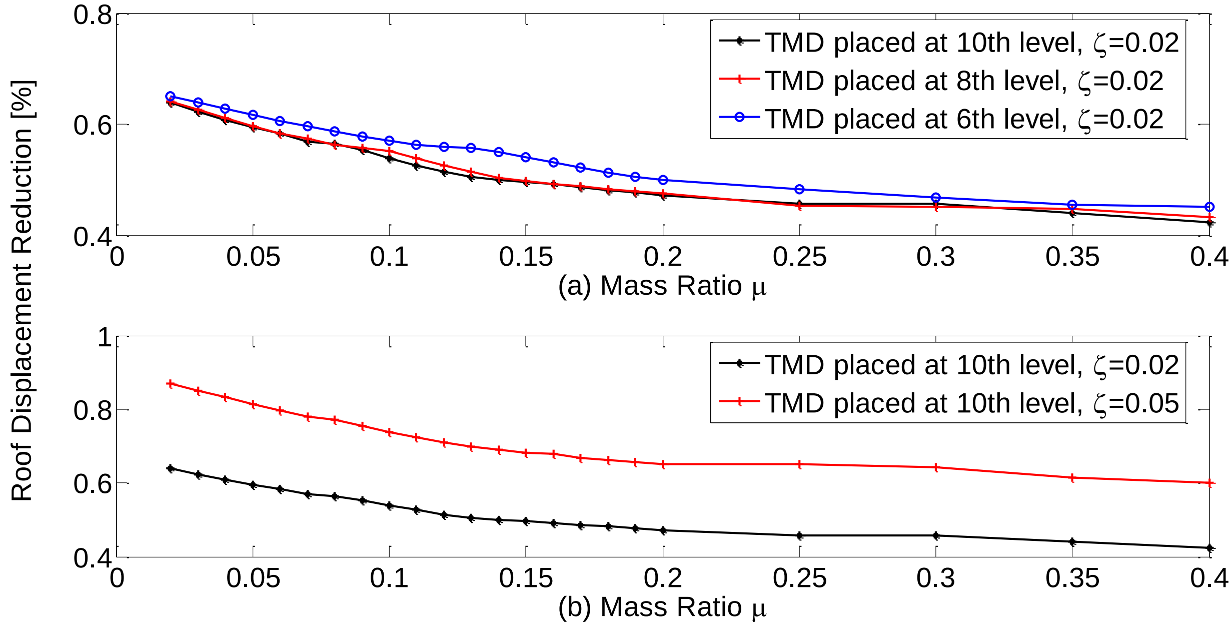

Figure 42: Roof displacement reduction, (a) structural damping ratio is 0.02; (a) structural damping ratio are 0.02 and 0.05

The effect of the damping ratio of the primary structure on the roof displacement reduction is also shown from Figure 42(b). It is observed that for a value of $\mu = 15\%$, the reduction in roof displacement for $\xi = 0.05$ and $\xi = 0.02$ is 68.26% and 49.57%, respectively. For $\mu = 25\%$, the reduction in roof displacement are 65.01% and 45.65%, respectively. It also shows that the effect of the TMD with higher structural damping ratio is less remarkable. However, the absolute displacement was still lower for the higher damping ratio. For example, for $\xi = 0.02$, the roof displacement was 4.2731in, whole it decreases to 2.8323in for $\xi = 0.05$ as expected. With a TMD and mass ratio is $\mu = 15\%$, the roof displacement for $\xi = 0.02$ was 2.118in, while the roof displacement for $\xi = 0.05$ was 1.933in.

4.3. Effect of the TMD on story drift

The story drift is defined as

$$\Delta_i = \frac{u_i - u_{i-1}}{H_i}$$

in which

u_i, u_{i-1} −displacement of level i and level $i-1$

H_i −story height of level i

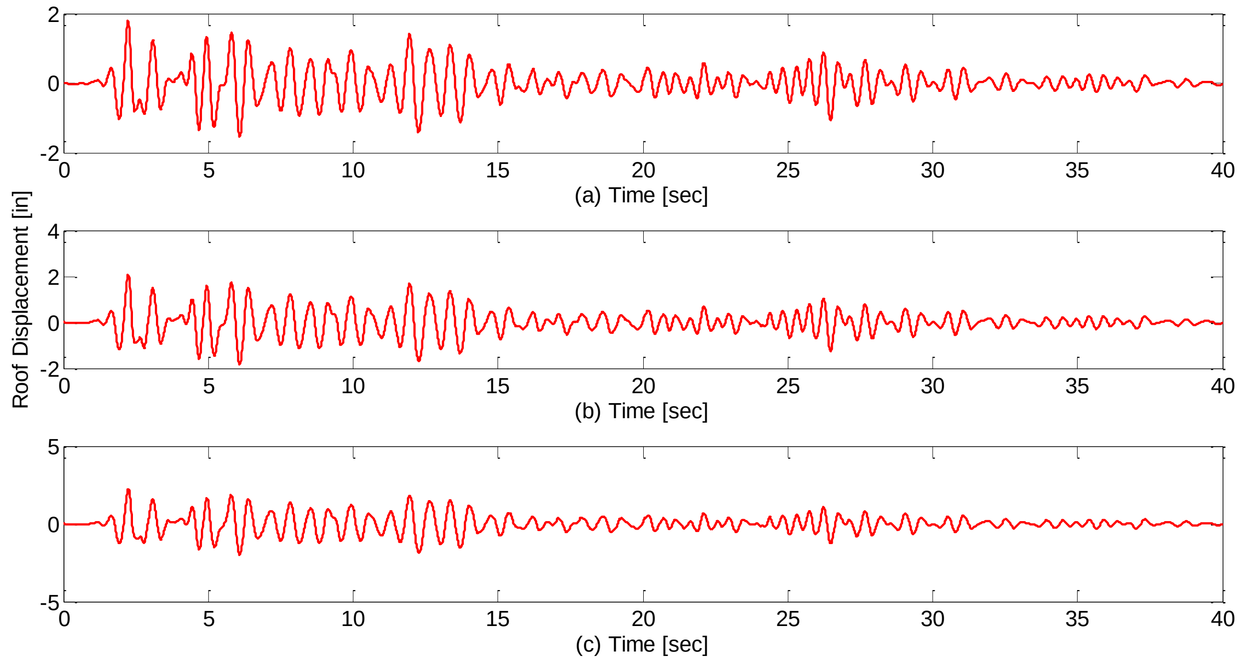

Figure 43: Displacement response with TMD placed at 10th level, (a) 6th level; (b) 8th level; (c) 10th level

Figure 43 shows the displacement of the 10-story building with the TMD placed at 10th level subjected to the El Centro ground motion. The displacement of 1st level to 4th level are shown from Figure 25(a) to (c), respectively. The mass ratio is 15%, specifically. The maximum displacement for each level are: 1.7827in for level 6; 2.0940in for level 8; and 2.2341in for level 10. It is found that although the maximum displacement increases as the level moves up, the story drift, 0.14% for level 6; 0.081 % for level 8; and 0.025% for level 10 drops down significantly.

Table 17: Story drift when TMD placed at 10th level with structural damping 0.02

Mass ratio, μ	Story drift, Δ_1	Story drift, Δ_2	Story drift, Δ_3	Story drift, Δ_4	Story drift, Δ_5
0.01	0.00344	0.00325	0.00295	0.00262	0.00223
0.05	0.00303	0.00287	0.00261	0.00228	0.00195

0.10	0.00278	0.00264	0.00242	0.00215	0.00183
0.15	0.00251	0.00236	0.00219	0.00193	0.00164
0.20	0.00253	0.00236	0.00210	0.00181	0.00151
0.25	0.00241	0.00226	0.00200	0.00170	0.00142
0.30	0.00227	0.00215	0.00199	0.00175	0.00153
0.35	0.00238	0.00224	0.00201	0.00178	0.00150
0.40	0.00228	0.00214	0.00193	0.00171	0.00143

Table 18: Story drift when TMD placed at 10th level with structural damping 0.02

Mass ratio, μ	Story drift, Δ_6	Story drift, Δ_7	Story drift, Δ_8	Story drift, Δ_9	Story drift, Δ_{10}
0.01	0.00181	0.00137	0.00101	0.00064	0.00020
0.05	0.00171	0.00136	0.00098	0.00061	0.00023
0.10	0.00150	0.00118	0.00085	0.00050	0.00015
0.15	0.00140	0.00111	0.00081	0.00052	0.00025
0.20	0.00119	0.00099	0.00076	0.00052	0.00024
0.25	0.00113	0.00093	0.00083	0.00055	0.00031
0.30	0.00129	0.00102	0.00081	0.00052	0.00024
0.35	0.00120	0.00091	0.00065	0.00034	0.00004
0.40	0.00115	0.00091	0.00062	0.00033	0.00004

Table 19: Story drift when TMD placed at 8th level with structural damping 0.02

Mass ratio, μ	Story drift, Δ_1	Story drift, Δ_2	Story drift, Δ_3	Story drift, Δ_4	Story drift, Δ_5
0.01	3.29097E-03	3.16042E-03	2.93194E-03	2.61528E-03	2.25278E-03
0.05	3.01319E-03	2.86250E-03	2.62639E-03	2.34444E-03	2.03194E-03
0.10	2.75208E-03	2.63889E-03	2.43819E-03	2.16458E-03	1.89514E-03
0.15	2.53056E-03	2.40000E-03	2.21875E-03	1.95833E-03	1.67222E-03

0.20	2.40208E-03	2.28333E-03	2.10486E-03	1.85486E-03	1.61181E-03
0.25	2.49861E-03	2.33194E-03	2.08194E-03	1.79375E-03	1.49306E-03
0.30	2.20208E-03	2.12222E-03	1.94097E-03	1.75486E-03	1.54861E-03
0.35	2.20347E-03	2.12222E-03	1.94028E-03	1.74653E-03	1.54028E-03
0.40	2.31181E-03	2.17222E-03	1.96181E-03	1.73194E-03	1.44861E-03

Table 20: Story drift when TMD placed at 8th level with structural damping 0.02

Mass ratio, μ	Story drift, Δ_6	Story drift, Δ_7	Story drift, Δ_8	Story drift, Δ_9	Story drift, Δ_{10}
0.01	1.89236E-03	1.50486E-03	1.07778E-03	6.24306E-04	1.83333E-04
0.05	1.74028E-03	1.37431E-03	9.98611E-04	5.43056E-04	1.59722E-04
0.10	1.60972E-03	1.27639E-03	9.37500E-04	4.94444E-04	1.47917E-04
0.15	1.44097E-03	1.15694E-03	9.07639E-04	3.45833E-04	1.16667E-04
0.20	1.37083E-03	1.08264E-03	8.36111E-04	4.20139E-04	1.23611E-04
0.25	1.17917E-03	8.62500E-04	6.88194E-04	3.93750E-04	1.15972E-04
0.30	1.32500E-03	1.12708E-03	8.66667E-04	3.92361E-04	1.16667E-04
0.35	1.30069E-03	1.10833E-03	8.39583E-04	3.86806E-04	1.13889E-04
0.40	1.15556E-03	9.08333E-04	7.61806E-04	3.06944E-04	9.86111E-05

Table 21: Story drift when TMD placed at 6th level with structural damping 0.02

Mass ratio, μ	Story drift, Δ_1	Story drift, Δ_2	Story drift, Δ_3	Story drift, Δ_4	Story drift, Δ_5
0.01	3.31875E-03	0.003190972	0.002959722	0.002641667	0.002276389
0.05	3.08472E-03	0.002972917	0.002750694	0.002451389	0.002140972
0.10	2.90694E-03	0.002738194	0.0025375	0.002269444	0.002
0.15	2.74514E-03	0.002618056	0.002420833	0.00214375	0.001839583
0.20	2.53681E-03	0.002478472	0.002340278	0.002128472	0.001863889
0.25	2.43750E-03	0.002350694	0.002157639	0.001945139	0.001722222

0.30	2.35556E-03	0.002270833	0.00208125	0.001884028	0.001663889
0.35	2.38750E-03	0.002222917	0.001976389	0.001754167	0.001617361
0.40	2.22708E-03	0.002149306	0.002013194	0.00184375	0.001663194

Table 22: Story drift when TMD placed at 6th level with structural damping 0.02

Mass ratio, μ	Story drift, Δ_6	Story drift, Δ_7	Story drift, Δ_8	Story drift, Δ_9	Story drift, Δ_{10}
0.01	0.001919444	0.001504167	0.001071528	0.000630556	0.000186111
0.05	0.001818056	0.001359028	0.000966667	0.00056875	0.000167361
0.10	0.001690278	0.001236806	0.000879167	0.000515972	0.000152083
0.15	0.001575	0.001195833	0.00085	0.000498611	0.000147222
0.20	0.001572917	0.000864583	0.000595139	0.000343056	0.00011875
0.25	0.001441667	0.00101875	0.000724306	0.000425	0.000125694
0.30	0.001510417	0.000917361	0.000665278	0.000402083	0.000120139
0.35	0.00143125	0.000935417	0.000661111	0.000388194	0.000114583
0.40	0.00146875	0.000891667	0.00064375	0.000384722	0.000113194

Table 23: Story drift when TMD placed at 10th level with structural damping 0.05

Mass ratio, μ	Story drift, Δ_1	Story drift, Δ_2	Story drift, Δ_3	Story drift, Δ_4	Story drift, Δ_5
0.01	0.0029375	0.002803472	0.002623611	0.002351389	0.00203125
0.05	0.002786806	0.002653472	0.002428472	0.002142361	0.001825694
0.10	0.002477083	0.002343056	0.00216875	0.001941667	0.0016625
0.15	0.00228125	0.002152778	0.001988889	0.001775694	0.001515972
0.20	0.002288889	0.0021625	0.001954167	0.001692361	0.001408333
0.25	0.002067361	0.001965278	0.001827083	0.001620833	0.001461806
0.30	0.002276389	0.002144444	0.001942361	0.001738194	0.001472917
0.35	0.002170139	0.002041667	0.001851389	0.001658333	0.001398611

0.40	0.002067361	0.001943056	0.001784722	0.001585417	0.001338889

Table 24: Story drift when TMD placed at 10th level with structural damping 0.05

Mass ratio, μ	Story drift, Δ_6	Story drift, Δ_7	Story drift, Δ_8	Story drift, Δ_9	Story drift, Δ_{10}
0.01	0.001702778	0.001361111	0.000975694	0.000580556	0.00018125
0.05	0.001492361	0.001156944	0.000832639	0.000493056	0.000209028
0.10	0.00138125	0.001113889	0.000797917	0.000479167	0.000159722
0.15	0.001284028	0.001023611	0.000736806	0.000455556	0.000211806
0.20	0.001151389	0.000860417	0.000620833	0.000475	0.000209028
0.25	0.001220833	0.00100625	0.000790278	0.000529167	0.000297222
0.30	0.001183333	0.000900694	0.000636806	0.000333333	3.125E-05
0.35	0.001122917	0.000889583	0.000611111	0.000323611	3.88889E-05
0.40	0.001125694	0.000875694	0.000604861	0.00035625	0.000116667

Table 17 through Table 24 show the story drift of the 10-story building structure with the TMD placed at various levels and with various structural damping ratio, respectively.

Figure 44 shows the effect of mass ratio on the story drift subjected to the El Centro ground motion. The same trend is observed that the story drift decreases with the increase of mass ratio. The effect of TMD for different mass ratio at various levels on story drift is given in Figure 45. It is observed that the story drift below the level where TMD was placed are similar. However, the TMD reduces the story drift above that level significantly.

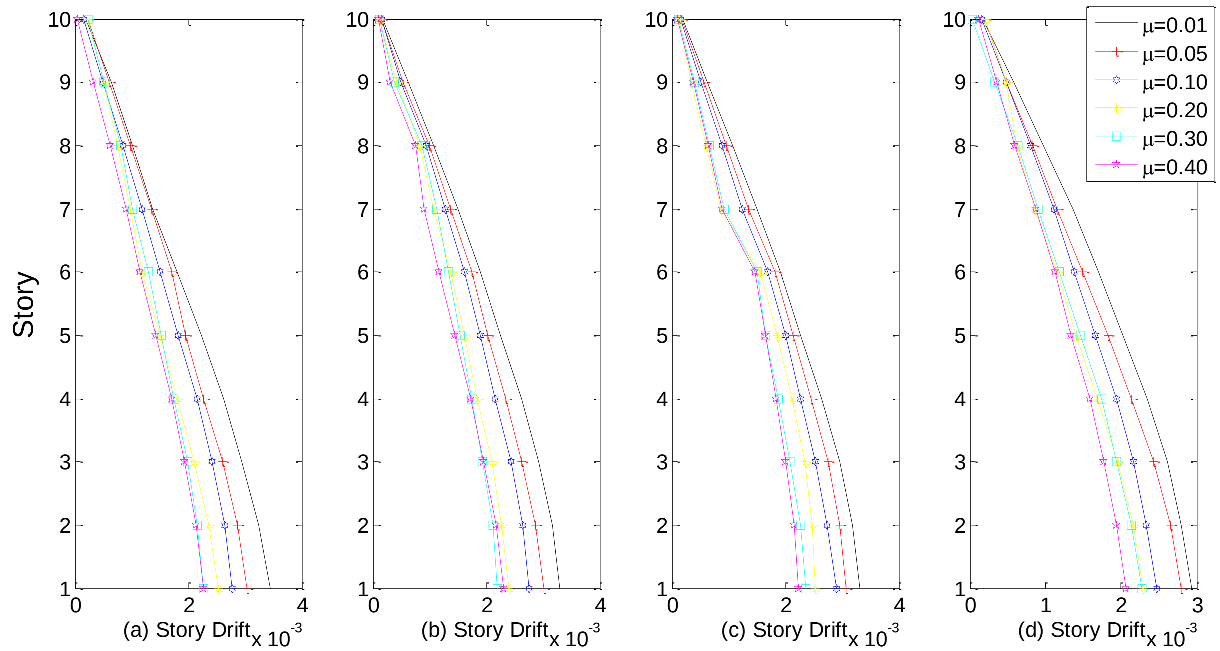

Figure 44: Story drift, (a) TMD placed at 10th level and damping ratio is 0.02; (b) TMD placed at 8th level and damping ratio is 0.02; (c) TMD placed at 6th level and damping ratio is 0.02; (d) TMD placed at 10th level and damping ratio is 0.05

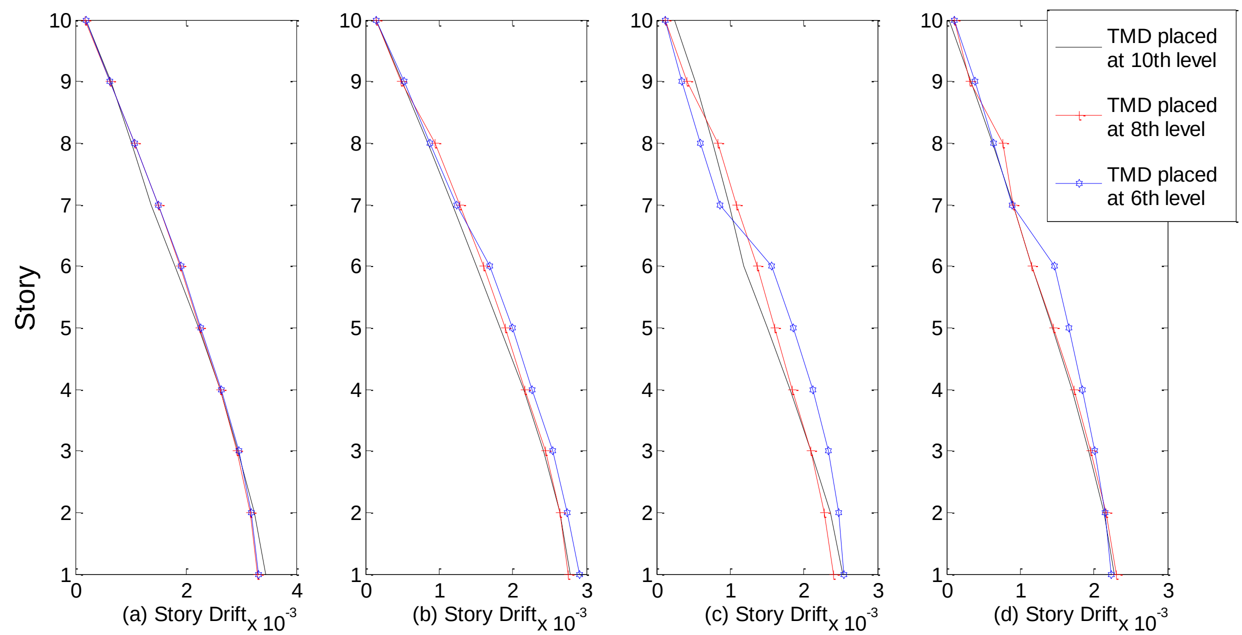

Figure 45: Effect of TMD at various levels on story drift, (a) mass ratio is 0.01; (b) mass ratio is 0.10; (c) mass ratio is 0.20; (d) mass ratio is 0.40

For the building structure with a TMD placed at 6th level, the story drift above 6th story is the smallest, while the story drift for the building structure with the TMD placed at 10th level becomes the largest. It is also observed that the difference of story drift between the TMD placed at 10th level and 8th level is considerably small, however, it is relatively obvious for the story drift with the TMD placed at 6th level.

4.4. Effect of TMD on the base shear

Similar with what was defined previously, the base shear of a building structure subjected to ground motion is very important in design. The base shear is defined as

$$V = \sum_{i=1}^{n} V_i = \sum_{i=1}^{n} (m_i \ddot{u}_i)$$

From the definition, the base shear is determined by the mass and the acceleration of the building. Although the TMD reduces the acceleration of the building, it, however, the TMD increases the mass of the building.

To evaluate the effect of the TMD on the base shear, base shear reduction is introduced. The base shear reduction is defined as the ratio of the base shear for the building with the TMD to the original base shear (without TMD). Table 25 shows the base shear reduction for the 10-story building structure subjected to the El Centro ground motion when the TMD is placed at various levels. It is observed that the increase of the mass ratio affects the base shear reduction in a significant way. For example, when the mass ratio is 1%, the base shear for the building with the TMD is 97.74% of the original base shear when the TMD placed at 10th level, and the structural damping ratio is 0.02. When the mass ratio is increased to 10%, the base shear decreases to 82.51% of the original base shear. Furthermore, when the mass ratio is 20%, the base shear is 72.02% of the original base shear. Also, when the mass ratio is increased to 40%, the base shear is 62.64% of the original one. That means when the mass ratio is less than 20%, increasing the mass of the TMD decreases the base shear remarkably. However, when the mass of the TMD is larger than 20% of the first mode mass of the primary system, increasing the mass of the TMD does not affect the base shear reduction a lot.

Figure 46 shows the effect of the TMD on the base shear. The similar trend is observed that increasing the mass ratio of the TMD decreases the base shear. The effect decreases slightly when the mass ratio is increasing for all cases. The base shear decreases with the increase of the damping ratio of the primary structure, while the base shear reduction increases with higher damping. For example, when the mass ratio is $\mu = 0.1$, and $\xi_1 = \xi_2 = 0.02$, the base shear is $10886kips$ and the reduction is 97.75% when the TMD placed at the 10th level, as shown in Figure 46(a). For $\xi_1 = \xi_2 = 0.05$, the base shear is $9992.6kips$ and reduction is 98.08% as shown in Figure 46(b), which is higher than that with lower structural damping ratio.

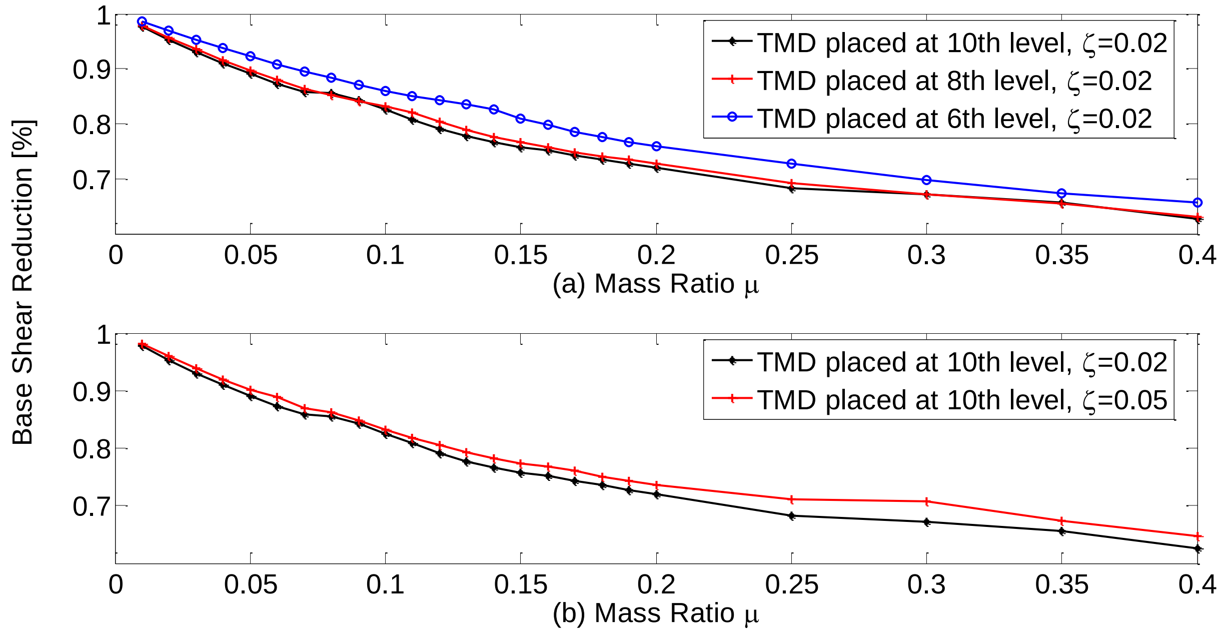

Figure 46: Base shear reduction of 10-story structure, (a) structural damping ratio is 0.02; (a) structural damping ratio are 0.02 and 0.05

Table 25: Base shear reduction

Mass ratio, μ	Structural Damping Ratio is 0.02: TMD placed at 10^{th} level	TMD placed at 8^{th} level	TMD placed at 6^{th} level	Structural Damping Ratio is 0.05: TMD placed at 10^{th} level
0.01	0.977463	0.979528	0.986621	0.980821
0.02	0.953039	0.9569	0.968932	0.959158
0.03	0.930233	0.9358	0.95277	0.938575
0.04	0.909581	0.915956	0.937416	0.919248
0.05	0.890365	0.897279	0.9226	0.901158
0.06	0.872766	0.879501	0.908503	0.888653
0.07	0.85858	0.863967	0.895035	0.869592
0.08	0.855886	0.852743	0.883003	0.863015
0.09	0.842956	0.841699	0.871599	0.847536
0.1	0.825177	0.832181	0.858759	0.832283
0.11	0.808117	0.820688	0.849511	0.817265
0.12	0.791506	0.804436	0.842866	0.804927
0.13	0.777319	0.78953	0.836132	0.792226
0.14	0.766634	0.775703	0.826434	0.782597
0.15	0.758014	0.765646	0.809195	0.774048
0.16	0.75119	0.756487	0.798061	0.767668
0.17	0.742929	0.748496	0.785849	0.760571
0.18	0.735207	0.740954	0.775613	0.750854
0.19	0.727754	0.734668	0.766724	0.743178
0.2	0.720212	0.727575	0.759091	0.736553
0.25	0.6825	0.692018	0.728203	0.710876
0.3	0.671276	0.672084	0.698213	0.707067

0.35	0.655922	0.655563	0.672802	0.673744
0.4	0.62647	0.63096	0.65646	0.646329

4.5. Effect of TMD in frequency domain

The effect of the TMD on the 10-story building subjected to the El Centro ground motion was also evaluated in frequency domain.

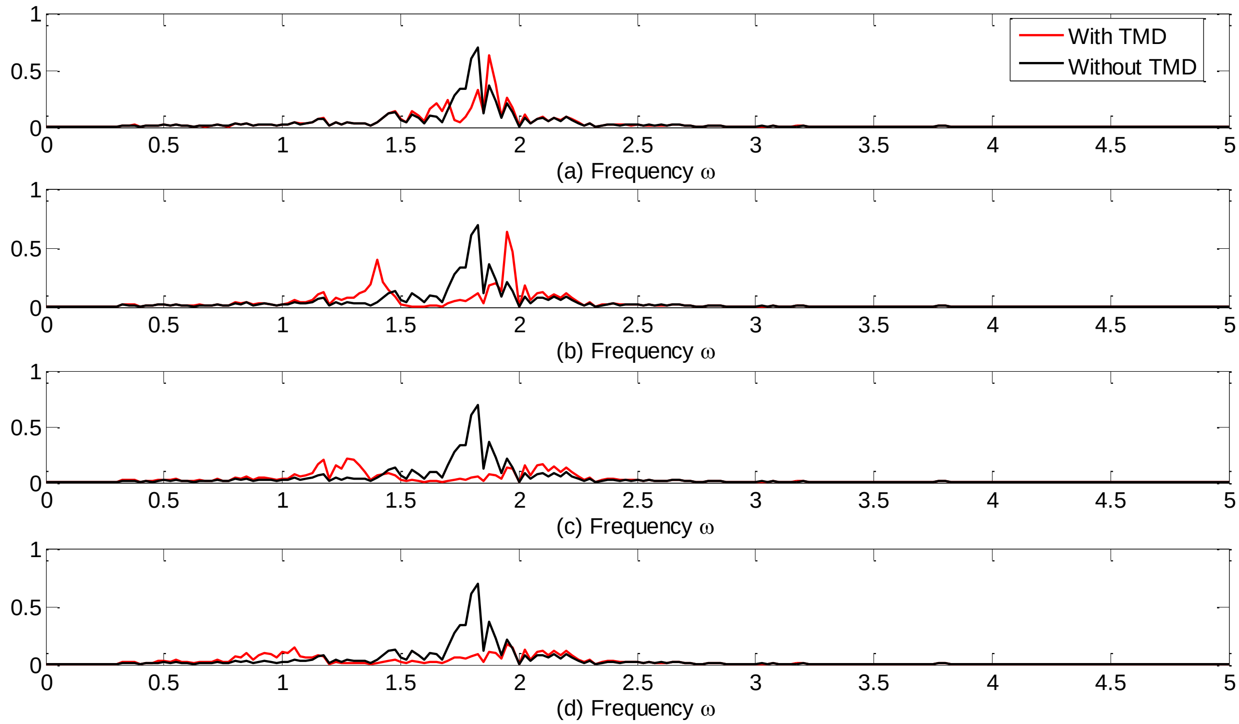

Figure 47: Effect of TMD on 10-story building in frequency domain when the TMD is placed at 4th level and the structural damping is 0.02, (a) $\mu = 0.01$; (b) $\mu = 0.10$; (c) $\mu = 0.20$; (d) $\mu = 0.40$

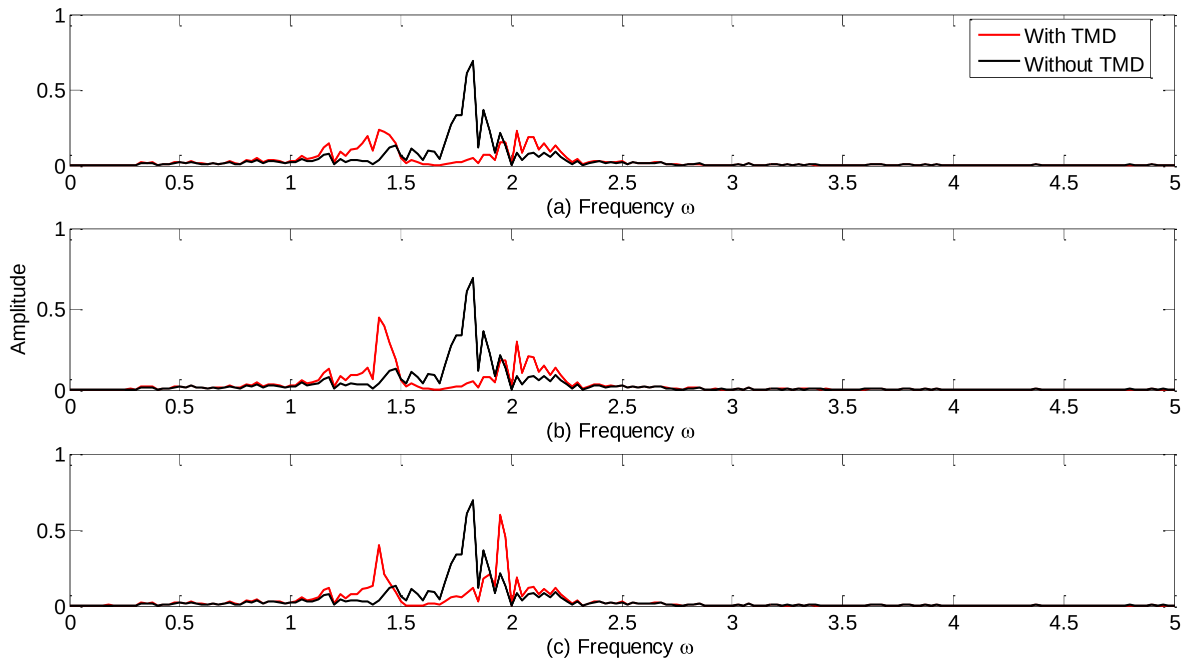

Figure 48: Effect of TMD on 10-story building in frequency domain when the structural damping is 0.02and $\mu = 0.15$, (a) TMD placed at 10th level; (b) TMD placed at 8th level; (c) TMD placed at 6th level

Figure 47 shows the effect of the TMD on the displacement in frequency domain. Comparing from Figure 47(a) to Figure 47(d) gives that when the mass ratio is 1%, the effect of the TMD is not obvious, with the increase of the mass ratio, the peak amplitude of the roof displacement response decreases remarkably.

Figure 48 shows the effect of the TMD at various levels. It is observed from Figure 48(a) that when the TMD is placed at the roof level, the peak amplitude of the displacement response is much lower than that without TMD. However, when the TMD is placed at 8th level and 6th level, it is found from Figure 48(b) and Figure 48(c)Figure 48 that the two peaks of the amplitude increase a lot. For example, when the TMD is placed at 8th level, the peak amplitude of the roof displacement with TMD is more than 50% of the original displacement amplitude; while when the TMD is placed at 6th level, the peak amplitude with TMD is approximately 80% of the original amplitude.

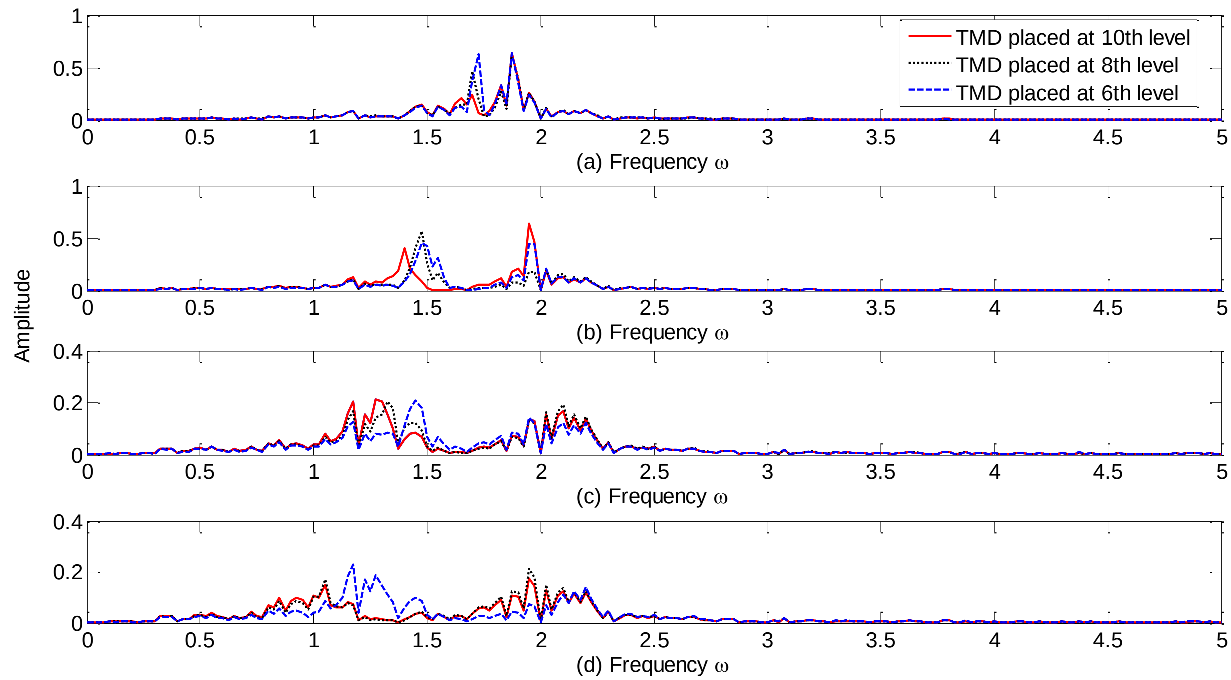

Figure 49: Effect of TMD on 10-story building in frequency domain, (a) $\mu = 0.01$; (b) $\mu = 0.10$; (c) $\mu = 0.20$; (d) $\mu = 0.40$

Figure 49 shows the effect of TMD at various levels on the 10-story building with various structural damping ratio. It is observed that for the 10-story building, the peak amplitude pf the displacement response decreases with the TMD placed at lower level. For example, when the TMD is placed at 6th level, the peak amplitude of the roof displacement is higher than that when the TMD is placed at 8th level, and also higher than that when TMD placed at 10th level. It is also found that with the increase of the mass ratio, the peak amplitude of the roof displacement response decrease. For example, for the 10-story building with TMD placed at 10th level, when the mass ratio is 1%, the peak amplitude is 0.633, when the mass ratio is 10%, the peak amplitude is 0.6329, and also when the mass ratio is 20%, the peak amplitude is 0.2142.

5. Comparison of the effect of the TMD on the 4-story building subjected to various ground motions

The effect of the TMD on the 10-story building subjected to the El Centro ground motion was evaluated in the previous sections. To compare the effect of the TMD under various ground motions, Altadena ground motion and Lexington ground motion were picked.

Table 26 shows the effect of the TMD on the roof displacement reduction of the 10-story building with structural damping ratio is 0.02 subjected to the Lexington ground motion. And Table 27 shows the effect of the TMD on base shear reduction of the 10-story building with structural damping ratio is 0.02 subjected to the Lexington ground motion. It is found that for Lexington ground motion, the TMD reduces the roof level displacement and the base shear. This is different from that for a 4-story building structure. For example, when the TMD is placed at 10th level, the roof displacement when the mass ratio 1% is 73.01% of the original. When the mass ratio is increased to 10%, the roof displacement is 80.73% of the original. However, when the mass ratio is 20%, the roof displacement is 104.18% of the original, which means the TMD amplifies the roof displacement slightly. Also, the TMD reduces the base shear subjected to Lexington ground motion. For instance, for the TMD placed at 10th level, when the mass ratio is 1%, the base shear is 69.9% of the original. When the mass ratio is 10%, the base shear is 62.32% of the original. Also, when the mass ratio is 20%, the base shear is 72.16% of the original base shear.

Table 26: Effect of TMD on the roof displacement reduction subjected to Lexington ground motion

	Roof Level Displacement		
Mass ratio, μ	TMD placed at 10th level	TMD placed at 8th level	TMD placed at 6th level
0.01	0.7301	0.7267	0.7193
0.02	0.7366	0.7346	0.7314
0.03	0.7322	0.736	0.7351
0.04	0.7317	0.7389	0.736
0.05	0.7365	0.7421	0.7369
0.06	0.7567	0.734	0.7392
0.07	0.7756	0.7501	0.727
0.08	0.7687	0.7685	0.7327

0.09	0.7876	0.7693	0.7441
0.10	0.8073	0.785	0.7571
0.11	0.8262	0.8017	0.7604
0.12	0.8466	0.8191	0.7686
0.13	0.8682	0.8345	0.7803
0.14	0.8909	0.8523	0.7925
0.15	0.9145	0.8712	0.8052
0.16	0.939	0.8907	0.8183
0.17	0.9641	0.9108	0.8319
0.18	0.9897	0.9313	0.8458
0.19	1.0157	0.9522	0.8557
0.20	1.0418	0.9734	0.869

Table 27: Effect of TMD on the base shear reduction subjected to Lexington ground motion

	Roof Level Displacement		
Mass ratio, μ	TMD placed at 10th level	TMD placed at 8th level	TMD placed at 6th level
0.01	0.699025	0.686157	0.701786
0.02	0.700029	0.678975	0.68051
0.03	0.721083	0.6911	0.718988
0.04	0.72256	0.703215	0.703369
0.05	0.719461	0.710841	0.714065
0.06	0.717569	0.688126	0.718274
0.07	0.684863	0.698021	0.732156
0.08	0.708833	0.646559	0.699894
0.09	0.669109	0.687489	0.730215
0.10	0.623236	0.650063	0.689507
0.11	0.592779	0.608833	0.757776

0.12	0.603813	0.578135	0.714403
0.13	0.61308	0.57966	0.678164
0.14	0.625147	0.589005	0.643392
0.15	0.641066	0.598764	0.611912
0.16	0.656955	0.608505	0.592509
0.17	0.673028	0.618148	0.601506
0.18	0.689111	0.62786	0.611594
0.19	0.705338	0.640216	0.599073
0.20	0.721633	0.652911	0.909422

Table 28 shows the effect of the TMD on the roof displacement for the 10-story building subjected to the Altadena ground motion. And Table 29 shows the effect of the TMD on the base shear for the 10-story building. It is found that for the displacement, the TMD reduces the displacement subjected to the Altadena ground motion. While for the base shear, the TMD amplifies the base shear when the mass ratio is approximately 1%. For instance, for the 10-story building with TMD placed at 10th level, when the mass ratio is 1%, the base shear is 103.05% of the original base shear. While when the mass ratio is 10%, the base shear is 84.75% of the original base shear. And when the mass ratio is 20%, the base shear is 75.56% of the original base shear.

Table 28: Effect of TMD on the roof displacement reduction subjected to Altadena ground motion

	Roof Level Displacement		
Mass ratio, μ	TMD placed at 10^{th} level	TMD placed at 8^{th} level	TMD placed at 6^{th} level
0.01	0.9061	0.9103	0.9439
0.02	0.8473	0.8474	0.8609
0.03	0.8413	0.8141	0.8466
0.04	0.8354	0.8355	0.8423
0.05	0.8296	0.8298	0.8381
0.06	0.8239	0.8242	0.834
0.07	0.8183	0.8188	0.83
0.08	0.8129	0.8135	0.826
0.09	0.8075	0.8083	0.8221
0.10	0.8023	0.8032	0.8182
0.11	0.7971	0.7983	0.8144
0.12	0.7921	0.7934	0.8107
0.13	0.7872	0.7887	0.8071
0.14	0.7824	0.7841	0.8035
0.15	0.7776	0.7796	0.7999
0.16	0.773	0.7752	0.7964
0.17	0.7685	0.7709	0.793
0.18	0.7641	0.7667	0.7896
0.19	0.7598	0.7626	0.7863
0.20	0.7556	0.7585	0.7831

Table 29: Effect of TMD on the base shear reduction subjected to Altadena ground motion

	Roof Level Displacement

Mass ratio, μ	TMD placed at 10th level	TMD placed at 8th level	TMD placed at 6th level
0.01	1.030543	1.031414	1.036557
0.02	0.999832	1.004555	1.021034
0.03	0.976195	0.982304	1.002834
0.04	0.953692	0.961365	0.987667
0.05	0.932291	0.941349	0.972921
0.06	0.911814	0.922121	0.958594
0.07	0.89247	0.903816	0.944666
0.08	0.873893	0.886194	0.931126
0.09	0.859902	0.869317	0.917965
0.10	0.847496	0.853006	0.905181
0.11	0.835709	0.837493	0.892733
0.12	0.82451	0.823702	0.880652
0.13	0.813563	0.812303	0.868886
0.14	0.803109	0.801388	0.857435
0.15	0.793138	0.790913	0.846299
0.16	0.783608	0.780606	0.835467
0.17	0.774508	0.77096	0.824919
0.18	0.76545	0.76144	0.814633
0.19	0.756759	0.752278	0.804641
0.20	0.748782	0.743451	0.79488

The roof displacement reduction and base shear subjected to Altadena and Lexington ground motion are also shown in Figure 50and Figure 51. For both ground motions, the displacement reduction and the base shear reduction have the similar trend. Figure 50(a) and Figure 51(a) indicate that the displacement reduction and base shear reduction decrease as mass ratio increases; while the decrease of displacement reduction and base shear reduction with the increase of mass ratio is found from Figure 50(b) and Figure 51(b).

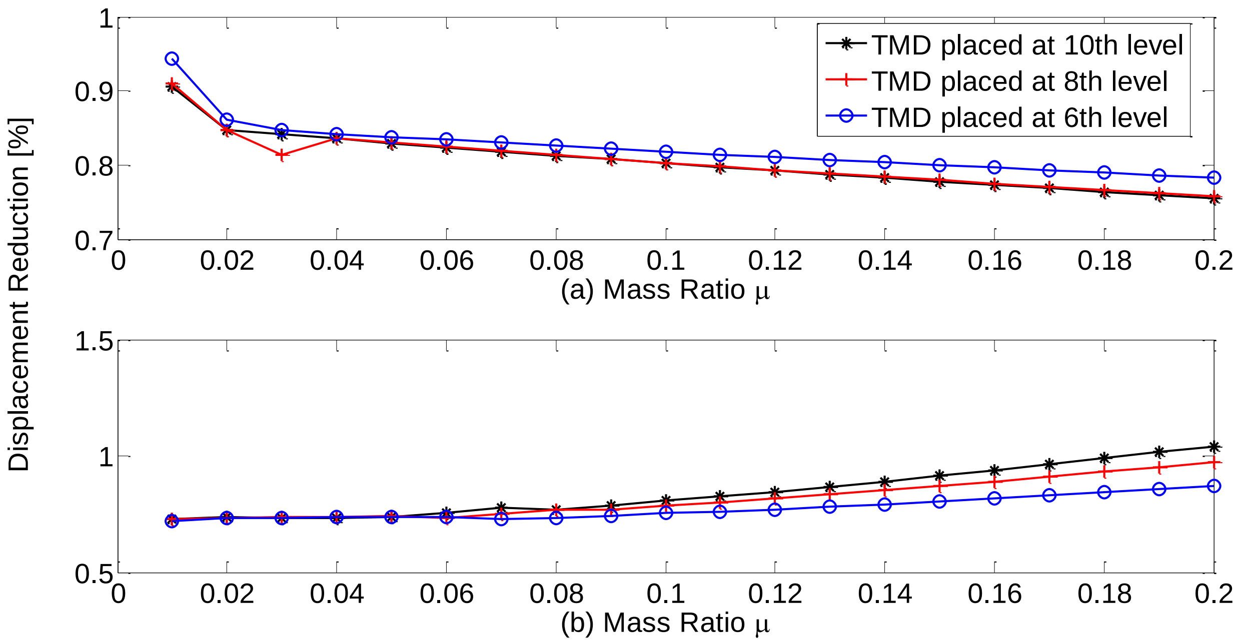

Figure 50: Displacement reduction of roof level of 10-story structure with $\xi_1 = \xi_2 = 0.02$, (a) subjected to Altadena ground motion; (b) subjected to Lexington ground motion

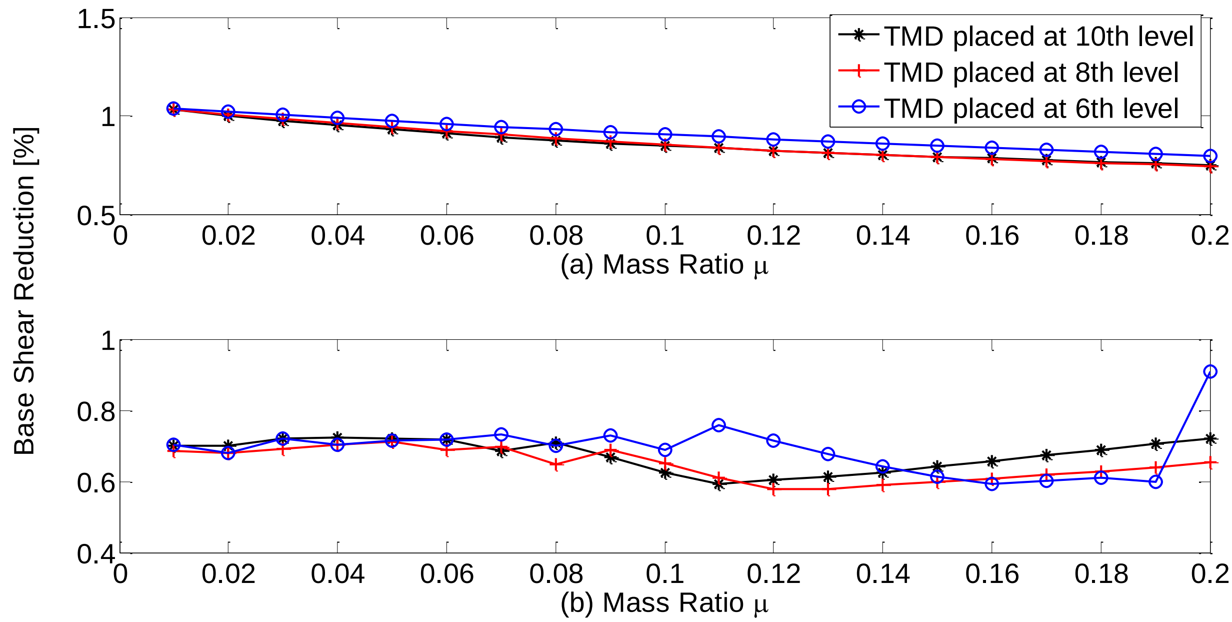

Figure 51: Base shear reduction of roof level of 10-story structure with $\xi_1 = \xi_2 = 0.02$, (a) subjected to Altadena ground motion; (b) subjected to Lexington ground motion

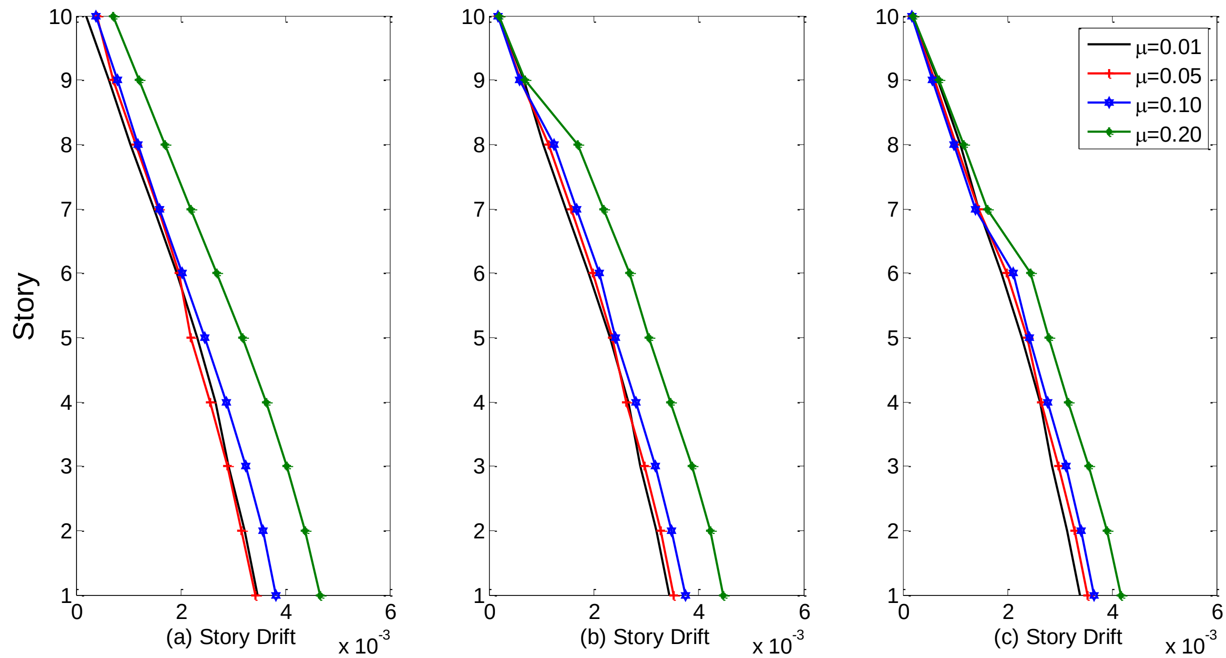

Figure 52: Story drift subjected to Lexington ground motion, (a) TMD placed at 10th level and damping ratio is 0.02; (b) TMD placed at 8th level and damping ratio is 0.02; (c) TMD placed at 6th level and damping ratio is 0.02

a

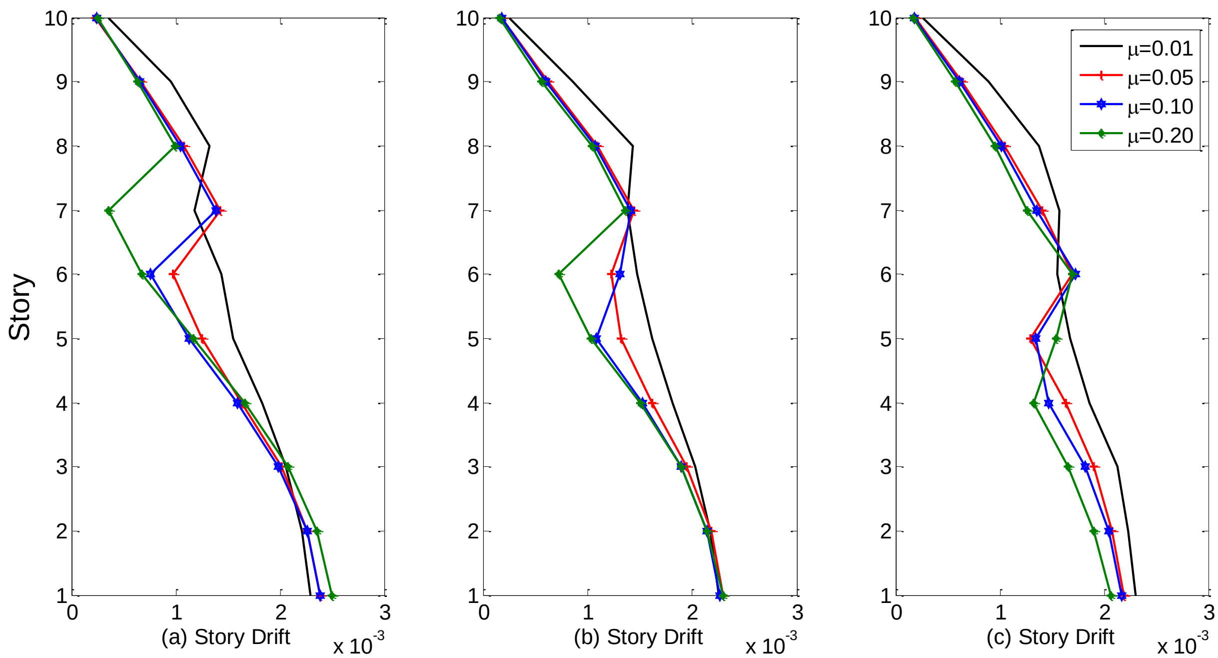

Figure 53: Story drift subjected to Altadena ground motion, (a) TMD placed at 10th level and damping ratio is 0.02; (b) TMD placed at 8th level and damping ratio is 0.02; (c) TMD placed at 6th level and damping ratio is 0.02

Figure 52 and Figure 53 show the story drift of the 10-story building subjected to the Lexington ground motion and the Altadena ground motion, respectively. It is found from the figures that for Lexington ground motion, the story drift decreases with higher level. And the increase of the mass ratio increases the story drift. For instance, when the mass ratio is 1%, the story drift Δ_{10} is 0.019%, when the mass ratio is 5%, the story drift, Δ_{10}, is 0.039. when the mass ratio is 10%, the story drift, Δ_{10}, is 0.079%, and when the mass ratio is 20%, the story drift is increased 0.12%. it is also found that the story drift decreases with the TMD placed at lower level. For example, for the mass ratio is 10%, when the TMD placed at 10th level, the story drift is $\Delta_{10}= 0.079\%$, when the TMD placed at 8th level, $\Delta_{10}= 0.017\%$; when the TMD placed at 6th level, $\Delta_{10}= 0.017\%$.

For the Altadena ground motion, an opposite trend is observed. The story drift decreases with the increase of the mass ratio. For instance, for the TMD placed at 10th level, when the mass ratio is 1%,

Δ_{10}= 0.036%, when the mass ratio is 5%, Δ_{10}= 0.023%, when the mass ratio is 10%, Δ_{10}= 0.025%, and when the mass ratio is increased to 20%, Δ_{10}= 0.025%.

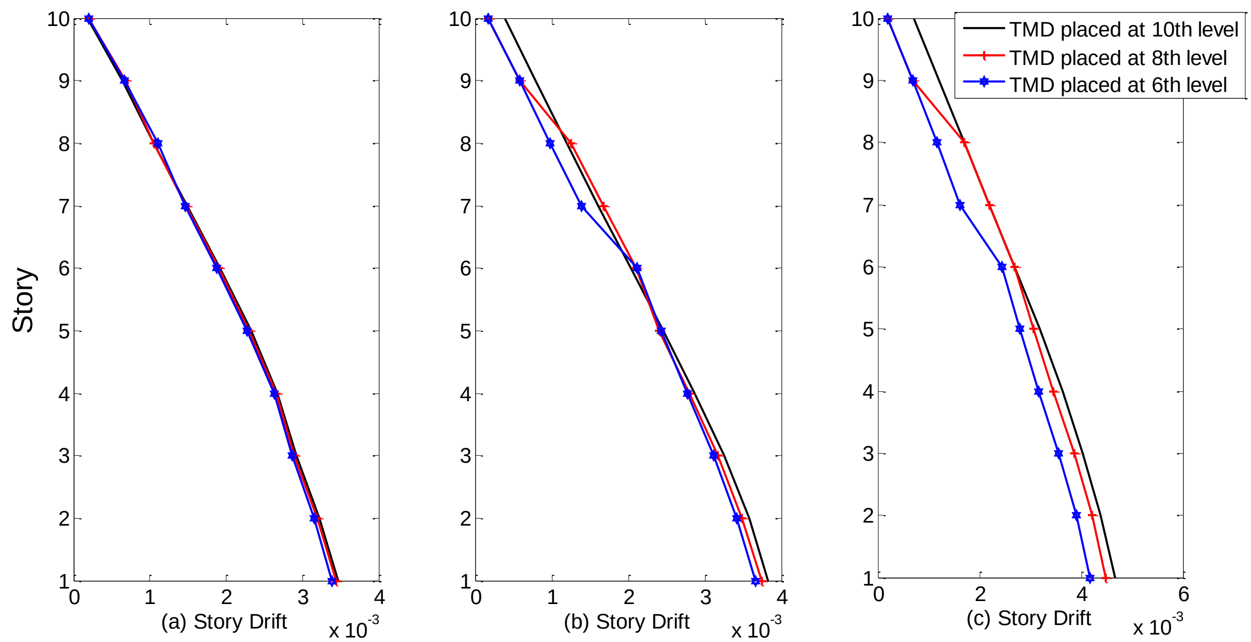

Figure 54: Effect of TMD at various levels on story drift subjected to Lexington ground motion, (a) mass ratio is 0.01; (b) mass ratio is 0.10; (c) mass ratio is 0.20

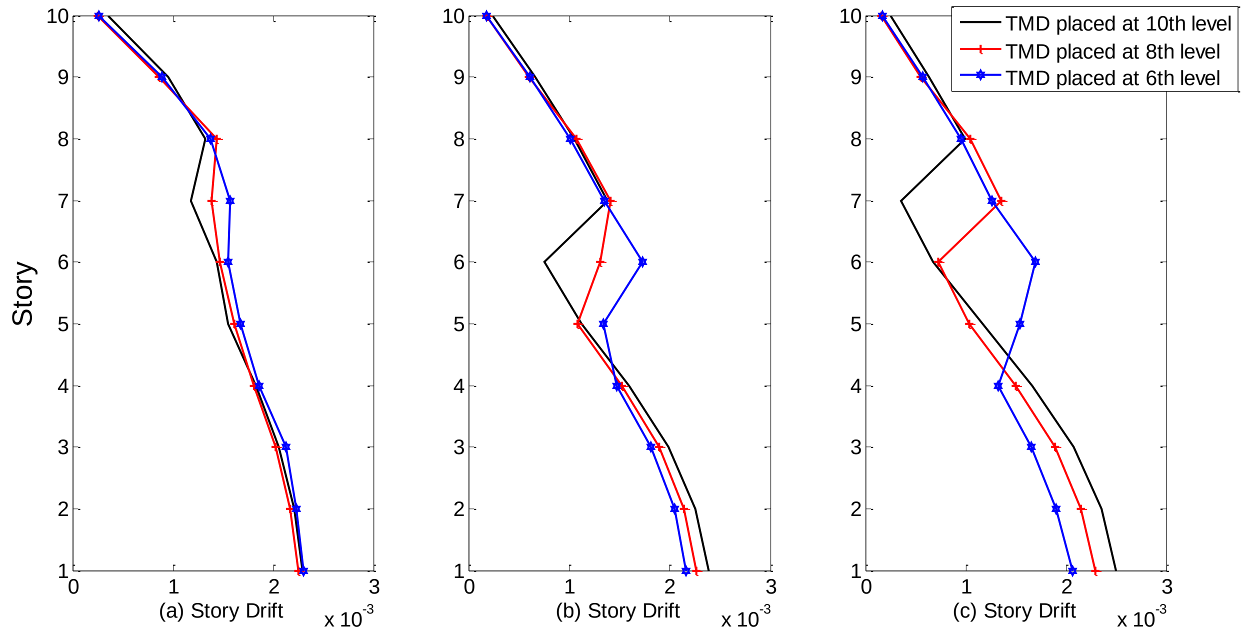

Figure 55: Effect of TMD at various levels on story drift subjected to Altadena ground motion, (a) mass ratio is 0.01; (b) mass ratio is 0.10; (c) mass ratio is 0.20

Figure 54 and Figure 55 show the effect of the TMD at various levels on the story drift of the 10-story building subjected to the Lexington ground motion and the Altadena ground motion, respectively. It is found from Figure 54 that for the Lexington ground motion, the TMD reduces the story drift above the level where the TMD is placed at significantly. For example, from Figure 54(b) and (c), a remarkable slope is observed above the level where the TMD is placed at indicating that the story drift is reduced via the TMD. From Figure 55, it is observed that although the TMD amplifies the story drift below the level where the TMD is placed at, it reduces the story drift significantly above that level. Which is not observed from the 10-story building subjected to the El Centro ground motion.

Conclusion and Recommendations

In this paper, a single TMD was placed at various levels of a 4-story building and a 10-story building, respectively, and various ground motions were used to evaluate the effect of TMD on reducing the roof displacement, story drift and base shear.

In a reasonable range of mass ratio, the roof displacement and base shear of both 4-story and 10-story building decrease as mass ratio increases. For a 4-story building subjected to El Centro, the amplitude of decrease of roof displacement and base shear are considerably large when mass ratio is less than 20%, while if larger than 20%, the decrease of displacement and base shear becomes much small. For Altadena ground motion, an optimally tuned TMD amplifies the roof displacement and base shear when mass ratio is less than 15% and between 4% to 12%, respectively. When subjected to Lexington, the optimally tuned TMD amplifies the base shear, while for roof displacement, it is enlarged when mass ratio is less than 25%. For a 10-story building, an optimally tuned TMD mitigates the displacement and base shear. The roof displacement and base shear decrease with the increase of mass ratio for El Centro and Altadena ground motions. While for Lexington ground motion, they increase as mass ratio increases.

TMD also affects the story drift. In the same range of mass ratio previously discussed, the story drift becomes smaller when mass ratio becomes larger. The amplitude of decrease drops down significantly from 0.00063 and 0.001 at 1st level to 0.00011 and 0.00014 at top level for 4-story and 10-story building respectively, as story is moving up. TMD also acts as a reducer of the story drift for the levels above where TMD is placed at. The story drift at roof level of a 10-story building with TMD at 6th level is 21.4% smaller than that of with TMD at 10th level, and for a 4-story building, placing the TMD at 3rd level makes the roof story drift 30% smaller than that of at 4th level.

Increasing the mass ratio of TMD, although, decreases the displacement and base shear, it adds on extra load on the structure. In addition, a TMD with practical mass ratio has opposite effects on story displacement and base shear subjected to different ground motions. Even so, a larger mass ratio of TMD mitigates the story drift. Furthermore, although a TMD placed at roof level has the best effect on mitigating displacement and base shear, a TMD placed at lower lever does decrease the story drift at the stories above where TMD attached.

Future research needs to focus on the use of multi-TMD on structures to mitigate the displacement, base shear story drift. It is highly needed to study the effect of using multi-TMD with one at roof level and the other at lower levels to maximize effect of vibration control subjected to various ground motions.

Appendix I

Matlab code for numerical integration using Newmark-β method.

```
clc;clear

g=386.1;

%g=9.81;      % SI unit

% Define the design parameters of the damper

n=8;   % Location of the damper

% ------------Input the parameters of the PRIMARY MASS-----------------

%M_diag=[3.26 3.26 3.26 3.26 3.26 3.26 3.26 3.26 3.26 1.358];  % Mass matrix for 10-story building

M_diag=[3.4 3.4 3.4 1.5];  % Mass matrix for 4-story building

nh=length(M_diag);

M=zeros(nh,nh);

for i=1:nh

    M(i,i)=M_diag(i);

end

Me=sum(M_diag);

disp('mass matrix')

M

%K_diag=[16927.32 16927.32 16927.32 16927.32 16927.32 16927.32 16927.32 16927.32 16927.32
16927.32];   % Stiffness matrix for 10-story building
```

```
K_diag=[11543.12 11543.12 11543.12 11543.12];  % Stiffness matrix for 4-story building

K=zeros(nh,nh);

K(1,1)=K_diag(1)+K_diag(2);

K(1,2)=-K_diag(2);

K(nh,nh)=K_diag(nh);

K(nh,nh-1)=-K_diag(nh);

for i=2:nh-1

   K(i,i-1)=-K_diag(i);

   K(i,i)=K_diag(i)+K_diag(i+1);

   K(i,i+1)=-K_diag(i+1);

end

disp('stiffness matrix')

K

%----------Determine the Natural period of the Primary Mass------------

Eig=inv(M)*K;

[vv,w]=eig(Eig);

for i=1:nh

   W(i)=sqrt(w(i,i));

end

[w2,a]=sort(W,'ascend');
```

```
omega=w2;
disp('The Natural Frequency')
omega
for i=1:nh
    ii=a(i);
    v_mode(:,i)=vv(:,ii);
    r(i)=1/max(abs(v_mode(:,i)));
    V_mode(:,i)=r(i)*v_mode(:,i);
end
disp('Norm normalized mode shapes')
V_mode
for i=1:nh
    Tao(i)=V_mode(:,i)'*M*ones(nh,1)/(V_mode(:,i)'*M*V_mode(:,i)); % Modal participation factor
    M_mode(i)=V_mode(:,i)'*M*V_mode(:,i);  % Modal mass
    Participation(i)=(V_mode(:,i)'*M*ones(nh,1))^2/M_mode(i); % Modal effective mass
end
disp('Mode Participation Factor is')
Participation
zeta(1)=0.02;
zeta(2)=0.02;
```

```
% Calculate the factors 'alpha' and 'beta'

A=[1 omega(1)^2;1 omega(2)^2];

B=[2*zeta(1)*omega(1);2*zeta(2)*omega(2)];

factor=A^-1*B;

disp('Alpha is')

factor(1)

disp('Beta is')

factor(2)

% Define the normalized damping matrix

mm=V_mode'*M*V_mode;

kk=V_mode'*K*V_mode;

cc=factor(1)*mm+factor(2)*kk;

C=(V_mode')^-1*cc*V_mode^-1;

disp('damping matrix')

C

% ---------------Input the GROUND EXCITATION---------------------------

Acc=importdata('C:\...\El Centro.txt');

ug=Acc.data(:,3)*g;

L=length(ug);

I=ones(nh,1);
```

```
F=M*I*ug';

% ---------------Input the EXCITATION FORCE----------------------------

P=zeros(nh,L);

% Define the time step

dt=0.01;

% Define the factor Alpha & Beta

alpha=0.5;

beta=0.1667;

% ---------------------Without TMD-----------------------------

U(:,1)=zeros(nh,1);

V(:,1)=zeros(nh,1);

% Define the calculation factor for vd(i+1),ad(i+1),v(i+1),a(i+1)

a1=1/(beta*dt*dt);

a2=-1/(beta*dt);

a3=-1/(2*beta);

a4=alpha/(beta*dt);

a5=-alpha/beta;

a6=dt*(1-(alpha/(2*beta)));

A=(M^-1)*(P(:,1)-F(:,1)-C*V(:,1)-K*U(:,1));

Kba=K+a1*M+a4*C;
```

```
D1=-M*a1-C*a4;

D2=M*a2+C*a5+C;

D3=M*a3+M+C*a6;

for i=1:L-1

    Fba(:,i)=P(:,i+1)-F(:,i+1)-D1*U(:,i)-D2*V(:,i)-D3*A(:,i);

    U(:,i+1)=(Kba^-1)*Fba(:,i);

    dV(:,i)=a4*(U(:,i+1)-U(:,i))+a5*V(:,i)+a6*A(:,i);

    dA(:,i)=a1*(U(:,i+1)-U(:,i))+a2*V(:,i)+a3*A(:,i);

    V(:,i+1)=V(:,i)+dV(:,i);

    A(:,i+1)=A(:,i)+dA(:,i);

end



% --------------------- Attached with TMD----------------------------

for j=1:20

    rou=0.15;   % Mass ratio

    for k=1:20

        zeta(j)=0.00+0.001*j;    % Damping ratio of the damper

        phi(k)=0.75+0.01*k;    % Frequency 7Ratio

% Input the parameters of the DAMPER

        md=M_mode(1)*rou;
```

```
    kd=md*(omega(1)*phi(k))^2;
    cd=2*zeta(j)*md*sqrt(kd/md);
% Assemble the matrix of damper
    Kd=zeros(nh,1);
    Cd=zeros(nh,1);
    Kd(n,1)=kd;
    Cd(n,1)=cd;
% Input the initial condition
    u(:,1)=zeros(nh,1);    % displacement of primary mass
    v(:,1)=zeros(nh,1);   % velocity of primary mass
    ud=0;                  % displacement of damper
    vd=0;                 % velocity of damper
% Define the calculation factor for vd(i+1),ad(i+1),v(i+1),a(i+1)
    H1=M+C*dt*K*dt*dt*beta;
    H2=C*dt*(1-alpha)+K*dt*dt*(0.5-beta);
    H3=C+K*dt;
    H4=K;
    H5=Kd*dt*dt*beta+Cd*dt*alpha;
    H6=Kd*dt*dt*(0.5-beta)+Cd*dt*(1-alpha);
    H7=Kd*dt+Cd;
```

```
    H8=Kd;

    B1=md+cd*dt*alpha+kd*dt*dt*beta;

    B2=cd*dt*(1-alpha)+kd*dt*dt*(0.5-beta);

    B3=cd+kd*dt;

    B4=kd;

    B5=-md;

    C2=H5*B5/B1;

    Dba=H1;

    Dba(:,n)=H1(:,n)-C2;

% -------------------------Numerical solution---------------------

% Input the initial condition

    a=(M^-1)*(P(:,1)-F(:,1)+Cd*vd-Kd*ud-C*v(:,1)-K*u(:,1));

    ad=(-md*a(n,1)-md*ug(1)-cd*vd-kd*ud)/md;

    for i=1:L-1

      Hba(:,i)=P(:,i+1)-F(:,i+1)+H6*ad(i)+H7*vd(i)+H8*ud(i)-H2*a(:,i)-H3*v(:,i)-H4*u(:,i);

      Bba(i)=B2*ad(i)+B3*vd(i)+B4*ud(i)+md*ug(i+1);

      C1(:,i)=Hba(:,i)-(H5*Bba(i)/B1);

      a(:,i+1)=(Dba^-1)*C1(:,i);             % acceleration of primary mass at time i+1

      ad(i+1)=(B5*a(n,i+1)-Bba(i))/B1;       % acceleration of damper at time i+1

      u(:,i+1)=u(:,i)+dt*v(:,i)+dt*dt*((0.5-beta)*a(:,i)+beta*a(:,i+1));
```

```
        v(:,i+1)=v(:,i)+dt*((1-alpha)*a(:,i)+alpha*a(:,i+1));

        ud(i+1)=ud(i)+dt*vd(i)+dt*dt*((0.5-beta)*ad(i)+beta*ad(i+1));

        vd(i+1)=vd(i)+dt*((1-alpha)*ad(i)+alpha*ad(i+1));

    end

    Maxu(j,k)=max(abs(u(nh,:)));

  end

end
```

Appendix II

1. Effect of the mass ratio of the TMD on the roof displacement response in frequency domain

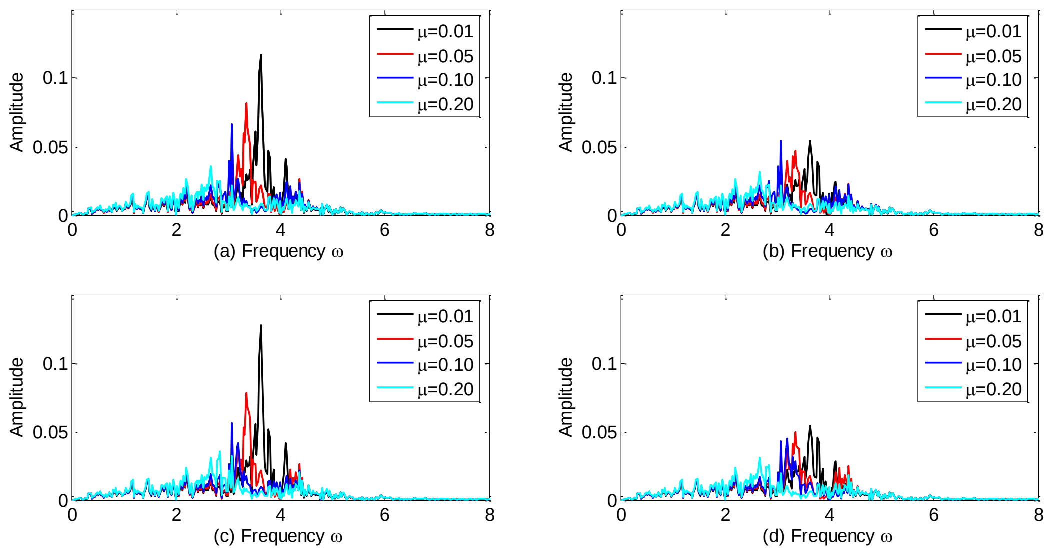

Figure 56: Frequency domain for 4-story building subjected to El Centro ground motion, (a) TMD placed at 4th level and $\xi = 0.02$; (b) TMD placed at 4th level and $\xi = 0.05$; (c) TMD placed at 3rd level and $\xi = 0.02$; (d) TMD placed at 3rd level and $\xi = 0.05$

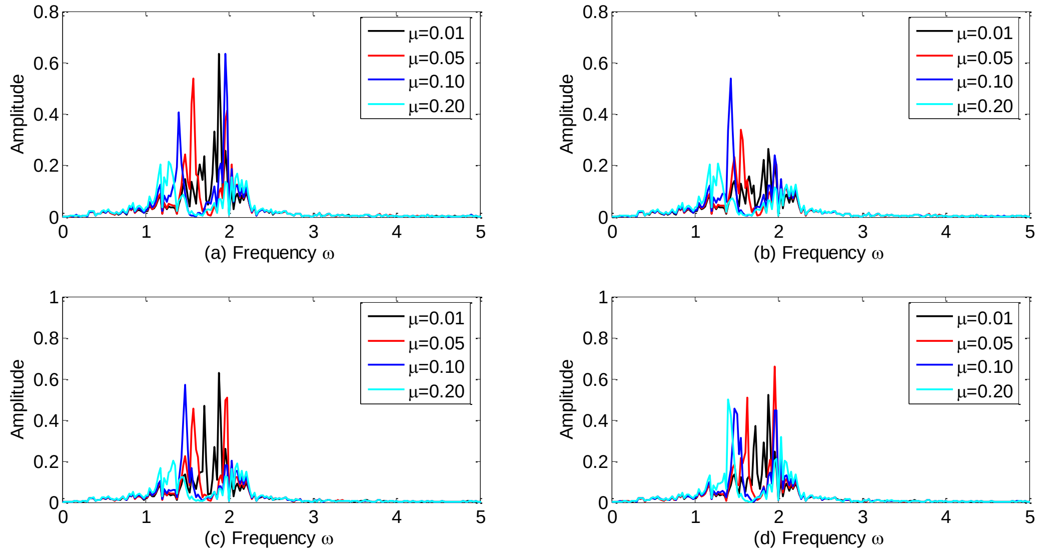

Figure 57: Frequency domain for 10-story building subjected to El Centro ground motion, (a) TMD placed at 10th level and $\xi = 0.02$; (b) TMD placed at 10th level and $\xi = 0.05$; (c) TMD placed at 8th level and $\xi = 0.02$; (d) TMD placed at 6th level and $\xi = 0.02$

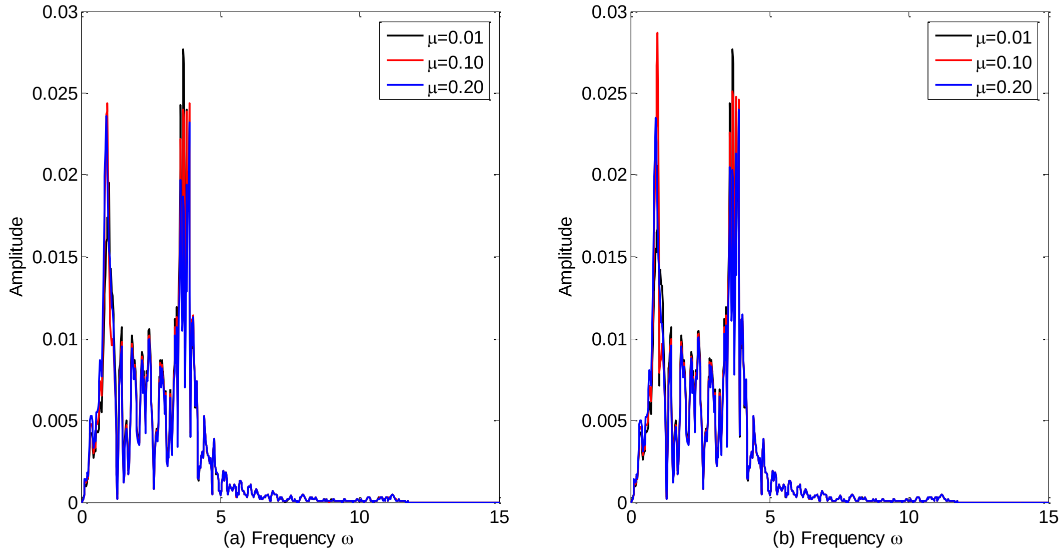

Figure 58: Frequency domain for 4-story building subjected to Lexington ground motion, (a) TMD placed at 4th level and $\xi = 0.02$; (b) TMD placed at 3rd level and $\xi = 0.02$

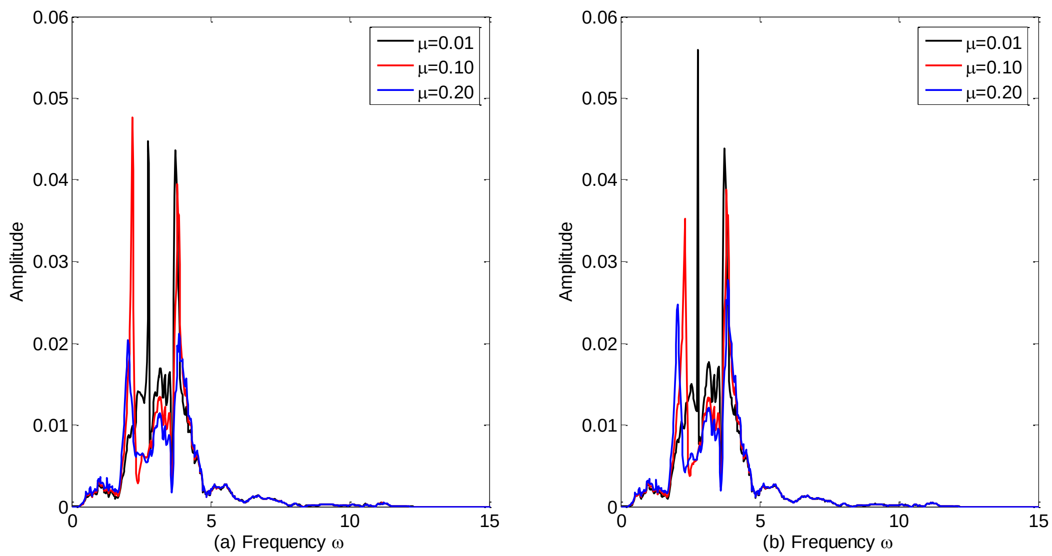

Figure 59: Frequency domain for 4-story building subjected to Altadena ground motion, (a) TMD placed at 4th level and $\xi = 0.02$; (b) TMD placed at 3rd level and $\xi = 0.02$

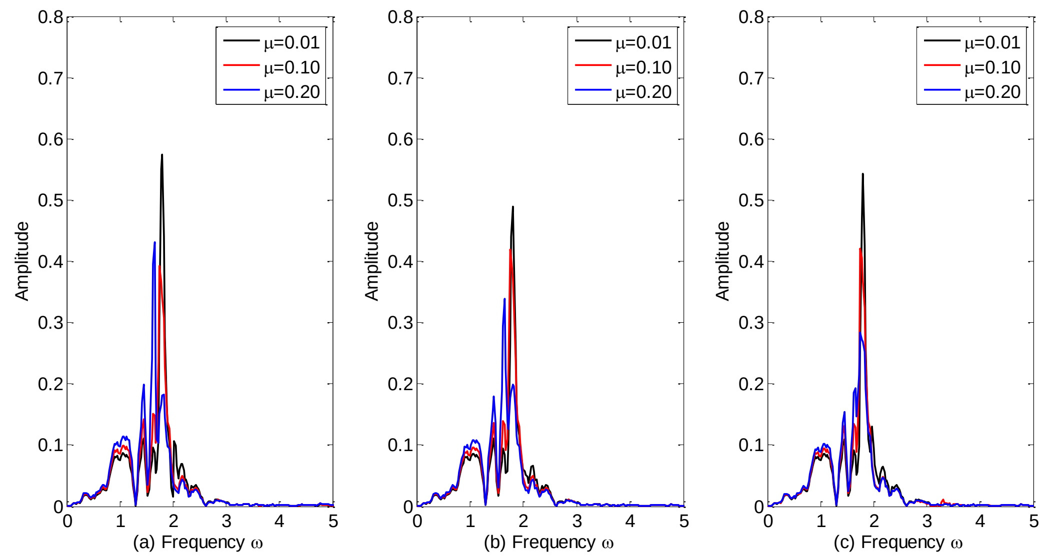

Figure 60: Frequency domain for 10-story building subjected to Lexington ground motion, (a) TMD placed at 10th level and $\xi = 0.02$; (b) TMD placed at 8th level and $\xi = 0.02$; (c) TMD placed at 6th level and $\xi = 0.02$

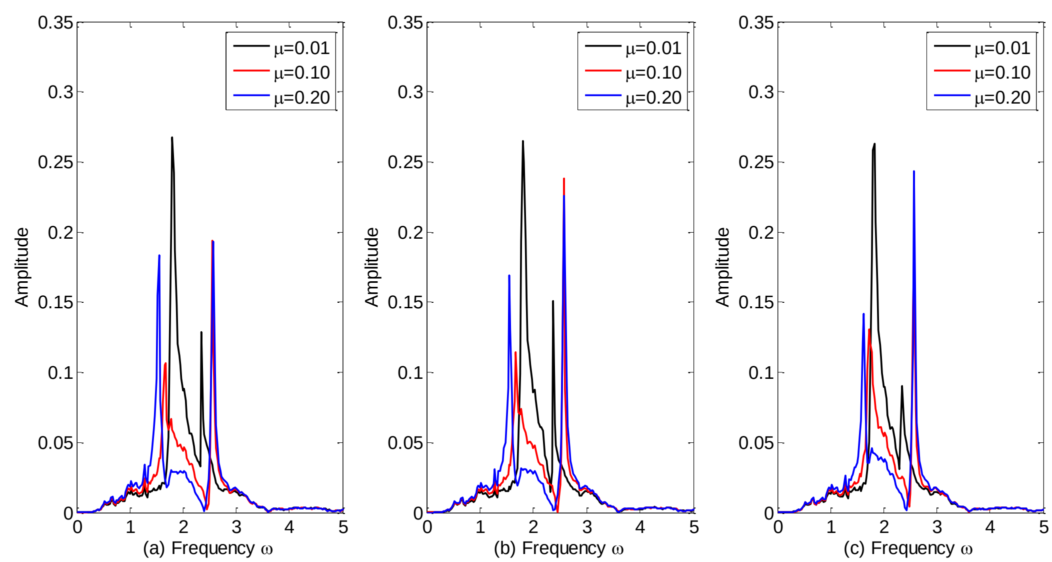

Figure 61: Frequency domain for 10-story building subjected to Altadena ground motion, (a) TMD placed at 10th level and $\xi = 0.02$; (b) TMD placed at 8th level and $\xi = 0.02$; (c) TMD placed at 6th level and $\xi = 0.02$

2. Effect of the TMD at various levels on the roof displacement response in frequency domain

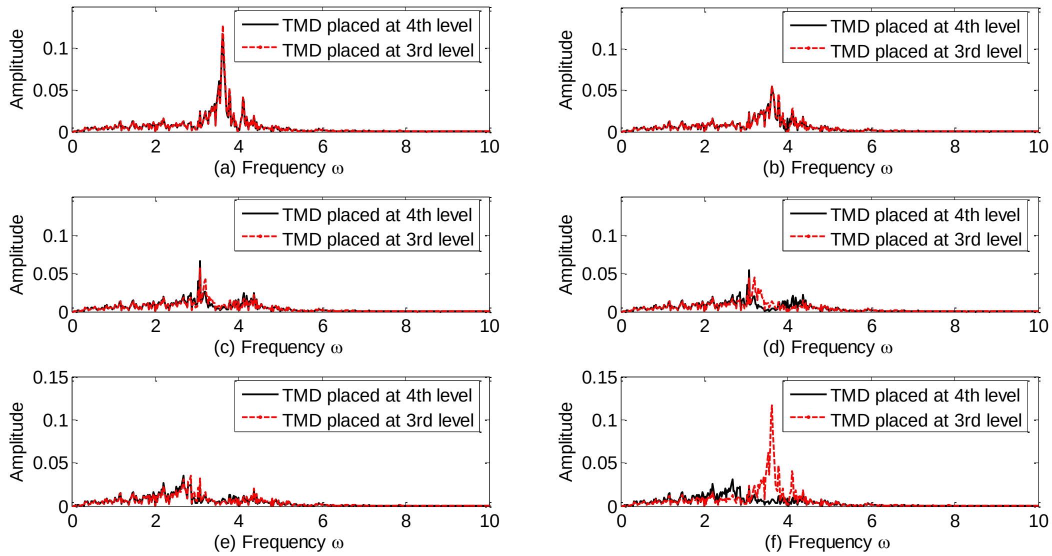

Figure 62: Frequency domain for 4-story building subjected to El Centro ground motion, (a) $\mu = 0.01$ and $\xi = 0.02$; (b) $\mu = 0.01$ and $\xi = 0.05$; (c) $\mu = 0.10$ and $\xi = 0.02$; (d) $\mu = 0.10$ and $\xi = 0.05$; (e) $\mu = 0.20$ and $\xi = 0.02$; (f) $\mu = 0.20$ and $\xi = 0.05$

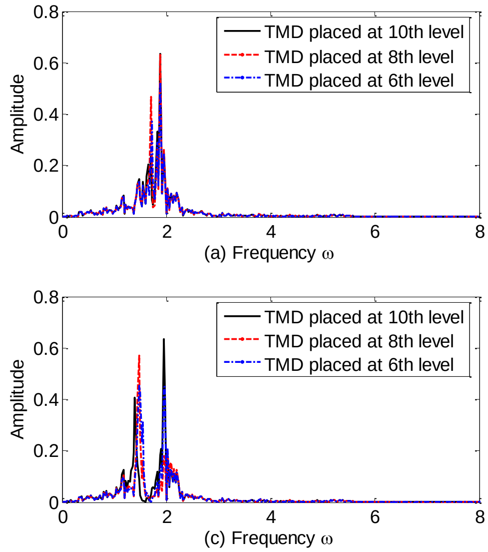

Figure 63: Frequency domain for 10-story building subjected to El Centro ground motion, (a) $\mu = 0.01$ and $\xi = 0.02$; (b) $\mu = 0.05$ and $\xi = 0.02$; (c) $\mu = 0.10$ and $\xi = 0.02$; (d) $\mu = 0.20$ and $\xi = 0.02$

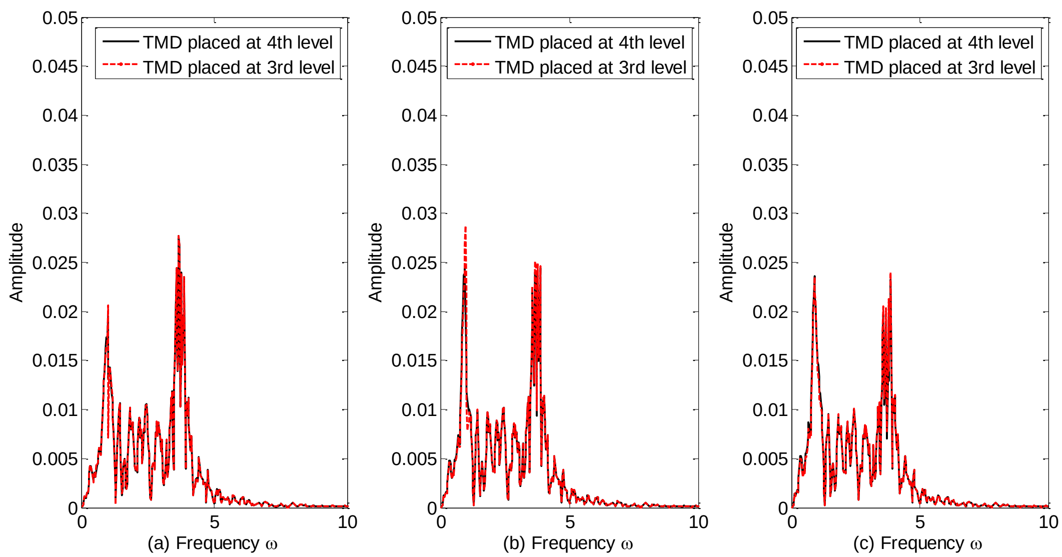

Figure 64: Frequency domain for 4-story building subjected to Lexington ground motion, (a) $\mu = 0.01$ and $\xi = 0.02$; (b) $\mu = 0.10$ and $\xi = 0.02$; (c) $\mu = 0.20$ and $\xi = 0.02$

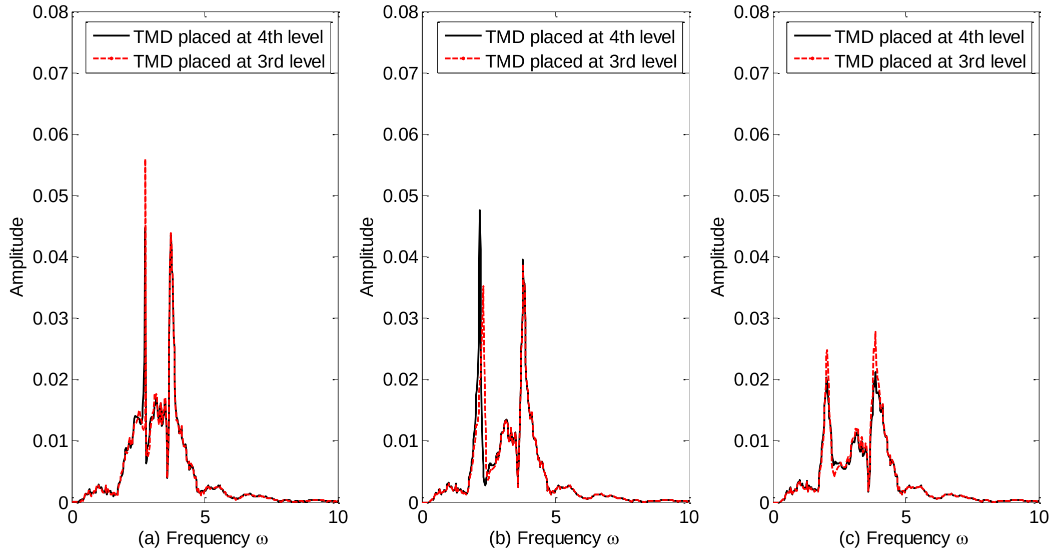

Figure 65: Frequency domain for 4-story building subjected to Altadena ground motion, (a) $\mu = 0.01$ and $\xi = 0.02$; (b) $\mu = 0.10$ and $\xi = 0.02$; (c) $\mu = 0.20$ and $\xi = 0.02$

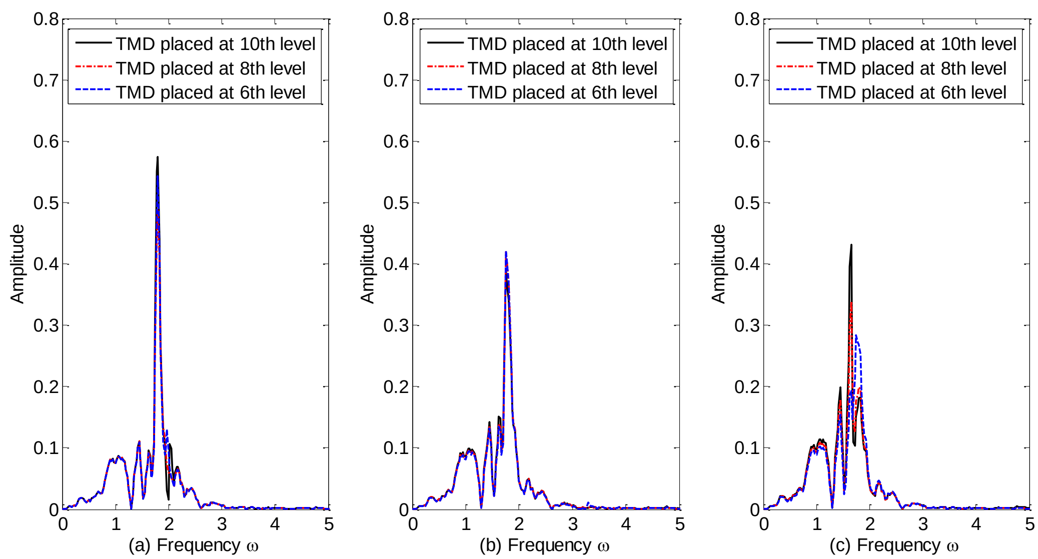

Figure 66: Frequency domain for 10-story building subjected to Lexington ground motion, (a) $\mu = 0.01$ and $\xi = 0.02$; (b) $\mu = 0.10$ and $\xi = 0.02$; (c) $\mu = 0.20$ and $\xi = 0.02$

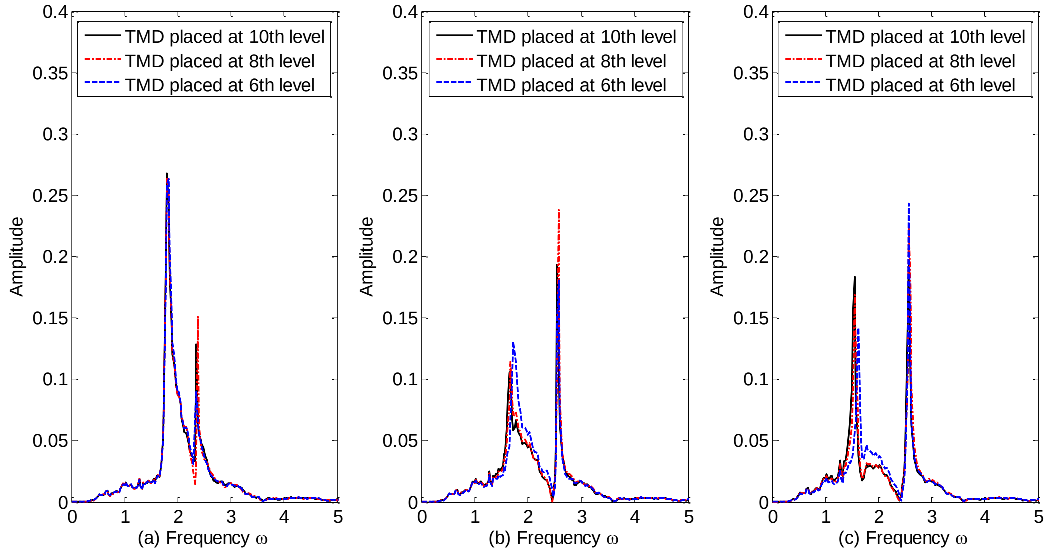

Figure 67: Frequency domain for 10-story building subjected to Altadena ground motion, (a) $\mu = 0.01$ and $\xi = 0.02$; (b) $\mu = 0.10$ and $\xi = 0.02$; (c) $\mu = 0.20$ and $\xi = 0.02$

3. Effect of the mass ratio of the TMD on the roof displacement in time domain

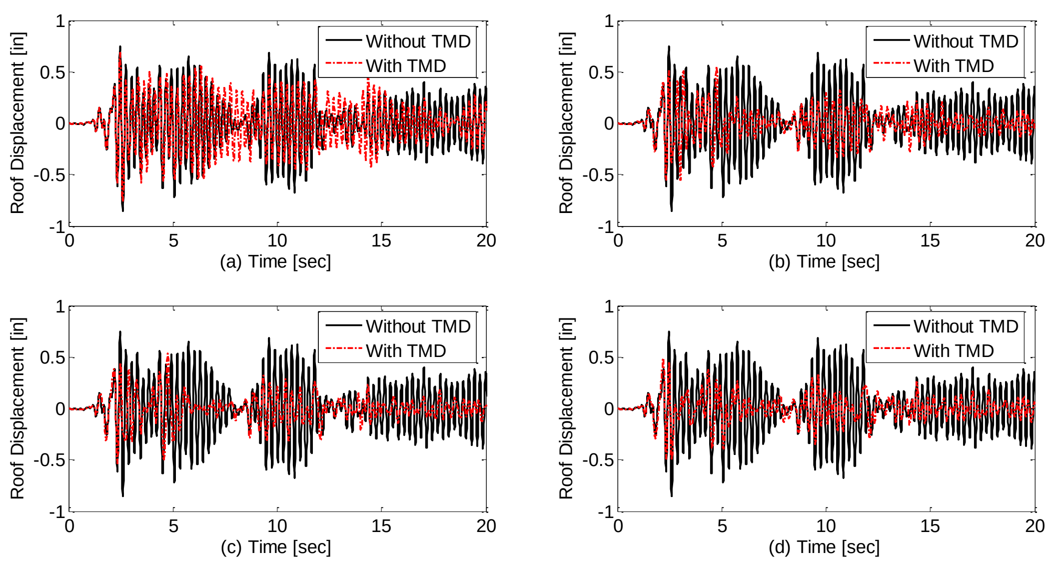

Figure 68: Roof displacement for the 4-story building with TMD placed at 4th level subjected to the El Centro ground motion, (a) $\mu = 0.01$; (b) $\mu = 0.10$; (c) $\mu = 0.20$; (d) $\mu = 0.40$

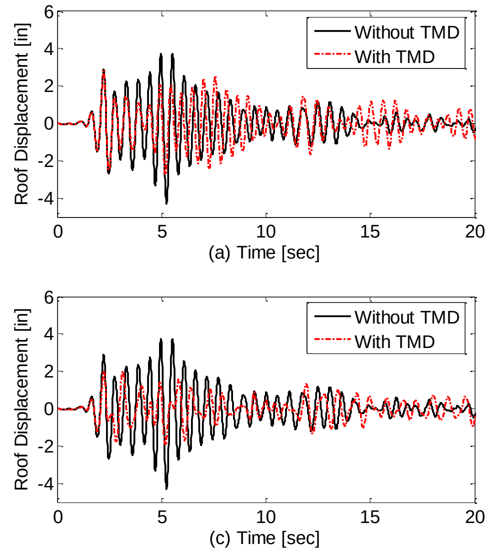

Figure 69: Roof displacement for the 10-story building with TMD placed at 10th level subjected to the El Centro ground motion, (a) $\mu = 0.01$; (b) $\mu = 0.10$; (c) $\mu = 0.20$; (d) $\mu = 0.40$

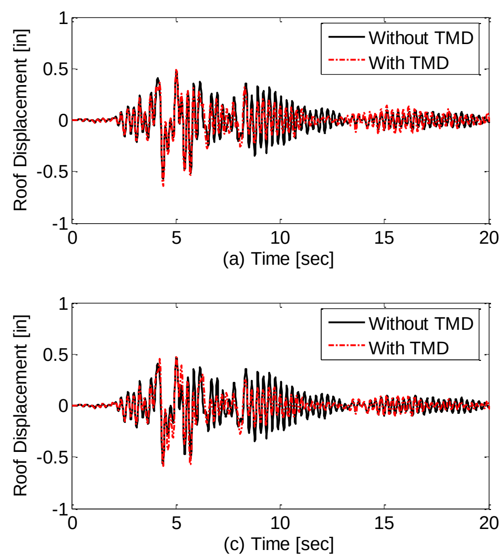

Figure 70: Roof displacement for the 4-story building with TMD placed at 4th level subjected to the Lexington ground motion, (a) $\mu = 0.01$; (b) $\mu = 0.10$; (c) $\mu = 0.20$; (d) $\mu = 0.40$

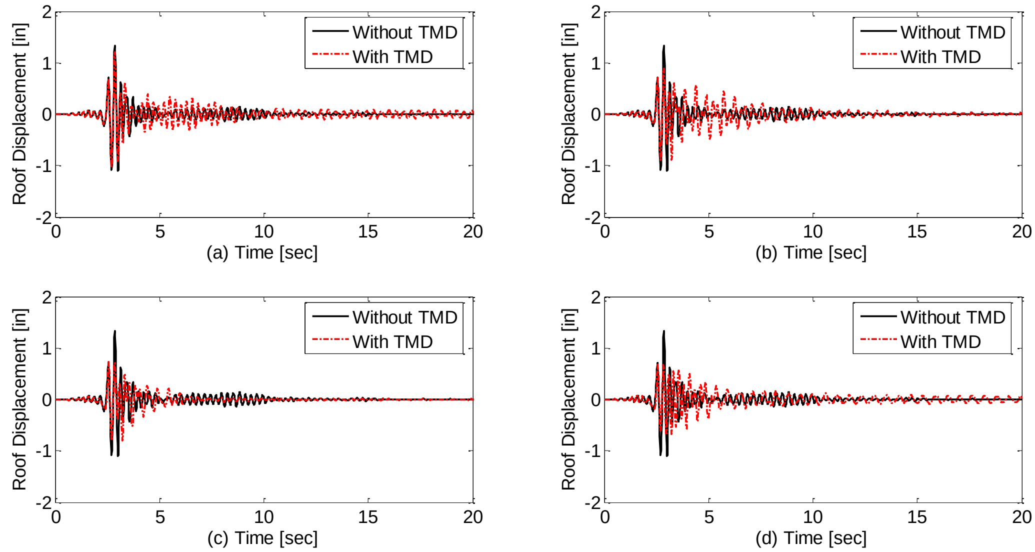

Figure 71: Roof displacement for the 4-story building with TMD placed at 4th level subjected to the Altadena ground motion, (a) $\mu = 0.01$; (b) $\mu = 0.10$; (c) $\mu = 0.20$; (d) $\mu = 0.40$

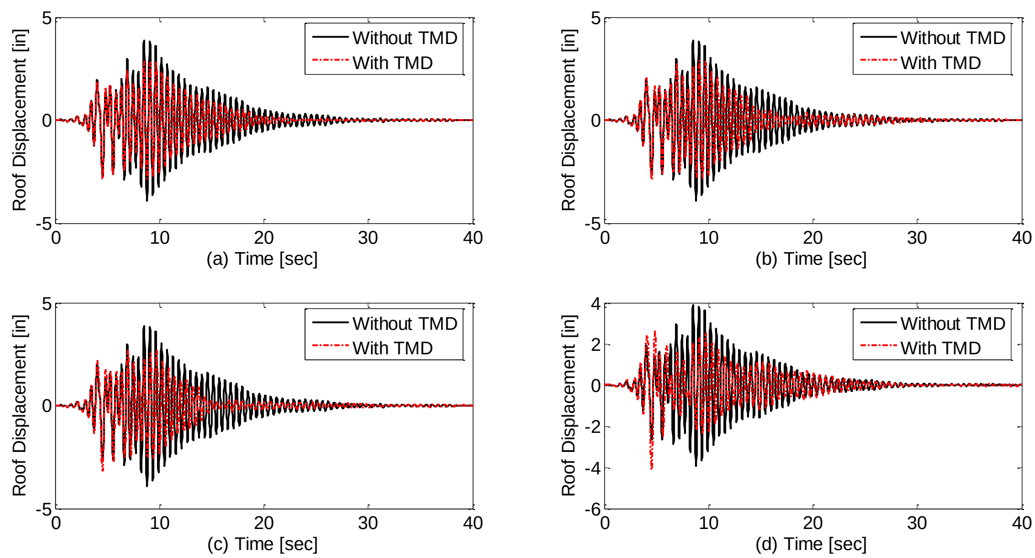

Figure 72: Roof displacement for the 10-story building with TMD placed at 10th level subjected to the Lexington ground motion, (a) $\mu = 0.01$; (b) $\mu = 0.05$; (c) $\mu = 0.10$; (d) $\mu = 0.20$

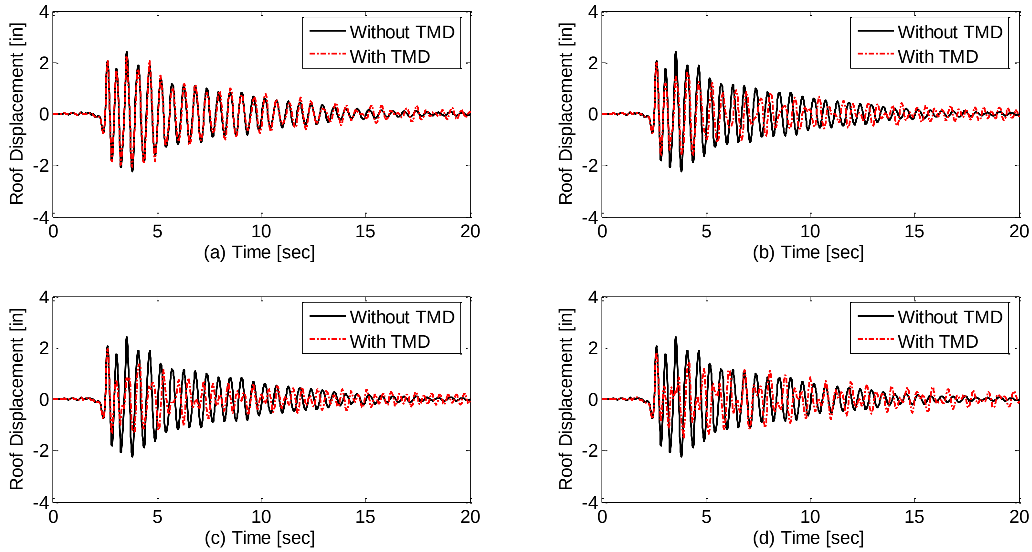

Figure 73: Roof displacement for the 10-story building with TMD placed at 10th level subjected to the Altadena ground motion, (a) $\mu = 0.01$; (b) $\mu = 0.05$; (c) $\mu = 0.10$; (d) $\mu = 0.20$

References:

1. http://en.wikipedia.org/wiki/Vibration_control
2. Chu, S.Y.; Soong, T.T.; Reinhorn, A.M. (2005). *Active, Hybrid and Semi-Active Structural Control*. John Wiley & Sons. ISBN 0-470-01352-4.
3. http://en.wikipedia.org/wiki/Active_vibration_control
4. http://articles.architectjaved.com/earthquake_resistant_structures/active-control-devices-for-earthquake-resistance/
5. Rasouli, SK.; Yahyai, M. (2002). *Control of response of structures with passive and active tuned mass damper.* Struct. Design Tall Build. 11, 1–14 (2002).
6. C.M. Wang, N. Yan and T. Balendra.(1999). *Control on Dynamic Structural Response Using Active-Passive Composite-Tuned Mass Dampers.* Journal of Vibration and Control 1999 5: 475
7. Abdel-Rohman M, Leipholz HHE. (1979). *General approach to active structural control.* Journal of Engineering Mechanics Division, ASCE 105(6): 1007–1023.
8. James Chang CH, Soong TT. (1980). *Structural control using active tuned mass* dampers. Journal of Engineering Mechanics Division, ASCE 106(6): 1091–1098.
9. Hrovat D, Barak P, Rabins M. (1983). *Semi-active versus passive or active tuned mass dampers for structural control.* Journal of Engineering Mechanics, ASCE 109(3): 691–705.
10. Feng Q, Shinozuka M.(1990). *Use of a variable damper for hybrid control of bridge response under earthquake. In: US national workshop on structural control researh 1990*. Los Angeles: University of Southern California; p. 10712.
11. Brogan WL. *Modern control theory*. Englewood Cliffs (NJ): Prentice-Hall; 1991.
12. McClamroch NH, Gavin HP.(1995). *Closed loop structural control using electrorheo-logical dampers.* In: American control conference. Washington (DC): American Automatic Control Council; 1995.
13. Dyke SJ, Spencer BF.(1996). *Seismic response control using multiple MR dampers*. In: 2nd international workshop on structural control. Hong Kong University of Science and Technology Research Center; 1996.
14. Inaudi JA. (1997). *Modulated homogeneous friction: a semi-active damping strategy*. Earthq Eng Struct Dyn 1997; 26(3):36176.
15. Song T T.(1990). *Active Structure Control. Theory and Practice*. Gongman, London and Wiley. New York; 1990.
16. Schmitendorf W E, Faryar J and Yang J N.(1994). *Robust Control Techniques for Buildings Under Earthquake Excitation*. Earthquake Engineering and Structural Dynamics, 1994; 23; 539–552.
17. Faryar J, Schmitendorf W E and Yang J N. H_∞ *Control for Seismic Excited Building with Acceleration Feedback*. ASCE, Journal of Engineering Mechanics, 1996; 121(9); 994–1002.
18. Kose I E, Schmitendorf W E, Faryar J and Yang J N. H_∞ *Active Seismic Response Control Using Static Output Feedback*. ASCE, Journal of Engineering Mechanics, 1996; 122(7); 651–659.
19. Kenzo N. *Control Performance Based on Control System Design Strategies for Active Structural Control.* JSME International Journal. Series C, 1995; 38(3); 367–378.
20. Laura M. Jansen and Shirley J. Dyke.(2000). *Semi-Active Control Strategies for MR Dampers: A Comparative Study*. ASCE, Journal of Engineering Mechanics, 2000; 126(8); 795–803.
21. McClamroch, N.H. and Gavin, H.P. (1995). *Closed Loop Structural Control Using Electrorheological Dampers*. Proc. of the Amer. Ctrl. Conf., Seattle, Washington, pp. 4173–77.
22. Leitmann, G. (1994). *Semiactive Control for Vibration Attenuation*. J. of Intelligent Material Systems and Structures," Vol. 5 September, pp. 841–846.
23. Buckle, Ian G.(2000). *Passive control of structures for seismic loads.* Bulletin of the New Zealand Society for Earthquake Engineering 33.3 (2000): 209-221.
24. Sadek, Fahim, et al.(1997). *A method of estimating the parameters of tuned mass dampers for seismic applications.* Earthquake Engineering and Structural Dynamics 26.6 (1997): 617-636.
25. Moreschi, Luis M. *Seismic design of energy dissipation systems for optimal structural performance.* Diss. Virginia Polytechnic Institute and State University, 2000.
26. Wiechert, E (1889); *Ueber elastische Nachwirkung*, Dissertation, Königsberg University, Germany

27. Thorby, Douglas.(2008). *Structural dynamics and vibration in practice: an engineering handbook.* Butterworth-Heinemann.
28. Krenk S. and Hogsberg J.R.,(2010). *Tuned Mass Dampers. Structural Dynamics Note 3.* Department of Mechanical Engineering, Technical University of Denmark, March, 2010.
29. J.*P.* Den Hartog,(1985) *Mechanical Vibrations (4th edn.)*, McGraw-Hill, New York, 1956. (Reprinted by Dover, New York, 1985).
30. J.E. Brock.(1946). *A note on the damped vibration absorber*, Journal of Applied Mechanics, Vol. 13, A284, 1946
31. Krenk, S., & Høgsberg, J. (2008). *Tuned mass absorbers on damped structures under random load*. Probabilistic Engineering Mechanics, 23(4), 408-415.
32. Gavin, H. (2001). Numerical integration for structural dynamics. *Department of Civil and Environmental Engineering, Duke University, Durham, NC*.
33. Ray W. Clough, Joseph Penzien. (1993). *Dynamics of structures*, McGraw-Hill, New York.
34. Pall, A. S., & Marsh, C. (1982). *Response of friction damped braced frames*. Journal of Structural Engineering, 108(9), 1313-1323.
35. Grigorian, C.E., Popov, E.P., *Slotted bolted connections for energy dissipation*. Proceeding of ACT-17-1 on seismic isolation, energy dissipation and active control, 1993. 2: p. 545-556.
36. Aiken, J.D., Kelly, J.M.(1990)., *Earthquake simulator testing and analytical studies of two energy-absorbing system for multistory structure*, in Report No. UCB/EERC-90/03. 1990,Earthquake Engineering Research Center, University of California, Berkeley, CA.
37. Tsiatas, G., Daly, K.(1994), *Controlling vibrations with combination viscour/friction mechanisms*. Proceedings of First World Conference on Structural Control, 1994. 1: p. WP4-3 - WP4-11.
38. Zheng Lu, Xilin Lu, and Sami F. Masri. *Optimum Design of Particle Dampers Under Random Excitation*. 7th International Conference on Urban Earthquake Engineering(7CUEE) & 5th International Conference on Earthquake Engineering 5ICEE), TokyoInstitute of Technology, Tokyo, Japan. March3-5, 2010.
39. Rana, R., & Soong, T. T. (1998). *Parametric study and simplified design of tuned mass dampers*. Engineering structures, 20(3), 193-204.
40. Hancock tower now to get dampersÕ, Eng. news record, 11 (1975).
41. Tuned mass dampers steady sway of sky scrapers in windÕ, Eng. news record, 28Ð29 (1977).